AD-A157 810 EXPERIMENTS IN LONG-WAVELENGTH COMMUNICATION USING MODULATED ELECTRON BEA..(U) PACIFIC-SIERRA RESEARCH CORP LOS ANGELES CA L E JOHNSON AUG 85 PSR-1513 1/2

UNCLASSIFIED RADC-TR-85-133 DNA001-84-C-0288 F/G 20/7 NL

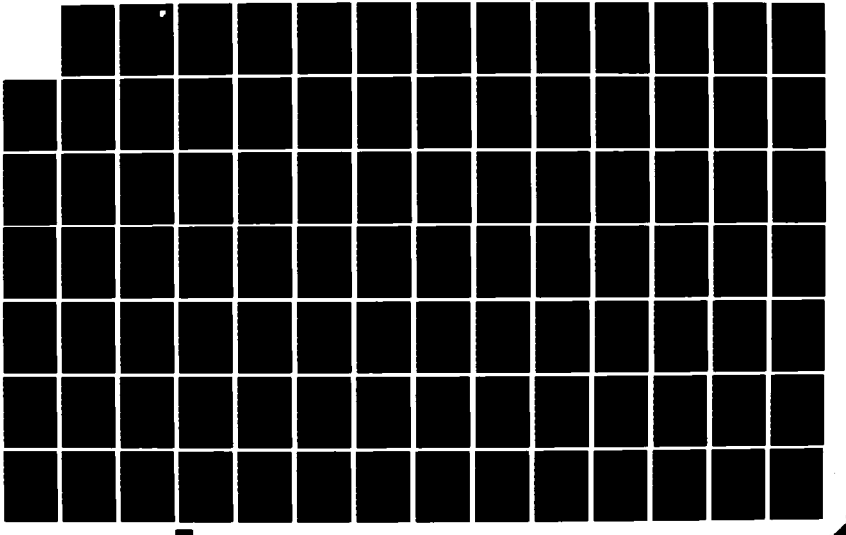

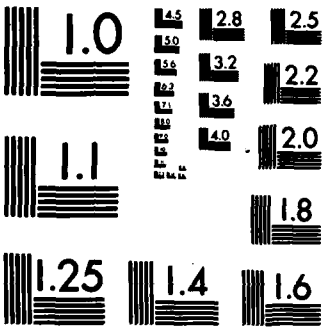

MICROCOPY RESOLUTION TEST CHART

)ARDS-1963-A

(2)

RADC-TR-85-133
Final Technical Report
August 1985

EXPERIMENTS IN LONG-WAVELENGTH COMMUNICATION USING MODULATED ELECTRON BEAM ANTENNAS: A Parameter Study

Pacific-Sierra Research Corporation

L. E. Johnson

APPROVED FOR PUBLIC RELEASE; DISTRIBUTION UNLIMITED

This effort was funded totally by the Defense Nuclear Agency

ROME AIR DEVELOPMENT CENTER
Air Force Systems Command
Griffiss Air Force Base, NY 13441-5700

This report has been reviewed by the RADC Public Affairs Office (PA) and is releasable to the National Technical Information Service (NTIS). At NTIS it will be releasable to the general public, including foreign nations.

RADC-TR-85-133 has been reviewed and is approved for publication.

APPROVED: Dallas T. Hayes

DALLAS T. HAYES
Project Engineer

APPROVED: Allan C. Schell

ALLAN C. SCHELL
Chief, Electromagnetic Sciences Division

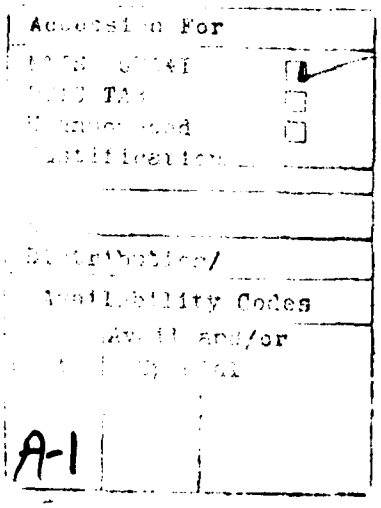

FOR THE COMMANDER: John A. Ritz

JOHN A. RITZ
Plans Office

If your address has changed or if you wish to be removed from the RADC mailing list, or if the addressee is no longer employed by your organization, please notify RADC (EEPS) Hanscom AFB MA 01731. This will assist us in maintaining a current mailing list.

Do not return copies of this report unless contractual obligations or notices on a specific document requires that it be returned.

UNCLASSIFIED
SECURITY CLASSIFICATION OF THIS PAGE

REPORT DOCUMENTATION PAGE

1a. REPORT SECURITY CLASSIFICATION UNCLASSIFIED	1b. RESTRICTIVE MARKINGS N/A
2a. SECURITY CLASSIFICATION AUTHORITY N/A	3. DISTRIBUTION/AVAILABILITY OF REPORT Approved for public release; distribution unlimited
2b. DECLASSIFICATION/DOWNGRADING SCHEDULE N/A	
4. PERFORMING ORGANIZATION REPORT NUMBER(S) PSR 1513	5. MONITORING ORGANIZATION REPORT NUMBER(S) RADC-TR-85-133
6a. NAME OF PERFORMING ORGANIZATION Pacific-Sierra Research Corporation 6b. OFFICE SYMBOL (If applicable)	7a. NAME OF MONITORING ORGANIZATION Rome Air Development Center (EEPS)
6c. ADDRESS (City, State and ZIP Code) 12340 Santa Monica Blvd Los Angeles CA 90025	7b. ADDRESS (City, State and ZIP Code) Hanscom AFB MA 01731
8a. NAME OF FUNDING/SPONSORING ORGANIZATION Defense Nuclear Agency 8b. OFFICE SYMBOL (If applicable)	9. PROCUREMENT INSTRUMENT IDENTIFICATION NUMBER
8c. ADDRESS (City, State and ZIP Code) Wash DC 20305	10. SOURCE OF FUNDING NOS. PROGRAM ELEMENT NO. 61102F; PROJECT NO. 2305; TASK NO. J2; WORK UNIT NO. 49

11. TITLE (Include Security Classification) EXPERIMENTS IN LONG-WAVELENGTH COMMUNICATION USING MODULATED ELECTRON BEAM ANTENNAS: A Parameter Study

12. PERSONAL AUTHOR(S)
L.E. Johnson

13a. TYPE OF REPORT	13b. TIME COVERED	14. DATE OF REPORT (Yr., Mo., Day)	15. PAGE COUNT
Final	FROM 15Jun84 TO 31Jan85	August 1985	124

16. SUPPLEMENTARY NOTATION
This effort was funded totally by the Defense Nuclear Agency

17. COSATI CODES		
FIELD	GROUP	SUB. GR.
17	02	
20	14	

18. SUBJECT TERMS (Continue on reverse if necessary and identify by block number)
BERT-I, Cerenkov radiation, Cyclotron radiation, Electron guns, ELF, VLF, VCAP, SEPAC, Virtual antennas (over)

19. ABSTRACT (Continue on reverse if necessary and identify by block number)

This preliminary study scopes the feasibility of producing electromagnetic signals from modulated beam antennas in the ionosphere and detecting those signals on the ground. Restricted to frequencies between tens of hertz and a megahertz, the report is essentially a handbook that gives predicted characteristics of the radiation produced by modulated electron beams employed in four different experiments. The first is hypothetical and is optimized for the generation of detection of long-wavelength radiation. The other three are BERT-I, SEPAC, and VCAP.

20. DISTRIBUTION/AVAILABILITY OF ABSTRACT UNCLASSIFIED/UNLIMITED ☒ SAME AS RPT. ☐ DTIC USERS ☐	21. ABSTRACT SECURITY CLASSIFICATION UNCLASSIFIED
22a. NAME OF RESPONSIBLE INDIVIDUAL Dallas T. Hayes	22b. TELEPHONE NUMBER (Include Area Code) (617) 861-4265 22c. OFFICE SYMBOL RADC (EEPS)

DD FORM 1473, 83 APR EDITION OF 1 JAN 73 IS OBSOLETE.

UNCLASSIFIED
SECURITY CLASSIFICATION OF THIS PAGE

Block 18. Subject Terms (Cont'd)

Long-wavelength communications
Low-frequency communications
Modulated electron beams
Spacelab 2

SUMMARY

This report lays the groundwork for analyzing the feasibility of producing electromagnetic signals from modulated electron beam antennas in the ionosphere and detecting the signals on the ground. It concentrates on frequencies between tens of hertz to a megahertz because higher frequencies are easily radiated from conventional antennas on spacecraft. This study is geared toward helping the military to develop low-frequency communication systems that use beam antennas.

It is well known that natural electric currents in the ionosphere and magnetosphere produce electromagnetic radiation of frequencies less than 1 MHz, and that radiation is regularly observed at the ground. Certain man-made electron beams ejected into the ionosphere have generated radiation at frequencies above 1 MHz--this radiation has been detected on the ground. As yet, however, no experiment has attempted to use modulated electron beams in the ionosphere to produce radiation of the modulation frequency or its harmonics, and to detect that radiation on the ground.

This detailed and extensive analysis necessarily incorporates several idealizations that tend to overstate the efficiency of the radiation. Nonetheless, this report suggests that a carefully controlled experiment may be able to produce long-wave radiation that can be detected on the ground.

This report is essentially a handbook that gives predicted characteristics of the radiation for four assumed experimental configurations. The first is hypothetical; it is optimized for the generation and detection of long-wavelength radiation using present-day or easily attainable technology. The other three are already planned and funded (their primary emphasis, however, is not on wave generation and detection measurements).

Further analysis is needed to design the optimal, long-wavelength experiment in detail. In addition, more theoretical work is suggested for an assessment of the impact of relaxing certain of the idealizations made in the beam/propagation models used in the present report.

PREFACE

This work represents the Pacific-Sierra Research Corporation (PSR) final report under contract DNA001-84-C-0288. The research was sponsored by the Rome Air Development Center (RADC) under Air Force Office of Scientific Research task number 2305J2, and the contract was administered by the Defense Nuclear Agency (DNA). The task performed under this contract is a parameter study of electromagnetic emissions from modulated electron beams in the ionosphere. It will be used to define an experiment that will evaluate the feasibility of long-wavelength communication using modulated electron beam antennas in the ionosphere.

CONTENTS

FIGURES

I. INTRODUCTION

This Pacific-Sierra Research Corporation (PSR) report is a parameter study of the characteristics of electromagnetic radiation that may be emitted by modulated nonrelativistic electron beams in the mid-latitude ionosphere. Two intentions motivate this work. The first is to design an optimal experiment for probing the physics of communication at very low frequency (VLF) and extremely low frequency (ELF) by means of an electron beam as a virtual antenna. The second is to examine the possibilities for communications research provided by planned, funded electron beam experiments.

Of the four experiments considered, the optimal experiment will employ an electron gun that we call the "future gun." Its parameters, at the leading edge of technical feasibility, will provide the maximum possible current at a given voltage. The future gun is intended for deployment on a rocket dedicated to communications research.

The other experiments analyzed here are not dedicated to communications, but they will utilize electron beams that are injected into the ionosphere and that are or may be modulated. The first experiment will be flown aboard a rocket, BERT-I, to be launched in April 1985. Devoted mainly to spacecraft charging, BERT-I will use a relatively low-power electron beam. Current plans are for an unmodulated beam, but the hardware could be modified to provide square wave modulation. The second utilizes a Vehicle Charging and Potential (VCAP) experiment gun, which will be placed on Spacelab 2, to be launched in mid-1985. Modulated electron beams will be ejected and electromagnetic fields will be measured in the near-field region. The third experiment is a joint Japanese and U.S. venture called SEPAC (Space Experiment with Particle Accelerators), which will be placed aboard three shuttle flights in August 1986. The gun on SEPAC is the most powerful of the three. Its beams will be modulated, and near-field measurements are planned for it.

The mathematical model employed for all the calculations presented here is from Harker and Banks.[1] That model calculates radiation

emission from a semi-infinite electron beam having a finite correlation length. The model, which is reviewed in Sec. II of this report, is coupled with simple estimates of the antenna gain and atmospheric attenuation to provide an overall, if highly simplified, model of the radiation received on the ground.

Section III encompasses a somewhat detailed analysis of the future gun. Because the interpretations of the results for the three other guns follow the patterns established for the future gun, those analyses are given in brief and only a few figures for those cases are presented in this report. Sections IV through VI are analytical results for the planned and funded guns--BERT-I is treated in Sec. IV, VCAP in Sec. V, and SEPAC in Sec. VI.

II. THEORY

MODEL

The Harker and Banks[1] model assumes that an infinite pulse train of electrons is emitted from the electron source at $z = 0$ and spirals around a magnetic field line with parallel and perpendicular velocities $v_{||}$ and $v_{\perp}$. The beam has zero diameter, has always been on and is not modified by the surrounding plasma. However, the magnitude of the current falls off exponentially in z with an e-folding length of ℓ. That falloff models a decreasing ability of the beam to radiate with increasing z.

The beam passes through a cold plasma in an ambient magnetic field. The plasma consists of electrons and one ion species [which we assume to be $(O^{16})^+$ in this parameter study] and is represented by the relative dielectric tensor

$$(\varepsilon_{ij}) = \begin{pmatrix} \varepsilon_1 & i\varepsilon_2 & 0 \\ i\varepsilon_2 & \varepsilon_1 & 0 \\ 0 & 0 & \varepsilon_3 \end{pmatrix} , \tag{1}$$

where

$$\varepsilon_1 = 1 - \frac{\delta^2(\Omega^2 - \varepsilon)}{(\Omega^2 - 1)(\Omega^2 - \varepsilon^2)} ,$$

$$\varepsilon_2 = \frac{\delta^2\Omega(1 - \varepsilon)}{(\Omega^2 - 1)(\Omega^2 - \varepsilon^2)} ,$$

$$\varepsilon_3 = 1 - \frac{\delta^2}{\Omega^2} , \tag{2}$$

and $\varepsilon = m_e/m_i$ is the electron-to-ion mass ratio, $\Omega = \omega/\omega_{ce}$ is the ratio of the (angular) frequency of the electromagnetic wave to the electron cyclotron frequency, and $\delta^2 = (\omega_{pe}^2 + \omega_{pi}^2)/\omega_{ce}^2$ is the normalized sum of the squares of the electron and ion plasma frequencies.

Maxwell's equations are solved by Fourier analysis. The resulting formula for power radiated takes the following form in the case of large ℓ:

$$P_r = \sum_{s=-\infty}^{\infty} \sum_{i=1}^{2} \sum_{p=1}^{\infty} \frac{I_B^2 R_0}{2\pi^2} \frac{\ell\omega_m}{c} \frac{\sin^2\left(\frac{\pi p b}{d}\right) G_i^2}{\varepsilon_1\left(\mu_1^2 - \mu_2^2\right) p} \quad \text{watts} . \tag{3}$$

In the above, c is the velocity of light; p labels the harmonic, so that $\omega = p\omega_m$, where ω_m is the angular modulation frequency of the beam; i labels the root of the dispersion relation; and s labels the radiation mode. The Cerenkov mode corresponds to s = 0, and the regular and anomalous cyclotron modes correspond to s = 1 and s = -1, respectively. The quantities μ_1^2 and μ_2^2 are the two roots or branches of the dispersion relation. Properties of those branches are summarized in Sec. 4.3 of *The Near-Earth and Interplanetary Plasma,* an excellent book by Al'pert.[2] In Eq. (3), I_B is the beam current in amperes, R_0 is the impedance of free space $R_0 = 377\ \Omega$, b is the length of the electron pulse, and d is the spacing between the front of the successive pulses. Finally, the quantity G_i^2 is the square of

$$G_i = -\frac{v_\perp}{v_\parallel} J_s'(u) \left[\varepsilon_1\varepsilon_3 + n^2(\varepsilon_1 - \varepsilon_3) - \varepsilon_1\mu_i^2\right]^{1/2}$$

$$+ J_s(u) \left\{ \left[\left(\mu_i^2 - \varepsilon_1\right)\left(n^2 - \varepsilon_1\right) - \varepsilon_2^2\right]^{1/2} \right.$$

$$\left. + \frac{v_\perp}{v_\parallel} \frac{s}{u} \left[\left(\mu_i^2 - \varepsilon_1\right)\left(\mu_i^2 - n^2 - \varepsilon_3\right)\right]^{1/2} \right\} , \tag{4}$$

where J_s and J_s' are the Bessel function of order s and its derivative and n is the parallel index of refraction $n = \mu_i \cos\theta$, where θ is the

angle between the direction of the ambient magnetic field and the wave normal (k vector). The parallel index of refraction at resonance satisfies the relationship

$$n = \frac{c}{v_{\parallel}} \left(1 - \frac{s}{\Omega}\right) , \tag{5}$$

and the quantity u is the gyroradius times the perpendicular component of the k vector:

$$u = \frac{v_{\perp} \Omega}{c} \left(\mu_i^2 - n^2\right)^{1/2} . \tag{6}$$

The solutions are further limited by the following requirements: (1) μ must be real, (2) $n^2 \leq \mu^2$, and (3) the power must be real [i.e., the product of any two of the radicands in Eq. (4) must be greater than or equal to zero]. Those three conditions define allowed and forbidden regions for emission of electromagnetic radiation from a modulated electron beam. The boundaries of those regions are complicated functions of the plasma density and composition, and of the strength of the ambient magnetic field. For combinations of the beam energy and modulation frequency that violate these requirements, the radiated power is set to zero in the following sections.

The e-folding or beam correlation length ℓ in the above is neither known nor is it modeled. In this report, we have divided out the length ℓ and calculated radiation emitted per unit beam length. A method of determining the minimum beam length needed to receive a signal on the ground under the most favorable circumstances of emission and propagation is given in the following subsection.

ROUGH ESTIMATES OF PROPAGATION

The electromagnetic radiation from a modulated electron beam will be detectable at the ground if its power at the receiver is higher than that of the background noise. Using this as a criterion, one can estimate the minimum beam correlation length necessary for a signal to noise

ratio greater than one. The following analysis is based on the linear theory given above.

Implicit in Harker and Banks's[1] theory is that the beam antenna has a gain G that depends on the beam correlation length ℓ. In the case of a beam radiating a power P_r, if the receiver is a distance R from the electron beam, the power/unit area P that reaches the receiver is approximately

$$P = \frac{A}{4\pi R^2} GP_r \ , \tag{7}$$

where A is a transmittance factor that depends on the attenuation of the radiation as it passes through the ionosphere. The values of A reported here are for transmission of the electromagnetic radiation vertically downward and ignore possible spreading, refraction, or reflection of the electromagnetic radiation. The ambient received noise in a particular frequency band is a measured quantity often expressed in the form p_0W_0, where p_0 is measured and is power/unit area per hertz and W_0 is the receiver bandwidth in hertz. The criterion, then, for the desired detectable signal is:

$$P > p_0W_0 \ . \tag{8}$$

In Eq. (7), R is known and P_r is given by Harker and Banks[1] in the form

$$P_r = p_r\ell \ , \tag{9}$$

where p_r is the radiated power per meter of beam correlation length. The transmittance factor for radiation through the entire ionosphere to the ground surface has been calculated by Booker, Crain, and Field[3] as a function of frequency for ambient day and night model ionospheres. We are justified using the results of Booker, Crain, and Field[3] for altitudes greater than 180 km, because most of the attenuation occurs below 180 km altitude.

The beam antenna gain G is

$$G = \frac{P_{max,\ radiated}}{\frac{1}{4\pi}\int P_{radiated}\ \delta\Omega} ,$$

$$\sim \frac{P_r}{\frac{1}{4\pi} P_r 2\pi\ \Delta(\cos\chi)} ,$$

or

$$G \sim \frac{2}{\Delta(\cos\chi)} , \tag{10}$$

where χ is the ray angle, $P_{radiated}$ is the radiated power, and $P_{max,\ radiated}$ is its maximum value. Equation (10) is approximately correct if the functions in the integrand of the power expression [Eq. (15) in Harker and Banks[1] and Eq. (4) above] are slowly varying over the interval where the term [Eq. (20) from Harker and Banks[1]]

$$W(k_\parallel) = \left[\left(\frac{v_\parallel}{\ell}\right)^2 + (\omega - k_\parallel v_\parallel - s\omega_{ce})^2\right]^{-1} , \tag{11}$$

is appreciable. Here $v_\parallel$ is the component of the electron velocity along the magnetic field, ω is the radiation frequency, $k_\parallel$ is the component of the wave vector along the magnetic field, s is the mode number, and ω_{ce} is the electron cyclotron frequency. The half value width of the function $W(k_\parallel)$ is

$$\Delta k_\parallel = \frac{2}{\ell} . \tag{12}$$

Using the following for the parallel index of refraction:

$$n = \frac{k_\parallel c}{\omega} ,$$

one can write

$$\Delta(\cos\chi) \simeq \Delta n \frac{d(\cos\chi)}{dn}$$

$$= \Delta n \frac{d\theta}{dn} \sin\chi \frac{d\chi}{d\theta}$$

$$\simeq \frac{2}{\ell}\left(\frac{c}{\omega}\frac{d\theta}{dn}\right) \sin\chi \frac{d\chi}{d\theta} , \qquad (13)$$

where θ is the angle of the k vector with respect to the magnetic field, and Eq. (12) has been used. The functions $d\theta/dn$ and $d\chi/d\theta$ are complicated functions of the ray angle χ, wave normal angle θ, radiation frequency ω, and parallel index of refraction n. The function $d\theta/dn$ is the inverse of Eq. (34) found in Harker and Banks[1]; $d\chi/d\theta$ is defined in Eq. (38) in Harker and Banks.[1]

Equation (8) can now be written as

$$\frac{A}{4\pi R^2} \frac{\ell^2 p_r}{\frac{c}{\omega}\frac{d\theta}{dn} \sin\chi \frac{d\chi}{d\theta}} > p_0 W_0 ,$$

or

$$\ell^2 > \ell_0^2 = \frac{4\pi R^2}{A}\left(\frac{p_0}{p_r}\right)\left(\frac{c}{\omega}\frac{d\theta}{dn}\right)\left(\sin\chi \frac{d\chi}{d\theta}\right) W_0 . \qquad (14a)$$

If the gain predicted by Eqs. (4) and (7) is unreasonably high (greater than 300 or 10^3, for example), experience suggests that an upper limit G_0 be artificially imposed. Equation (7) or (14a) then becomes

$$\ell_0 = \frac{4\pi R^2}{A}\left(\frac{p_0}{p_r}\right)\frac{1}{G_0} . \qquad (14b)$$

Equation (14a) or (14b) gives the absolute minimum beam correlation length ℓ_0 for which a signal may be detectable at a distance R away from the electron beam. The value ℓ_0 gives a lower bound to the correlation length. Because of the numerous idealizations in the beam and propagation physics (all of which ignore effects that degrade the signal), lengths greater than ℓ_0 may be needed. However, beams shorter than ℓ_0 will not suffice. Therefore, if ℓ_0 is short, the beam probably can radiate sufficient energy for detection before it disintegrates, but we have no assurance of that. For combinations of parameters that cause ℓ_0 to be very long, the experiment may not be feasible at all.

PRESENTATION OF CALCULATIONAL RESULTS

The important findings are displayed in graphical form in the following sections. The graphs show the power radiated per unit length of the electron beam, plotted against the kinetic energy of the electron beam and its modulation frequency. Many of the graphs take two forms. The first form is a three-dimensional plot showing the five highest orders of magnitude for the radiated power, which is useful for easily identifying and scanning the region where the peak power is generated. Figure 1 is an example of that kind of plot. The second form is a contour plot of the power, which is useful for reading numerical values of the power and for identifying null or forbidden regions where no power at all is radiated. Figure 2 is an example of the contour plots. The contours in all the figures are labeled by the common logarithm of the radiated power, in watts per meter. Note that the contour labels in the region below 0.1 kHz in Fig. 2 are preceded by a minus sign, whereas above 10 kHz many contours are positive.

In some regions the radiated power falls quickly to zero as the modulation frequency or the beam energy changes. These regions appear on the contour plots as closely spaced parallel lines that are not labeled because of lack of space near the contours. Such a region appears on Fig. 2 in the rectangle between 10 and 1000 kHz and between 60 and 100 keV. On some of the figures, small unlabeled diamonds appear in regions otherwise devoid of radiation. These indicate the existence of narrow regions of allowed radiation that were not well

mapped by the coarse grid calculated for the contour plot. Such regions are not of interest in beam experiments, as will be shown in Sec. III.

Each figure has additional labels that characterize the electron beam and the ionospheric plasma. The pitch angle of the beam is α in degrees, the beam power is P_{BEAM} in watts, P labels the radiation harmonic plotted, s labels the mode, ω_{CE} is the angular electron plasma frequency in radians per second, Ω_{pi} is the ratio of the ion plasma frequency to the electron plasma frequency, and I_B in amperes, which appears on some plots, is the beam current.

The dispersion relation that determines the magnitude, direction, and polarization of the electromagnetic radiation has, in general, two solutions at a given frequency. Because the propagation characteristics of the two solutions differ, each is treated separately in most of the graphical presentations in this report. Each curve is labeled "root 1" or "root 2" according to whether it corresponds to one or the other of the solutions. Figures 1 and 2 are root 1 solutions and Figs. 3 and 4 are root 2 solutions. It is a general characteristic of the root 1 solutions that the highest powers are radiated above the lower hybrid frequency and below the electron gyrofrequency (from 7.5 kHz to 1.3 MHz in Figs. 1 and 2). The three-dimensional and contour plots look like a sloping mesa or plateau in that region, and for that reason the region is called the "central plateau" in the sections that follow. Figures 3 and 4 show that the root 2 solutions tend to have more structure than the root 1 solutions and fill up regions forbidden to root 1, although they have power levels generally much lower than the root 1 levels. The specific trends will be analyzed in more detail in the following sections.

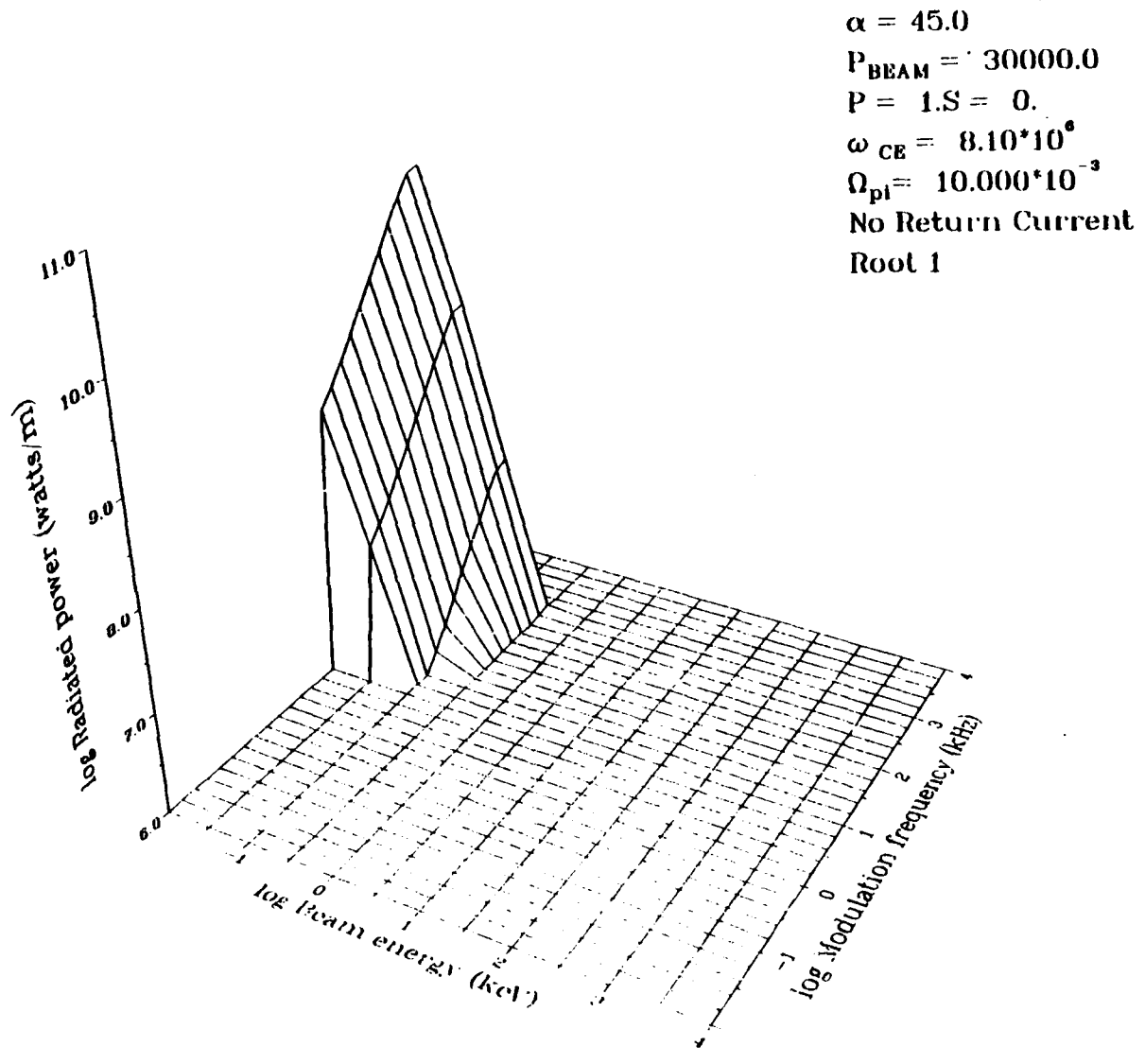

Fig. 1--Daytime radiated power at 100 km for 45 deg pitch angle (root 1, future gun).

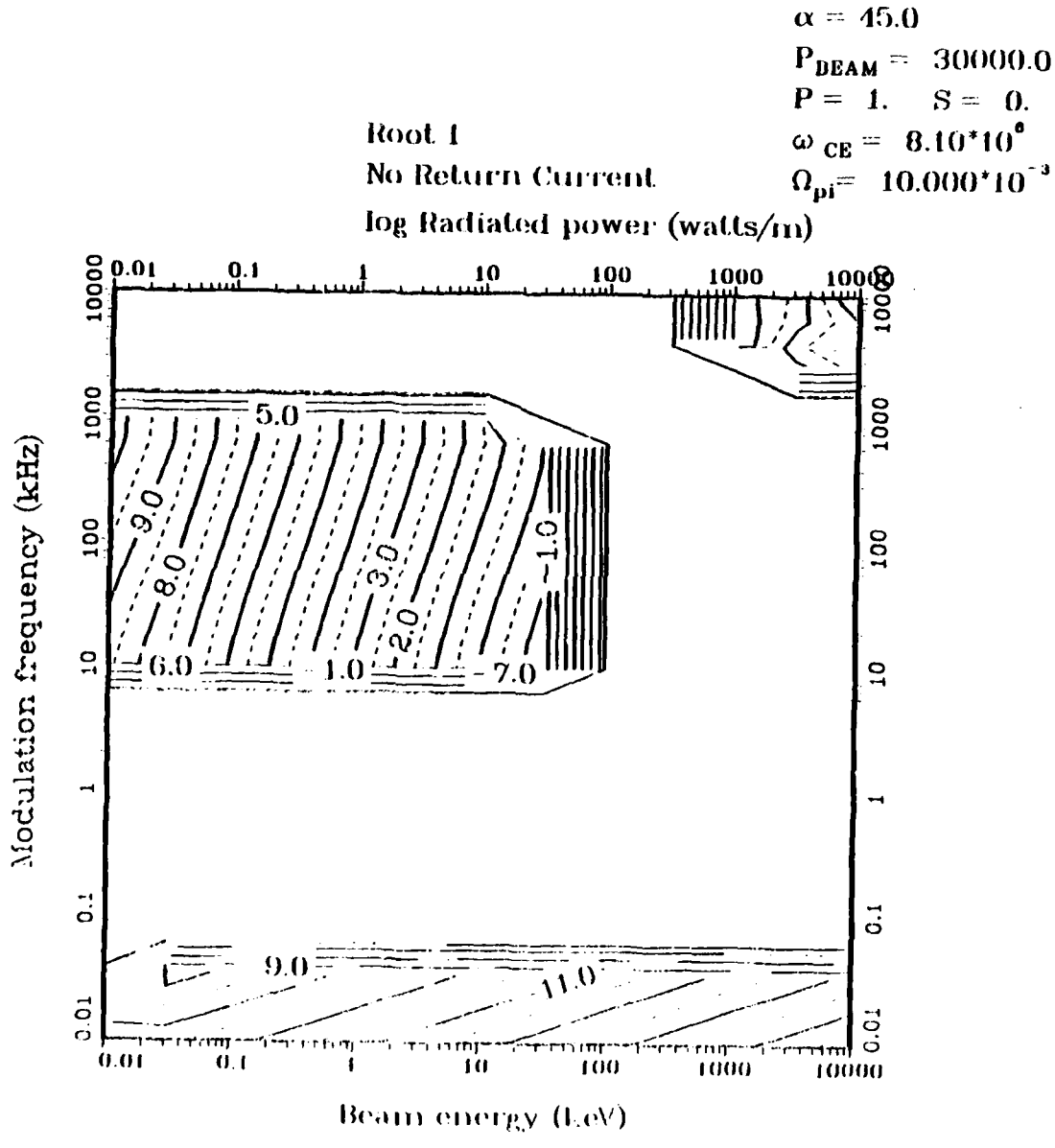

Fig. 2--Contours of daytime radiated power at 100 km for 45 deg pitch angle (root 1, future gun).

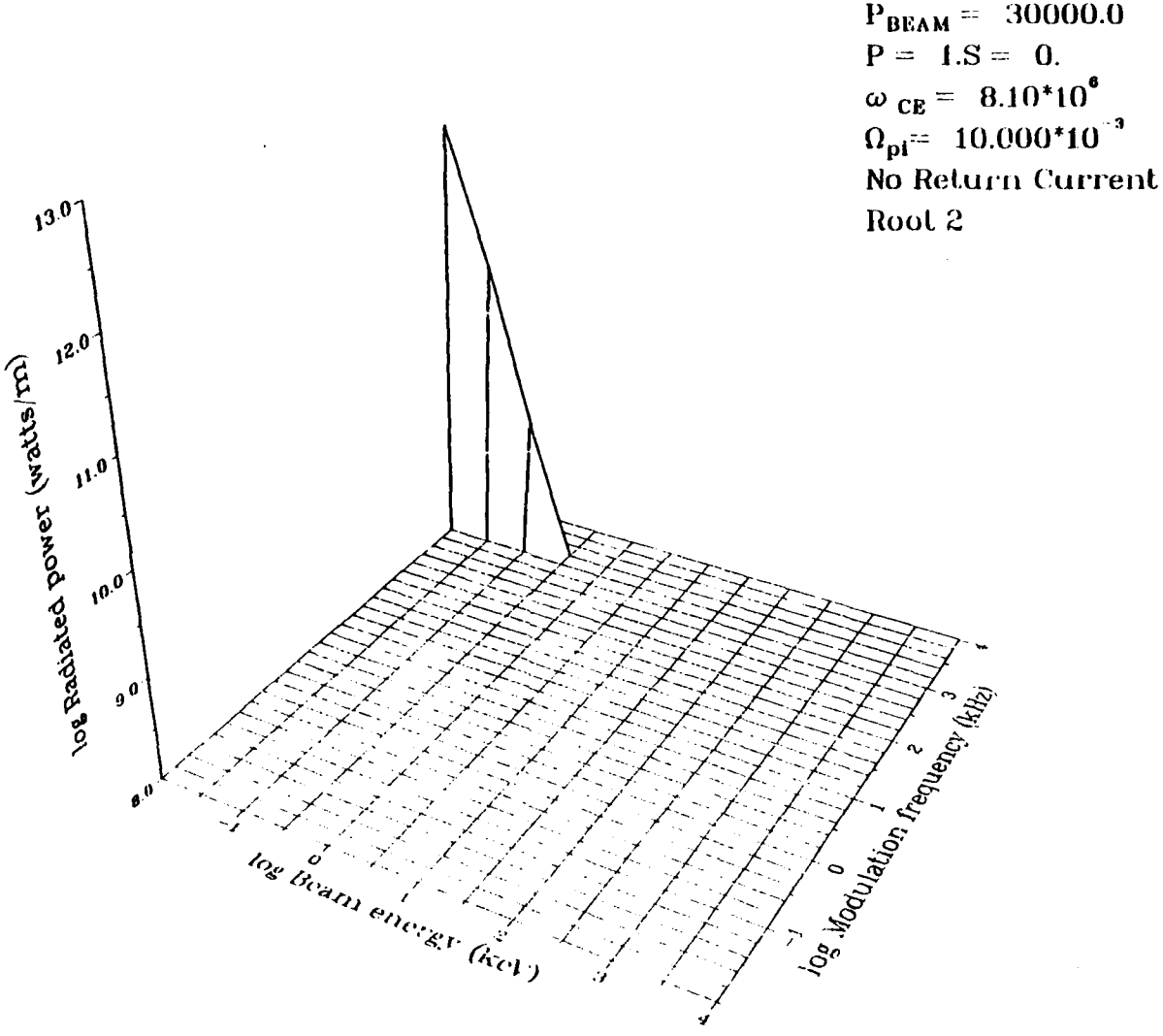

Fig. 3--Daytime radiated power at 100 km for 45 deg pitch angle (root 2, future gun).

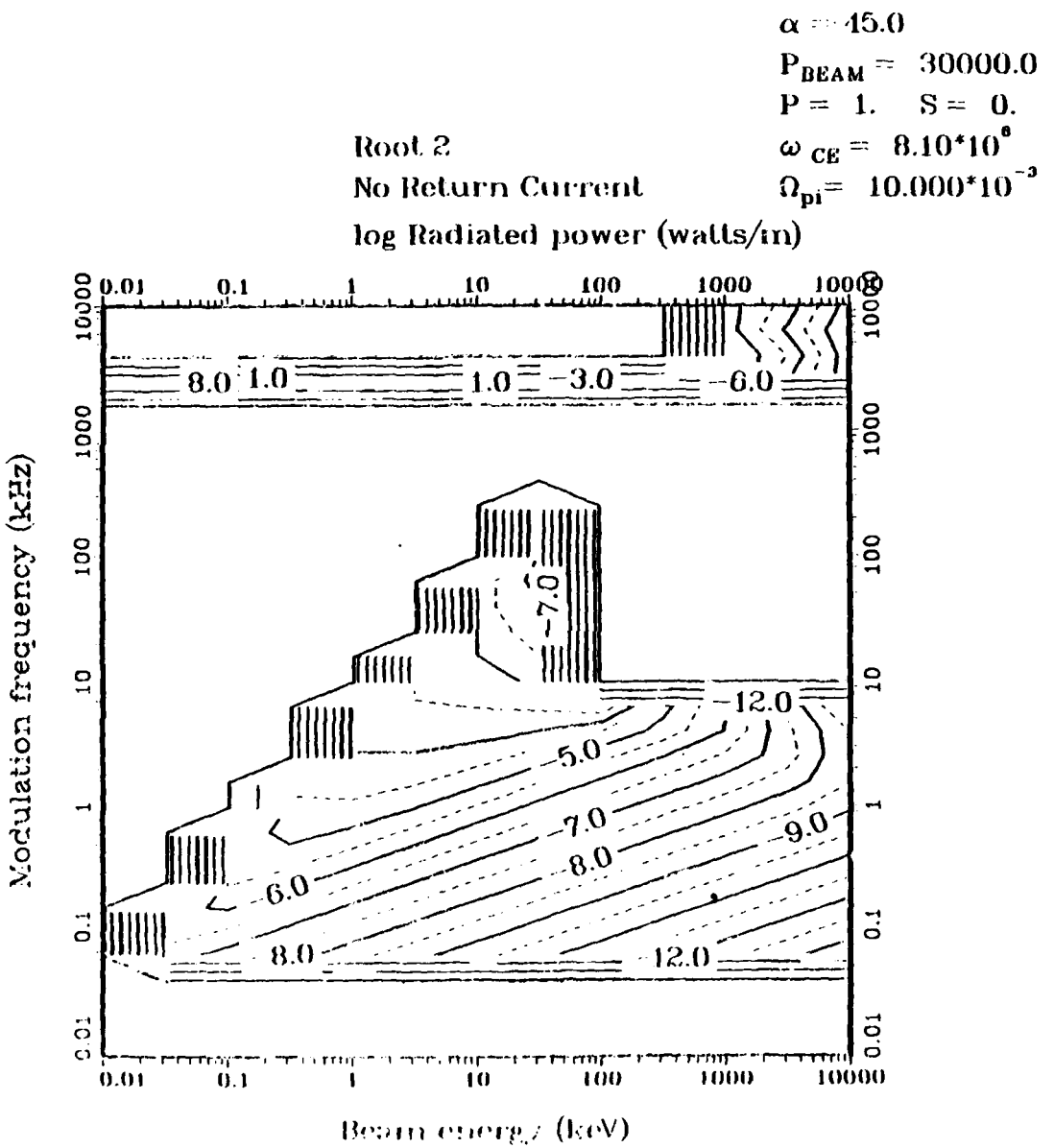

Fig. 4--Contours of daytime radiated power at 100 km for 45 deg pitch angle (root 2, future gun).

III. FUTURE GUN

CHOICE OF PARAMETERS

The parameter studies for the future gun were based on the observation[4] that the most powerful nonrelativistic electron gun flown on a rocket to date delivered 30 kW the entire duration of the flight (6 min). The highest current achieved so far is about 100 A. For a given voltage, the current from a cathode is space-charge limited, a relation that is often expressed in terms of the perveance p_g of the gun:

$$p_g = \frac{I_{MAX}}{V^{3/2}} , \tag{15}$$

where I_{max} is the maximum current that can be extracted at voltage V. Higher currents can be achieved, however, by increasing the number of cathodes, changing the cathode geometry, or by using several guns in parallel.

It is not clear what the lower limit of usable gun voltages are, but a Japanese sounding rocket, K-9M-41, successfully injected thermal (0.1 eV) electron beams into the ionosphere.[5] Tsutsui, Matsumoto, and Kimura[5] did not give the beam currents. The lower limit on the beam energy is limited by the power desired in the beam. To obtain, for example, 1 kW in the beam, a 10 V beam would require 100 A current. But typical electron gun perveances are on the order of a few times 10^{-6} $(A/V^{3/2})$, which implies that 10^5 to 10^6 cathodes are needed for a 10 V gun to deliver 1 kW into the electron beam. Because this is an unreasonable number of cathodes, and although we have no reason to suspect (except for intuition, based on terrestrial communications experience) that 1 kW beam energy is essential to communications, we have chosen 10 eV as the lower limit to the beam energy in our analysis.

The upper limit to achievable voltages is in the relativistic range. Our analysis is inherently nonrelativistic, however, so its usefulness is questionable much beyond 50 keV. Nonetheless, we chose 10^7 eV as the top end of the parameter study--not because we deemed

the results at such high energies acceptable, but to make trends stand out more clearly on the graphs. As the pitch angle of electron injection and the electron cyclotron frequency are varied, features of the radiated power shift along the beam energy axis. Thus, power peaks that appear in the nonrelativistic theory at high beam energy move to lower beam energies as emission parameters change.

The analysis of the future gun was done assuming a rocket flight launched at White Sands, New Mexico. The radiation was calculated for electron beam emission into the ionosphere at altitudes of 100, 200, 300, and 400 km for day and night flights. Table 1 summarizes the ionospheric parameters we assumed in the calculations. We chose pitch angles of 0.1, 45, and 89.9 deg.

One set of calculations was performed assuming a constant beam power of 30 kW at all beam voltages. The other assumed a constant current of 100 A at all beam voltages. In most of the figures, we show only the power that goes into radiation at the fundamental frequency. This is most of the power that goes into the radiation for a square wave modulated beam at VLF. It is perhaps 1/10 to 1/50 of the total power that goes into the radiation at lower frequencies for a square wave beam (the rest goes into higher harmonics in the allowed radiation region). For a sinusoidally modulated beam, the fundamental represents all the radiated power.

Calculations show that for much of the parameter space the theoretical index of refraction at resonance is very high (in some regions the resonant index of refraction is greater than 10^6 or 10^9) for radiation into the regular, anomalous, and higher-order cyclotron modes. In those regions the resonant indices are much larger than those for radiation into the Cerenkov mode; therefore, total internal reflection of the signal will be more likely for cyclotron modes than for Cerenkov modes. Radiation in the Cerenkov mode may therefore dominate the radiation that actually reaches the ground. For that reason, the higher-order modes are not considered except in a sample calculation at 200 km, which is discussed later.

This calculation of radiated power ignores all warm plasma and collisional effects. Those effects will reduce the predicted radiation

TABLE 1.

Ionospheric Parameters for Future Gun Calculation.

Altitude (km)	Electron Gyrofrequency (Hz)	Ion Gyrofrequency (Hz)	Time	Electron Plasma Frequency (Hz)	Ion Plasma Frequency (Hz)	Lower Hybrid Frequency (Hz)
100	1.29×10^6	43.8	Day	2.2×10^6	1.29×10^4	7.52×10^3
			Night	2.69×10^6	1.57×10^3	
200	1.23×10^6	41.7	Day	6.02×10^6	3.52×10^4	7.16×10^3
			Night	1.13×10^6	6.61×10^3	
300	1.17×10^6	39.7	Day	1.02×10^7	5.96×10^4	6.82×10^3
			Night	4.11×10^6	2.40×10^4	
400	1.11×10^6	37.7	Day	8.98×10^6	5.25×10^4	6.47×10^3
			Night	4.21×10^6	2.46×10^4	

at low altitudes (100 km) and will reduce the predicted resonant values of the refractive index for cyclotron emission,

MAGNITUDE OF RADIATED POWER

Figures 1 through 32 show the radiated power into the Cerenkov mode at the fundamental frequency for the four altitudes considered here, for day and night flights, and for constant beam power. In all those figures, the pitch angle has been set to 45 deg. Figures 1 through 4 are for a day flight at 100 km, and Figs. 5 through 8 are for night at 100 km. Figures 9 through 12 are for a day flight at 200 km, and Figs. 13 through 16 are for night at that altitude. Similarly, Figs. 17 through 20, and 21 through 24 are for 300 km, day and night, respectively, and Figs. 25 through 28, and 29 through 32 are for 400 km, day and night, respectively.

Several important conclusions can be drawn from these figures. There are regions in parameter space where there is no radiation at all, and the locations of those regions change with altitude and depend on the time of day. The easiest way to get an overview of those dependences is to look at contours of the total radiation summed over both roots of the dispersion relation. Figures 33 and 34 show contours of total radiated power at 100 and 400 km, respectively, during the day. Figure 33 shows that at 100 km during the day there are three regions in which there is no radiation: above approximately 4 MHz and less than 300 keV; between 10 kHz and 2 MHz and above 100 keV; and a triangular region less than 7 kHz and less than 500 eV. At 400 km, the first region increases in size and joins the second, so there is hardly any radiation for beam energies above 1.5 MHz, and none from 10 kHz to 1 MHz for beam energies above 3 keV. The third region almost disappears at 400 km, though a remnant of it exists near 8 kHz below 100 eV.

The same effect occurs at night (as Figs. 35 and 36 show) although the limits are pushed to higher beam energies. It is significant that at night the forbidden region at the low frequencies is much larger below 1 kHz than it is during the day.

In general, the structures that are displayed in the figures move to the lower beam energies as the altitude increases. (There are also

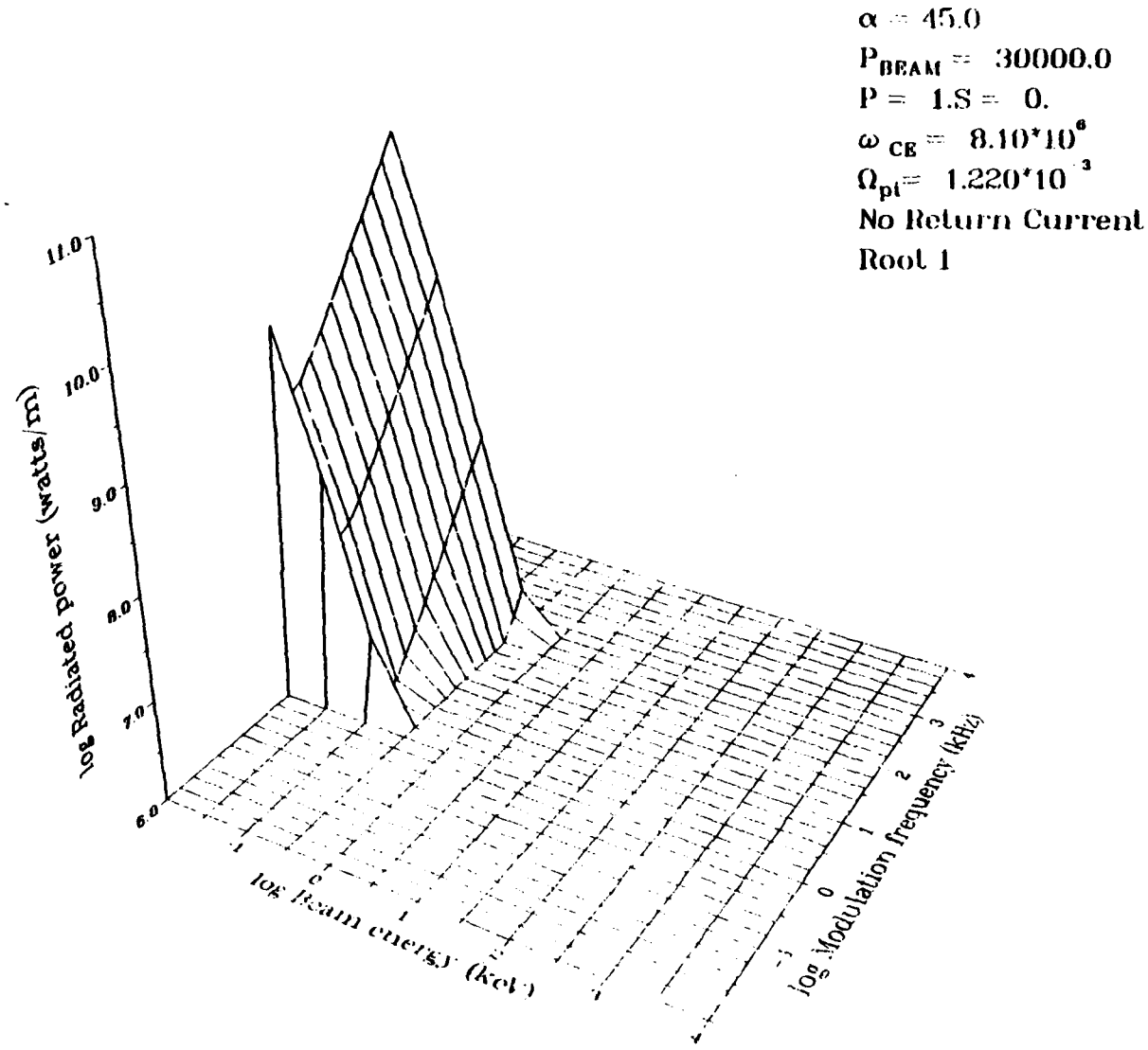

Fig. 5--Nighttime radiated power at 100 km for 45 deg pitch angle (root 1, future gun).

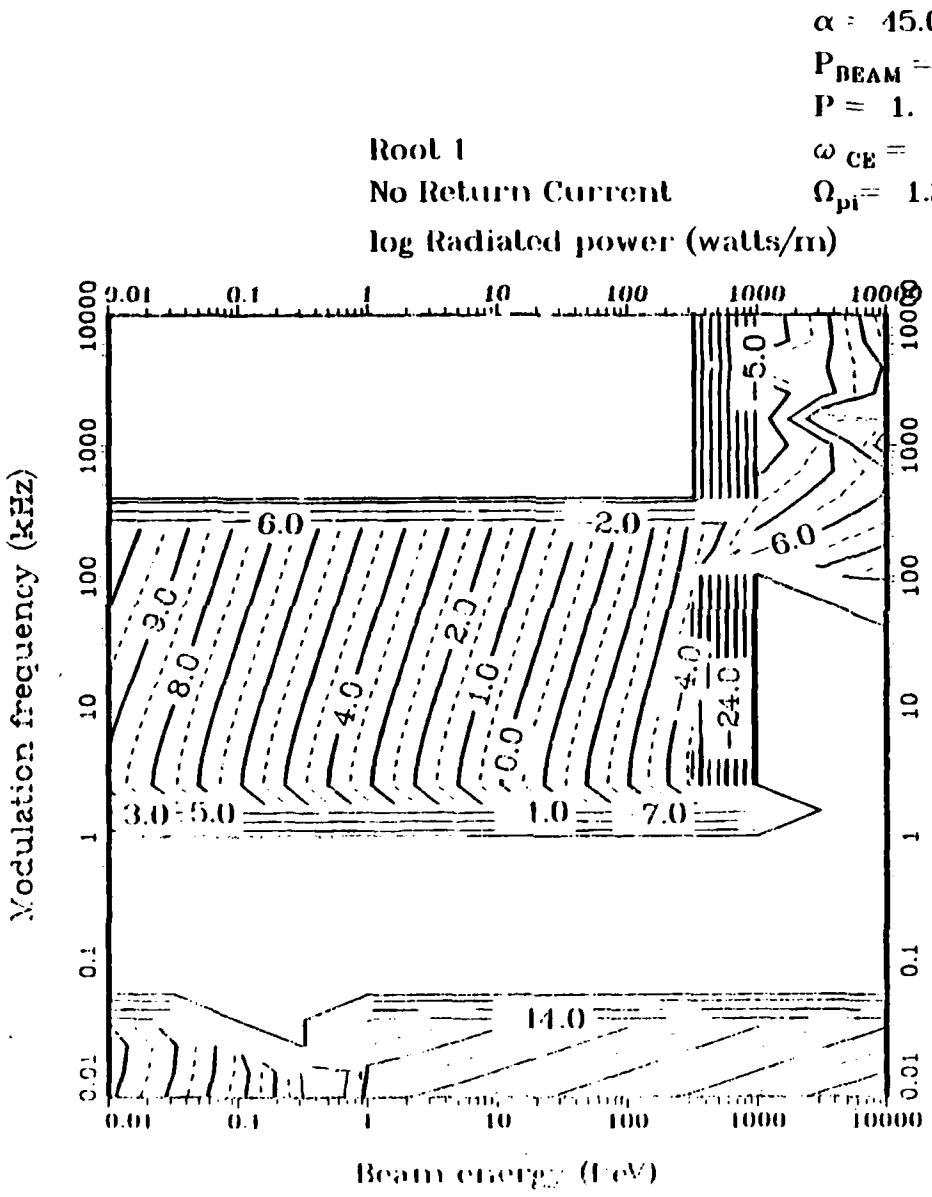

Fig. 6--Contours of nighttime radiated power at 100 km for 45 deg pitch angle (root 1, future gun).

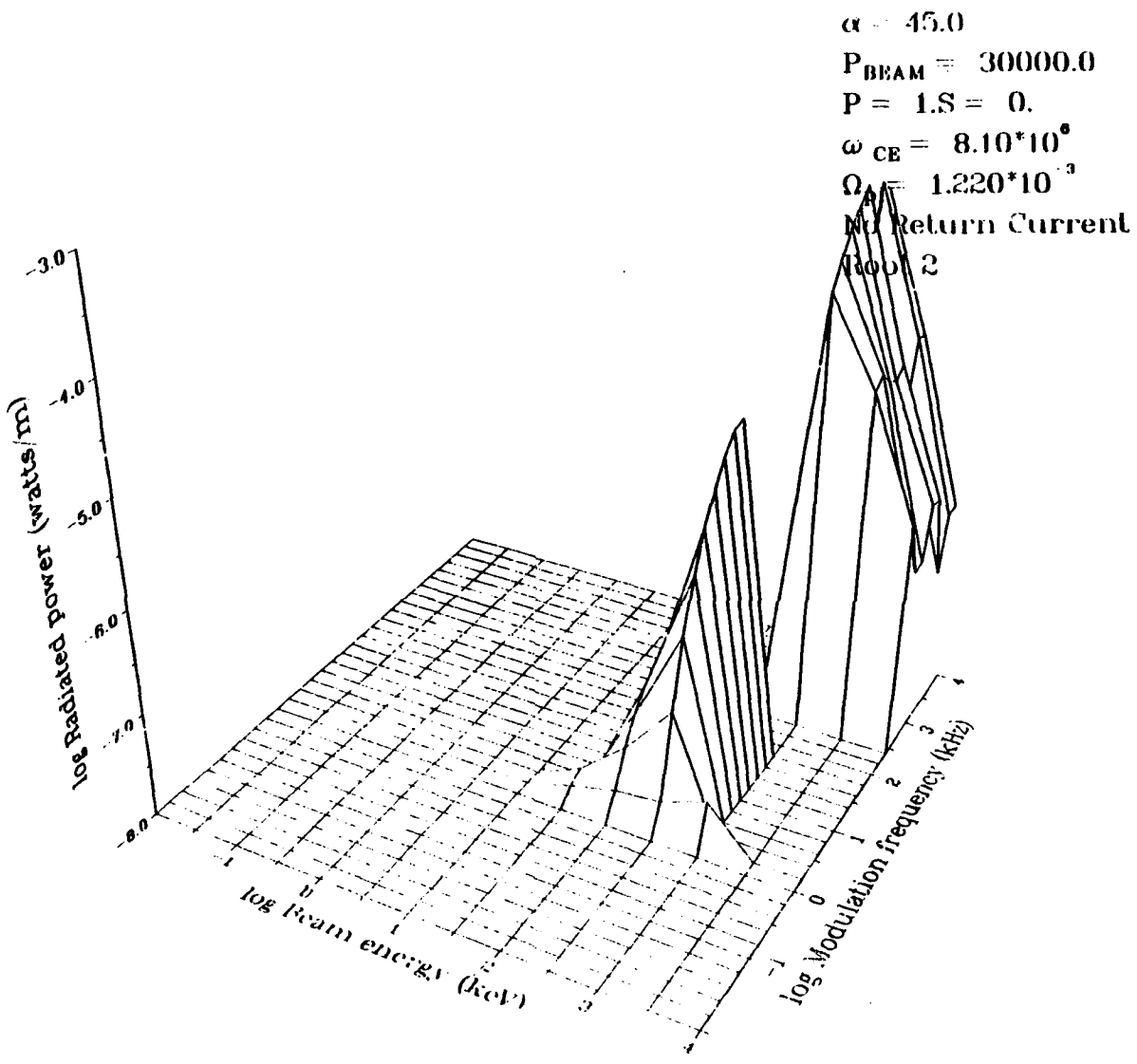

Fig. 7--Nighttime radiated power at 100 km for 45 deg pitch angle (root 2, future gun).

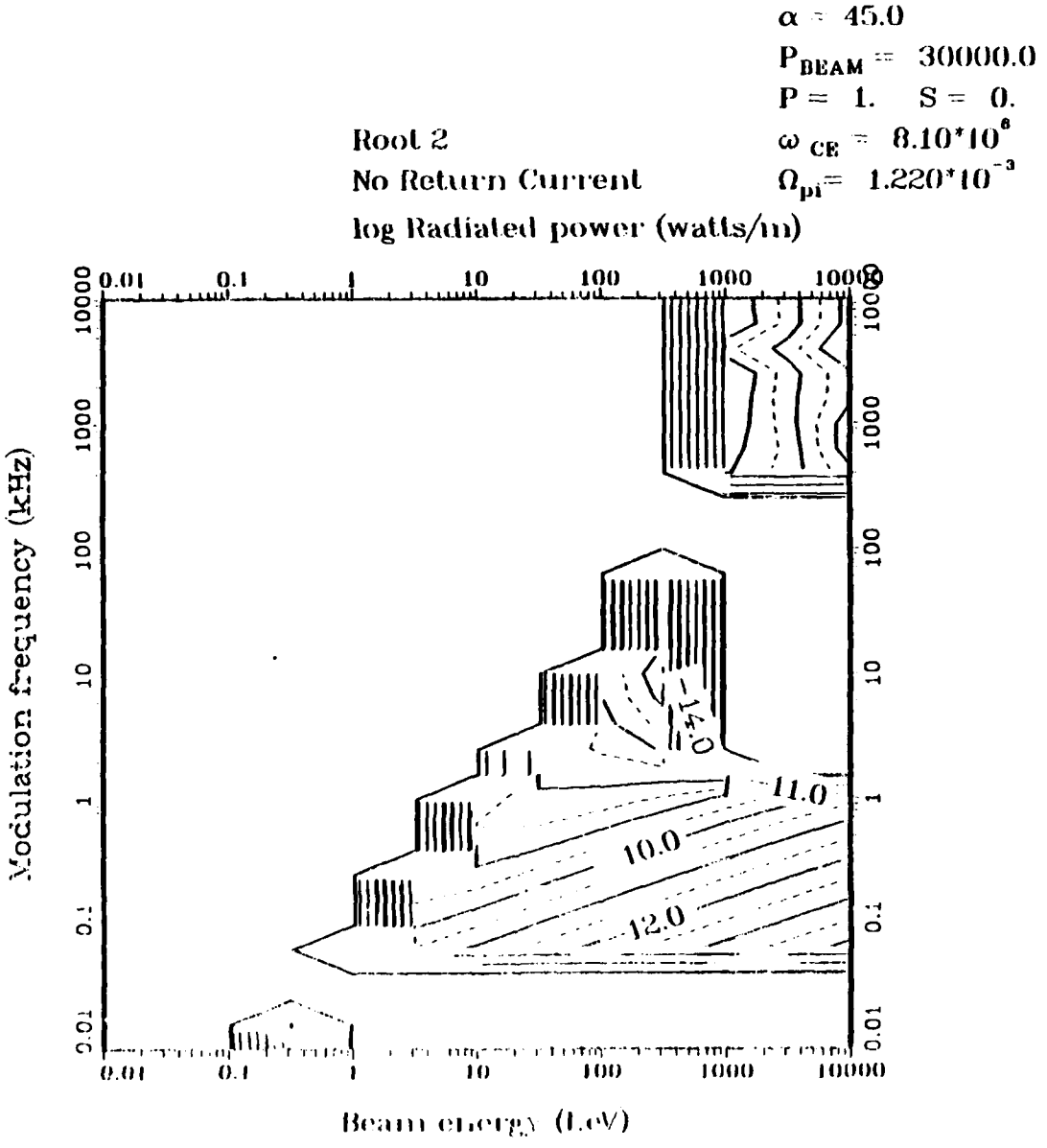

Fig. 8--Contours of nighttime radiated power at 100 km for 45 deg pitch angle (root 2, future gun).

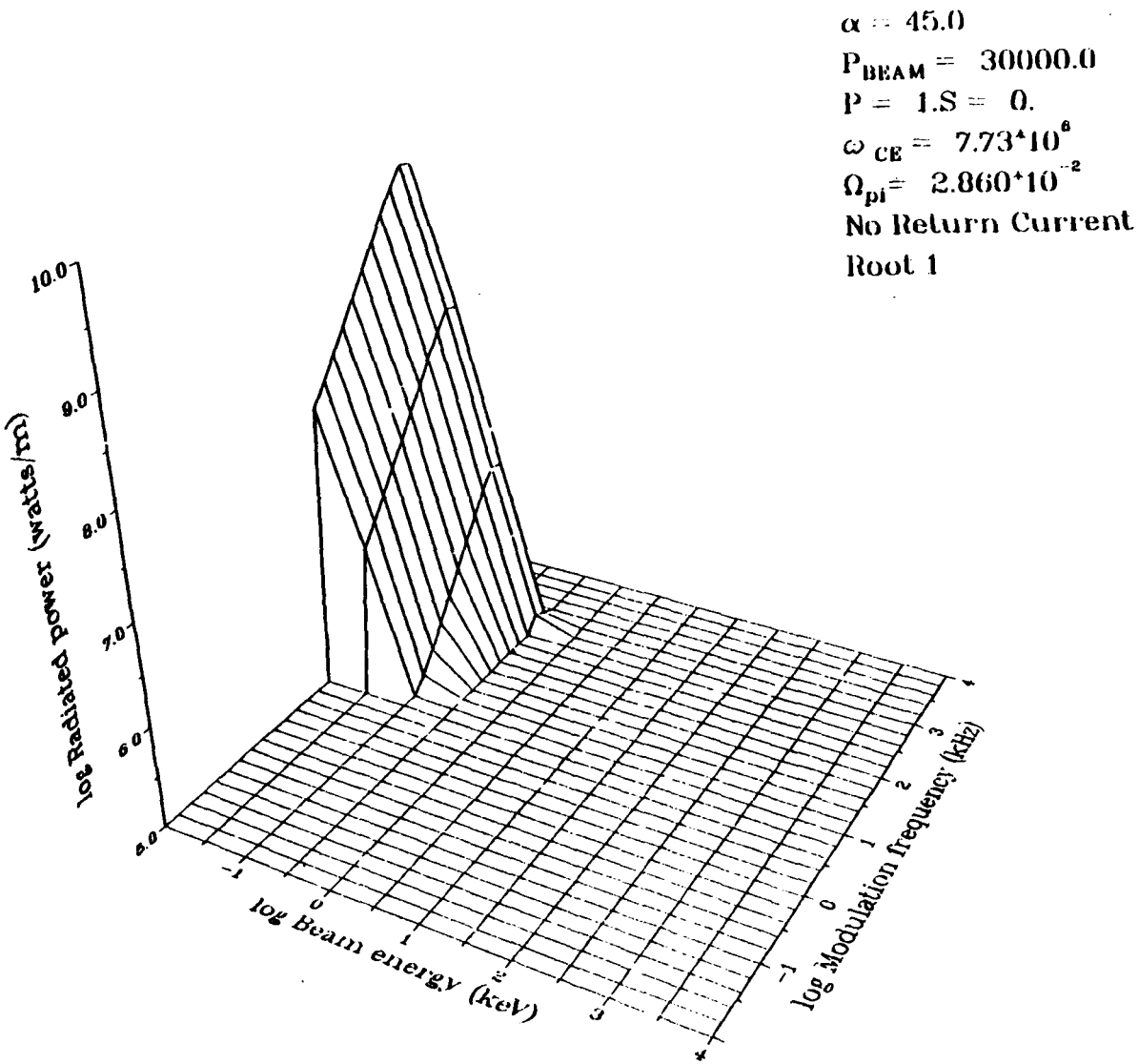

Fig. 9--Daytime radiated power at 200 km for 45 deg pitch angle (root 1, future gun).

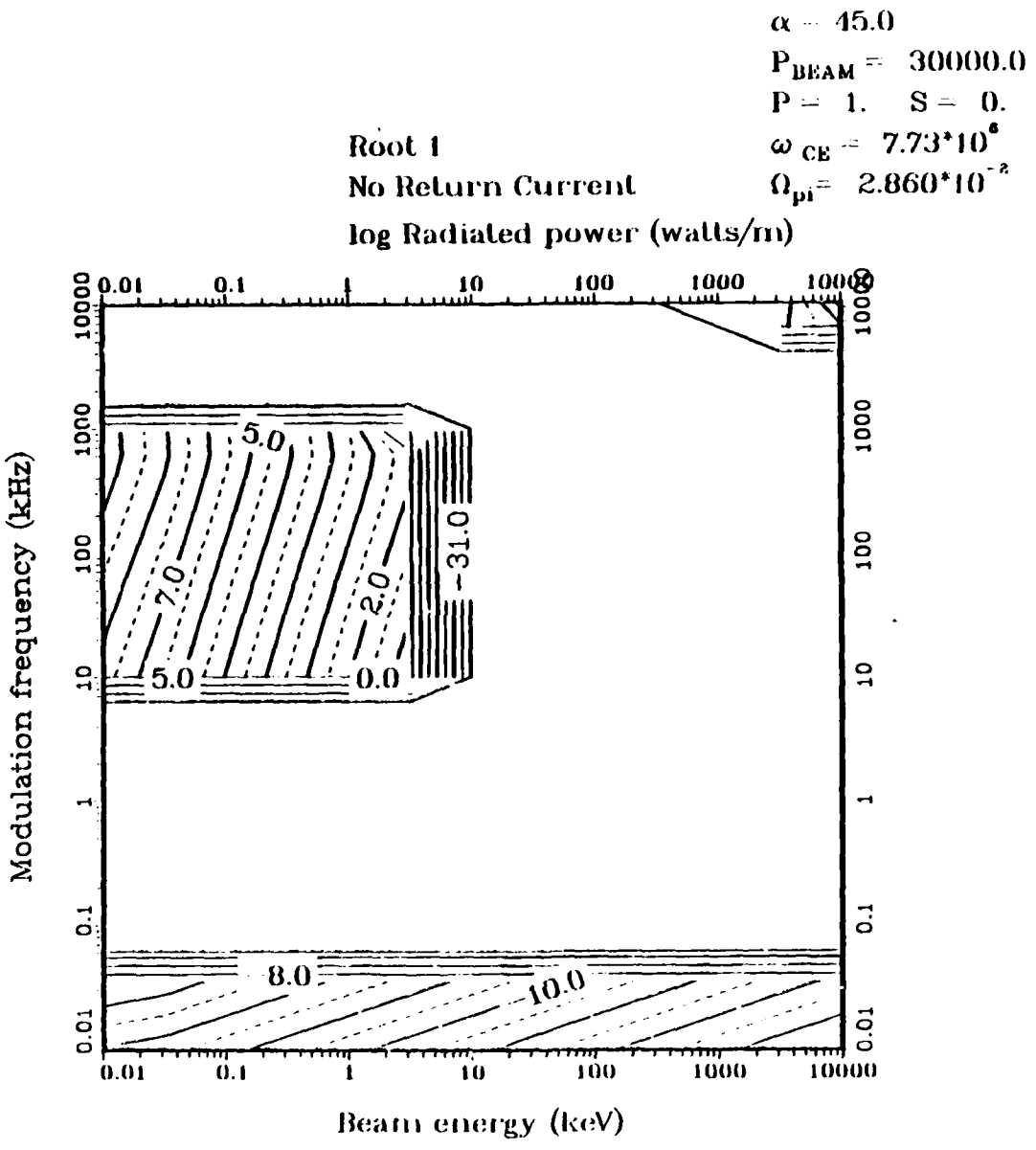

Fig. 10--Contours of daytime radiated power at 200 km for 45 deg pitch angle (root 1, future gun).

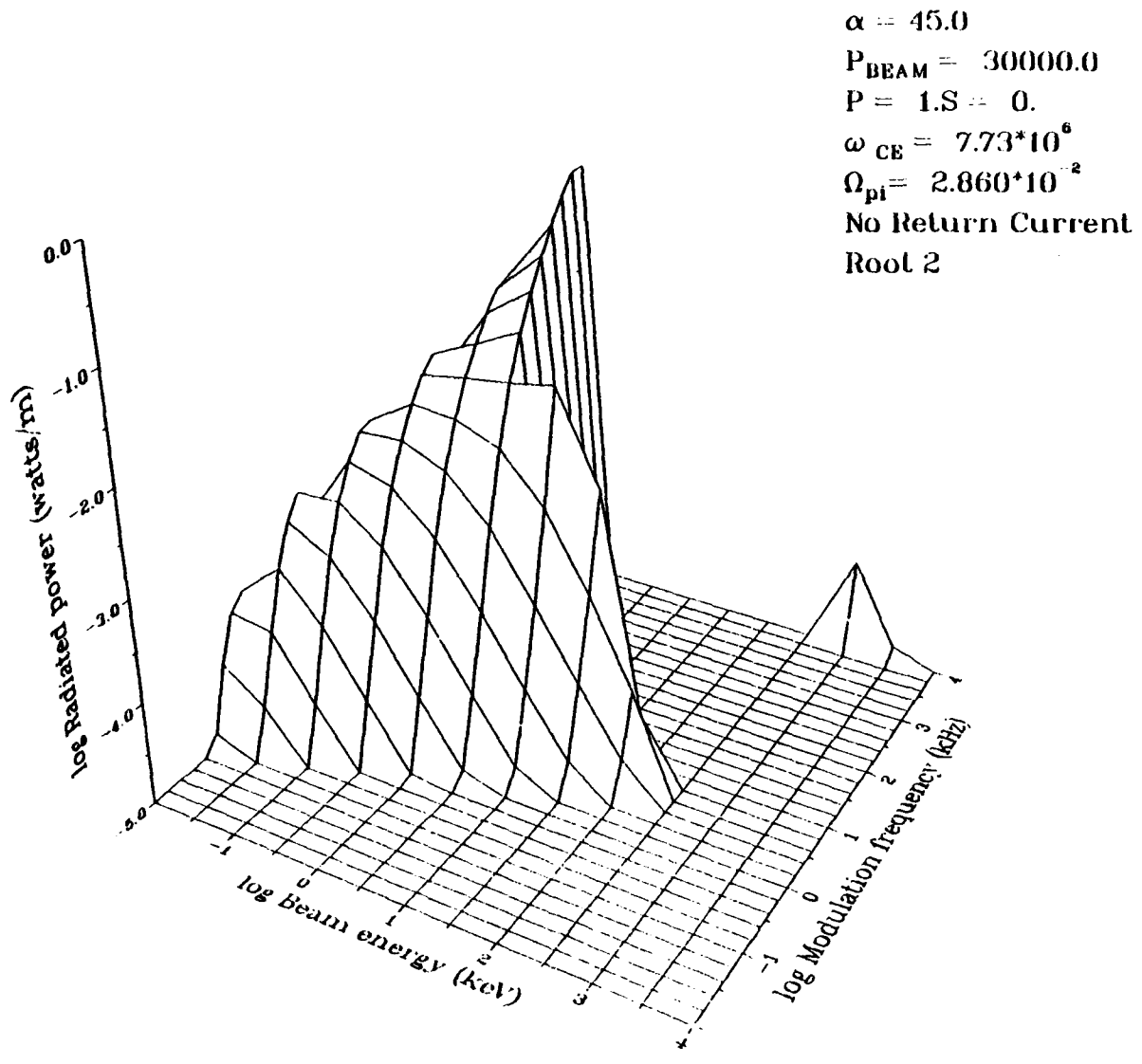

Fig. 11--Daytime radiated power at 200 km for 45 deg pitch angle (root 2, future gun).

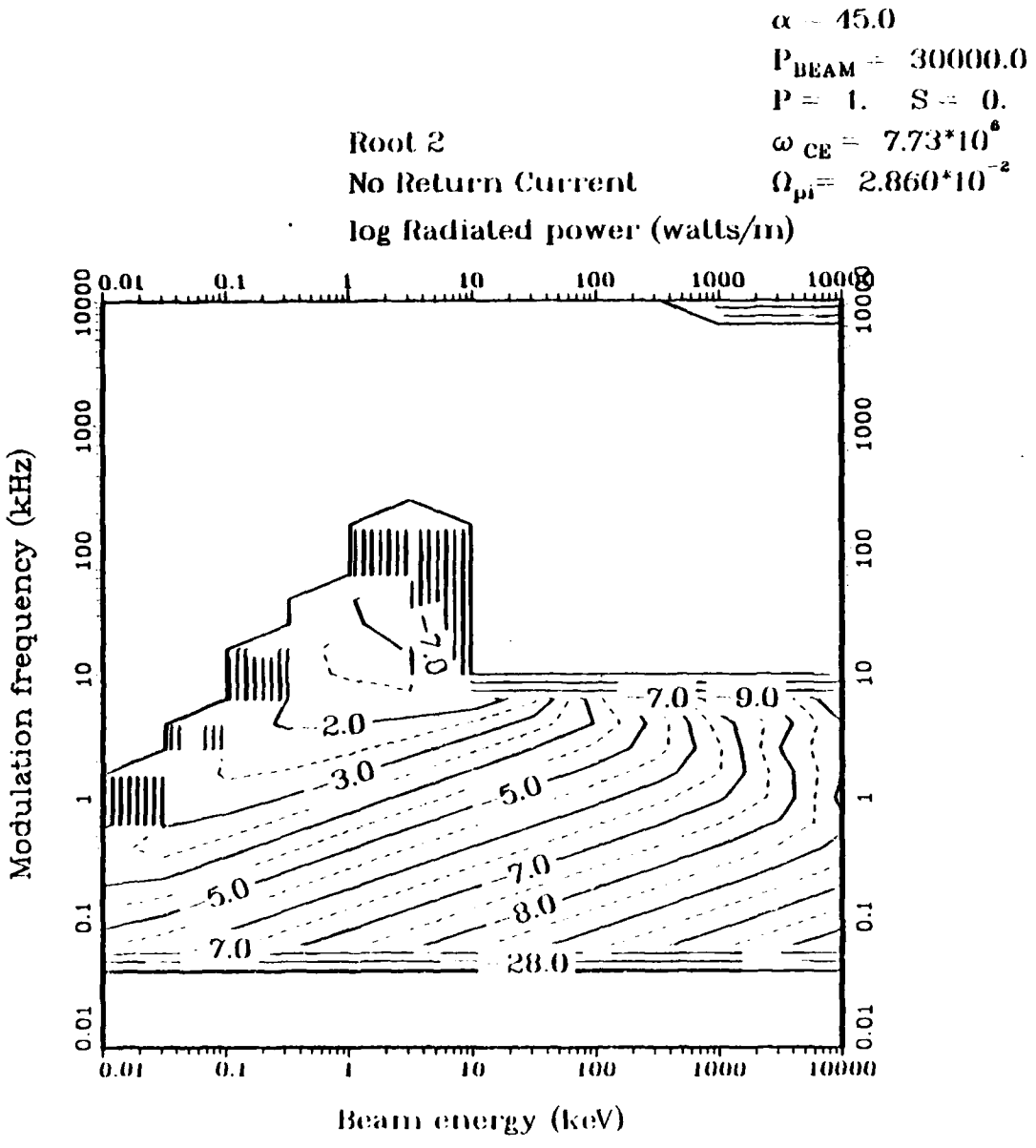

Fig. 12--Contours of daytime radiated power at 200 km for 45 deg pitch angle (root 2, future gun).

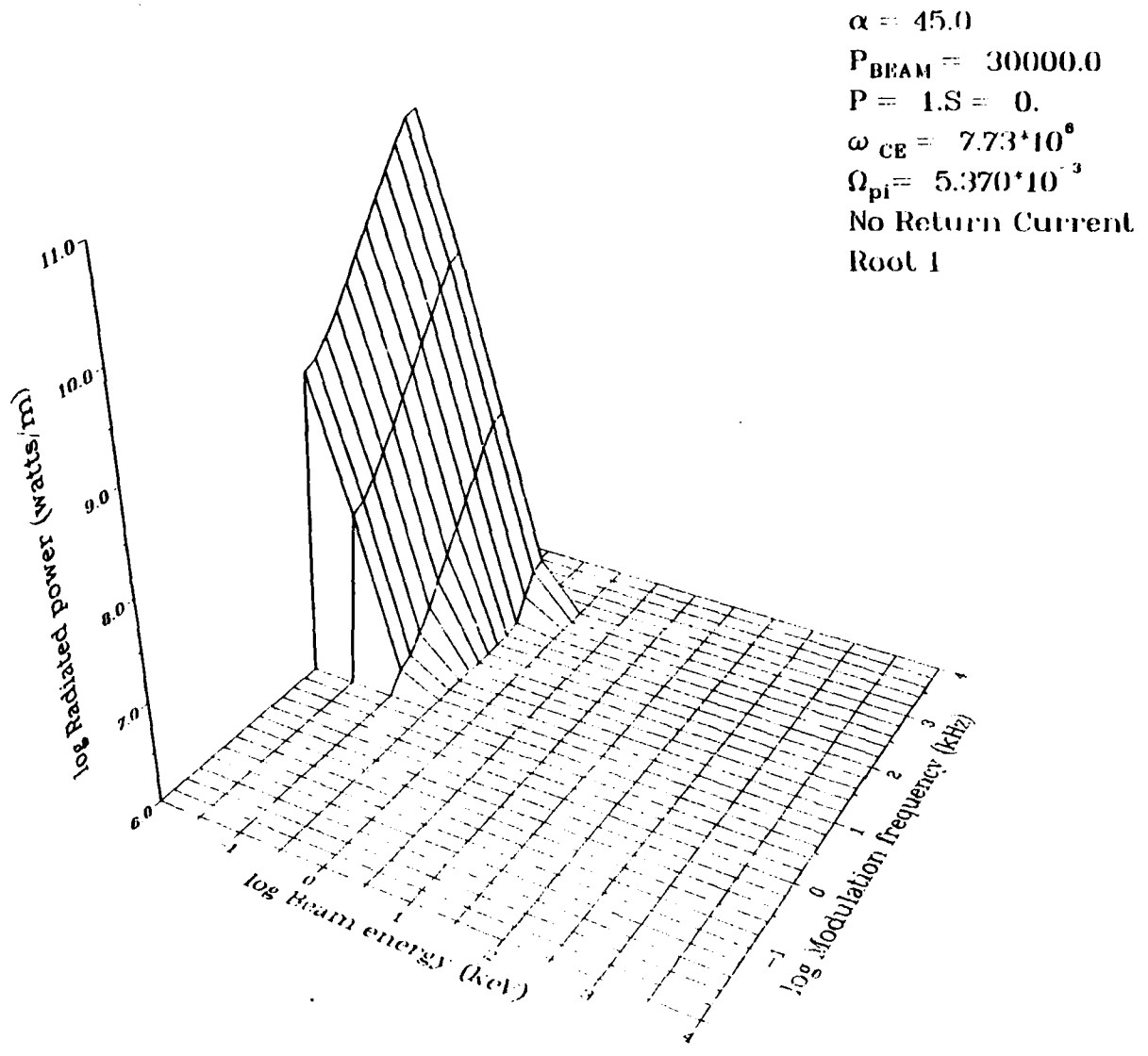

Fig. 13--Nighttime radiated power at 200 km for 45 deg pitch angle (root 1, future gun).

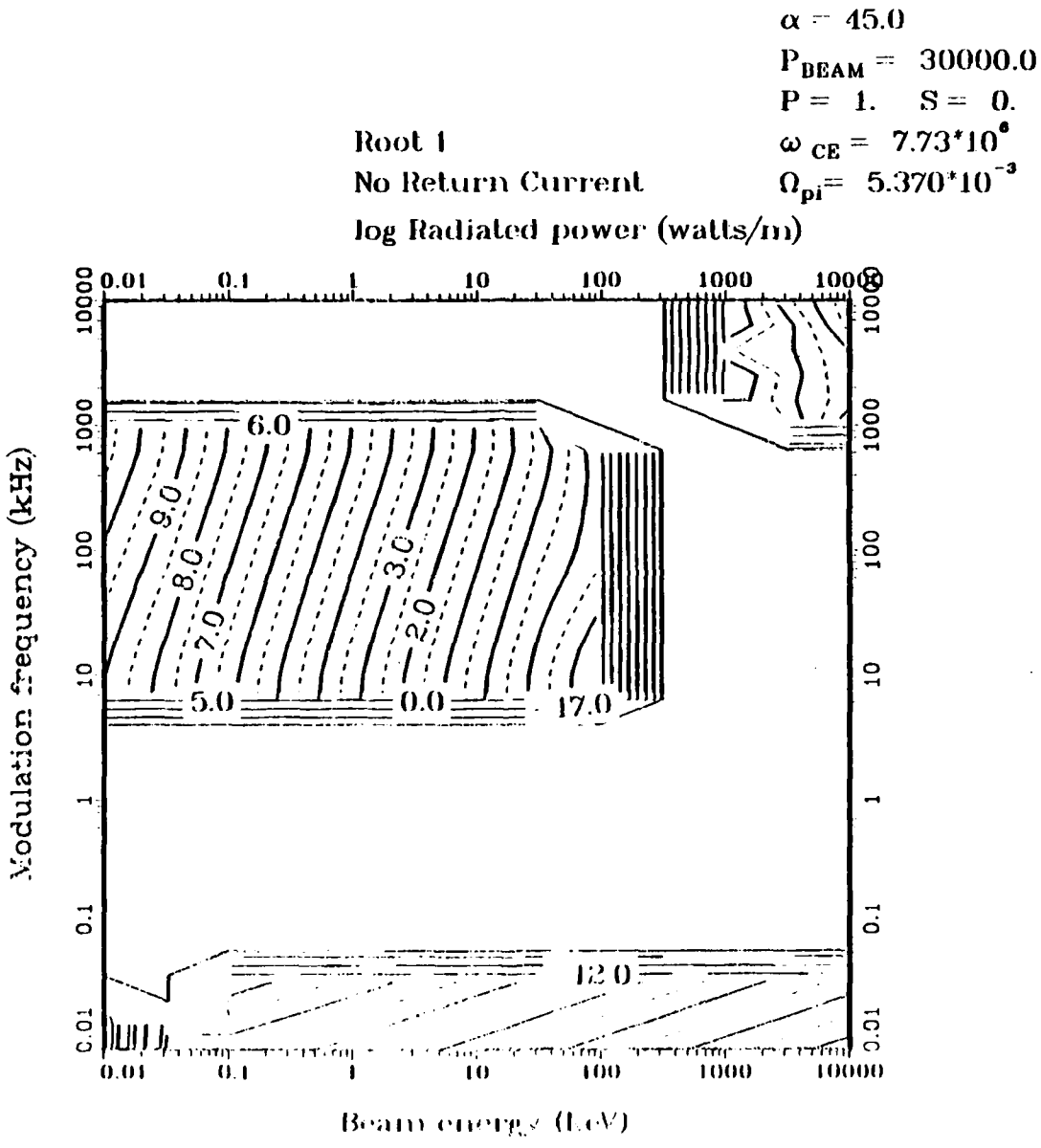

Fig. 14--Contours of nighttime radiated power at 200 km for 45 deg pitch angle (root 1, future gun).

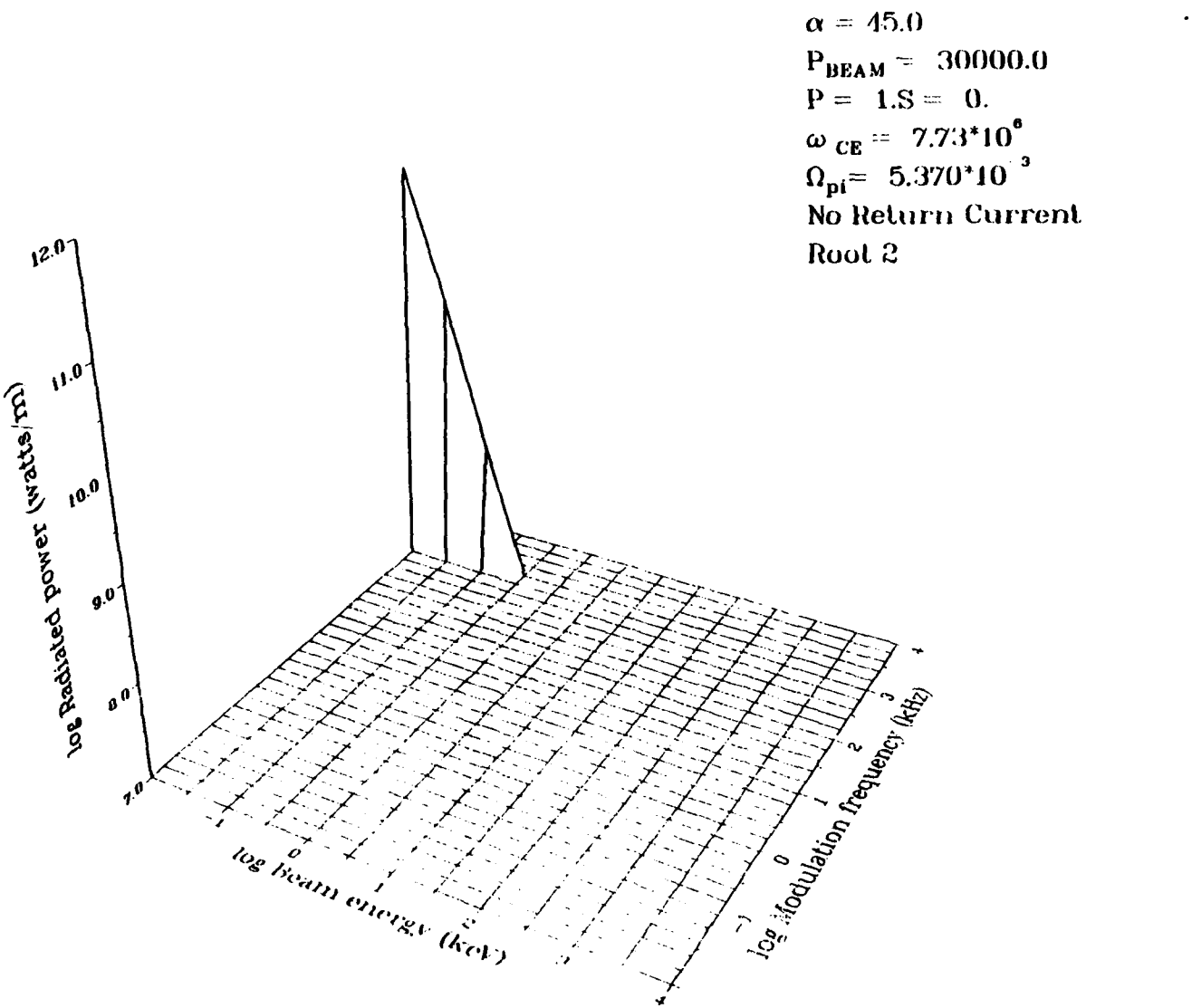

Fig. 15--Nighttime radiated power at 200 km for 45 deg pitch angle (root 2, future gun).

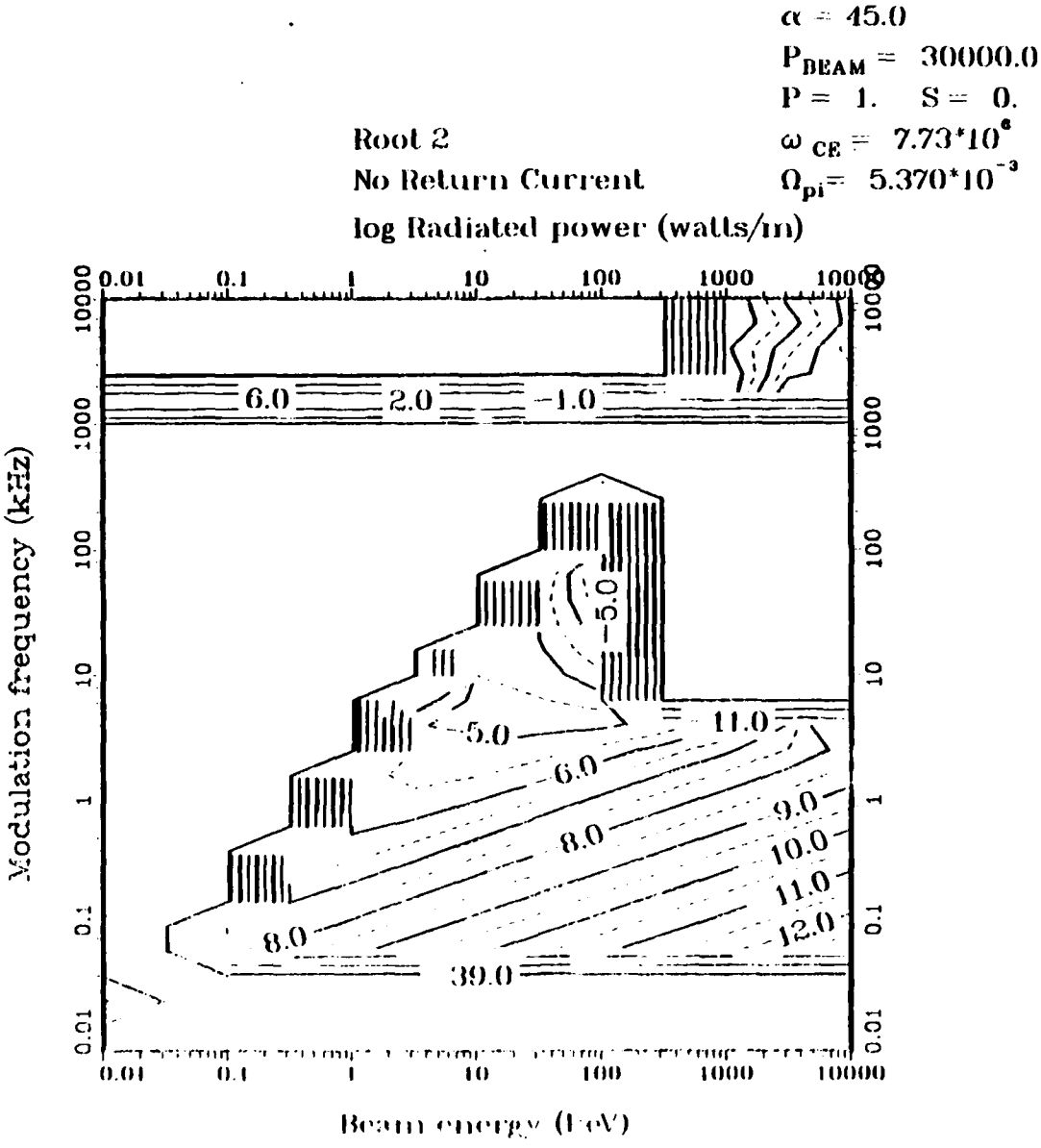

Fig. 16--Contours of nighttime radiated power at 200 km for 45 deg pitch angle (root 2, future gun).

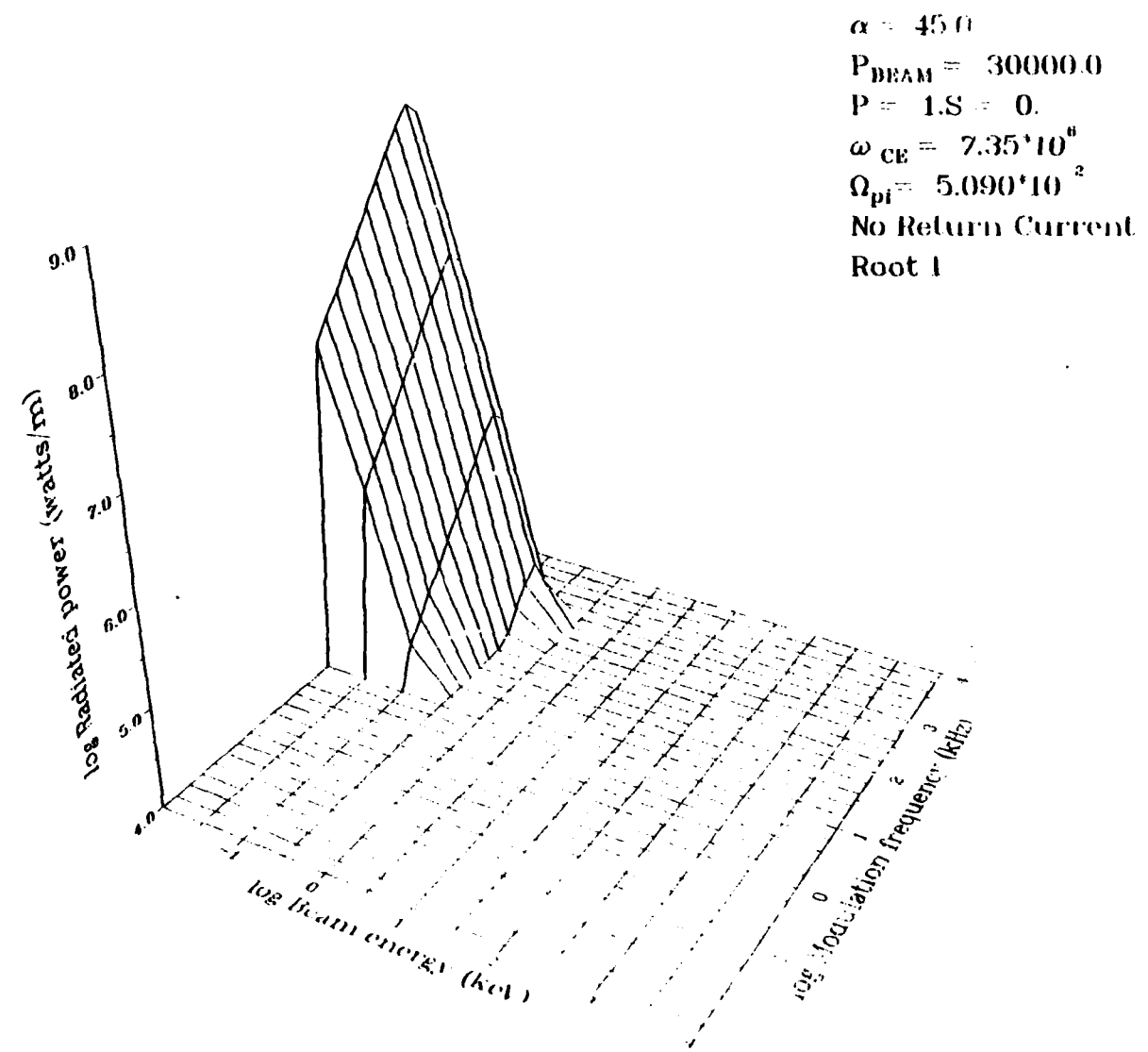

Fig. 17--Daytime radiated power at 300 km for 45 deg pitch angle (root 1, future gun).

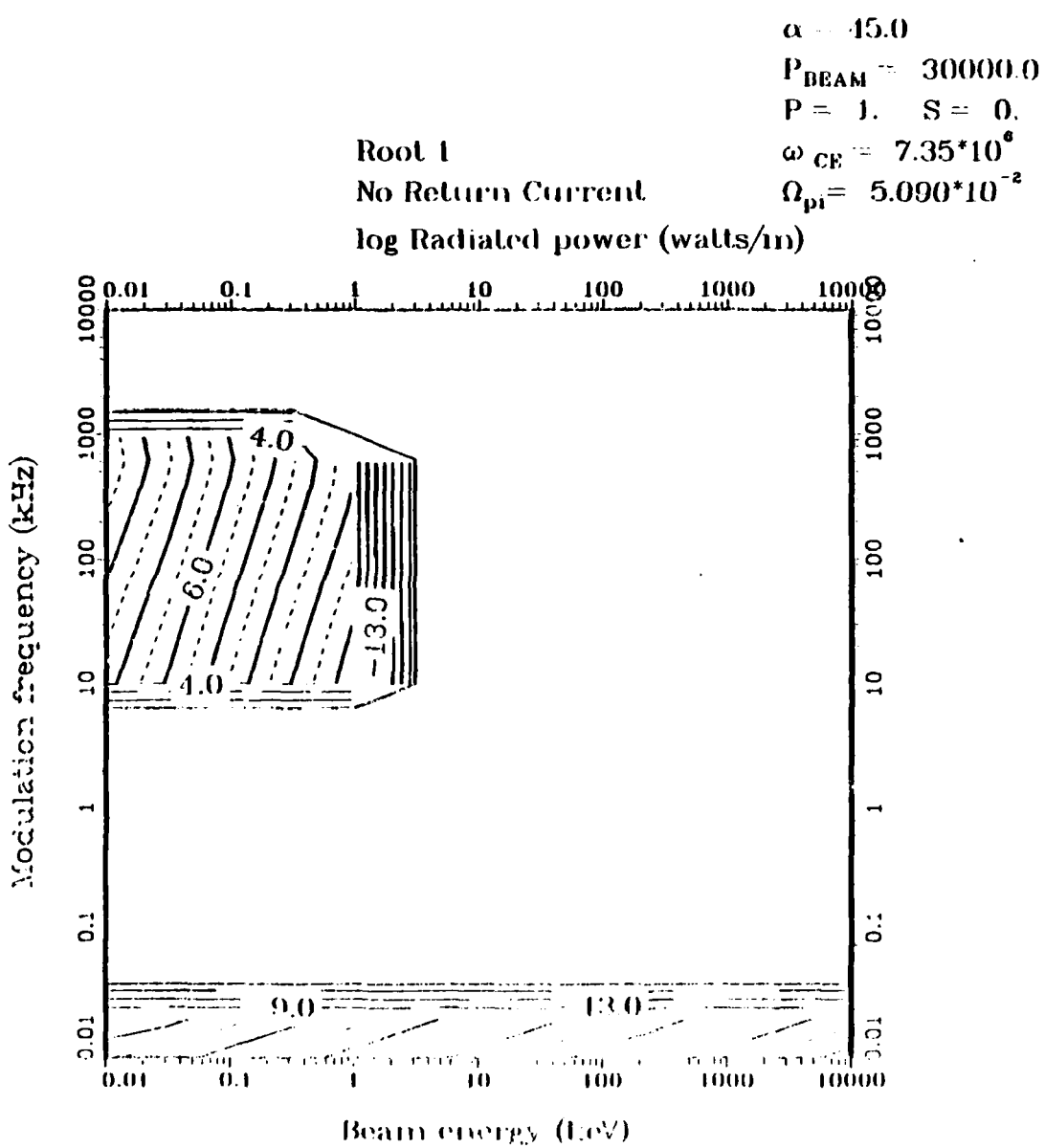

Fig. 18--Contours of daytime radiated power at 300 km for 45 deg pitch angle (root 1, future gun).

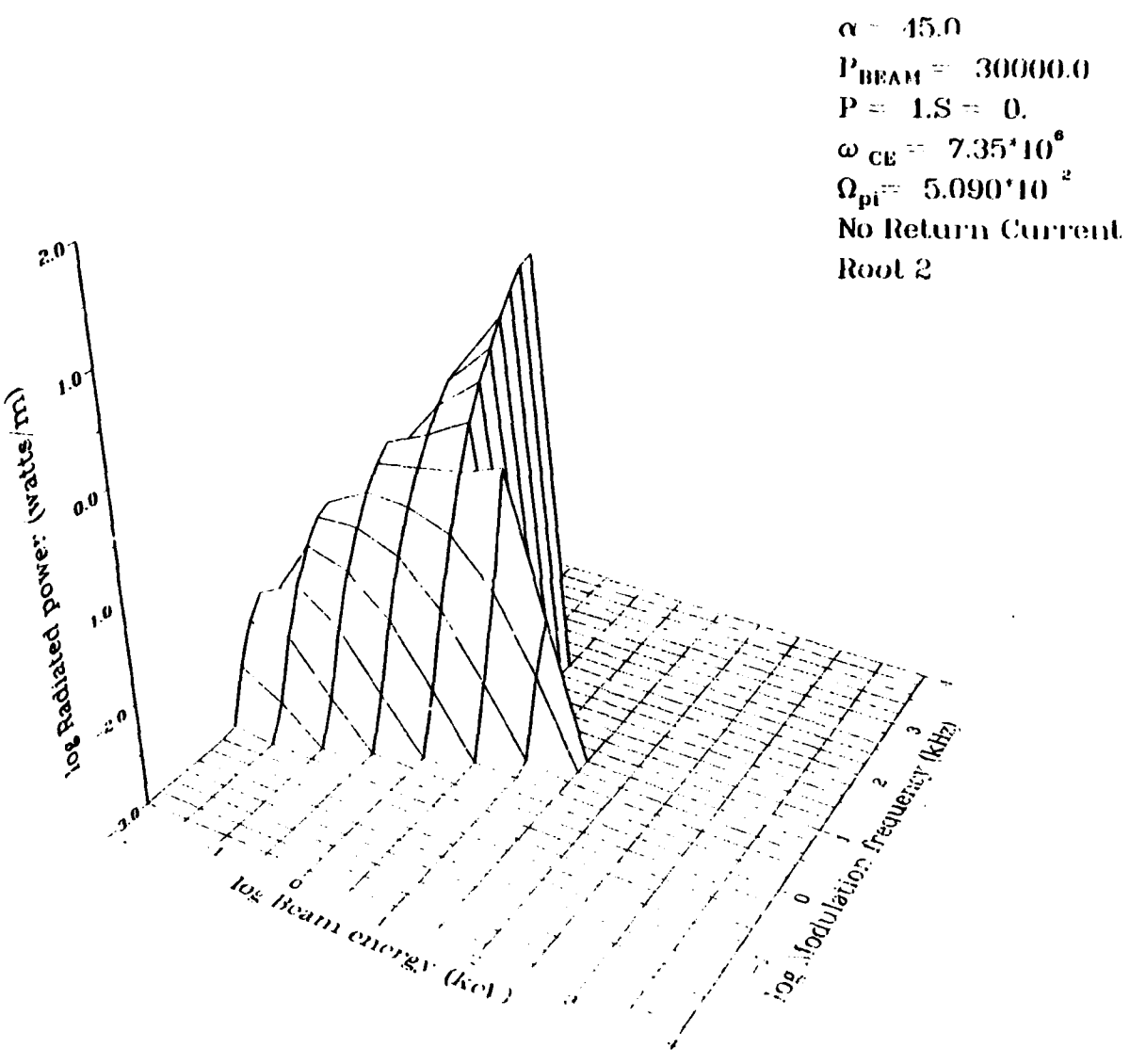

Fig. 19--Daytime radiated power at 300 km for 45 deg pitch angle (root 2, future gun).

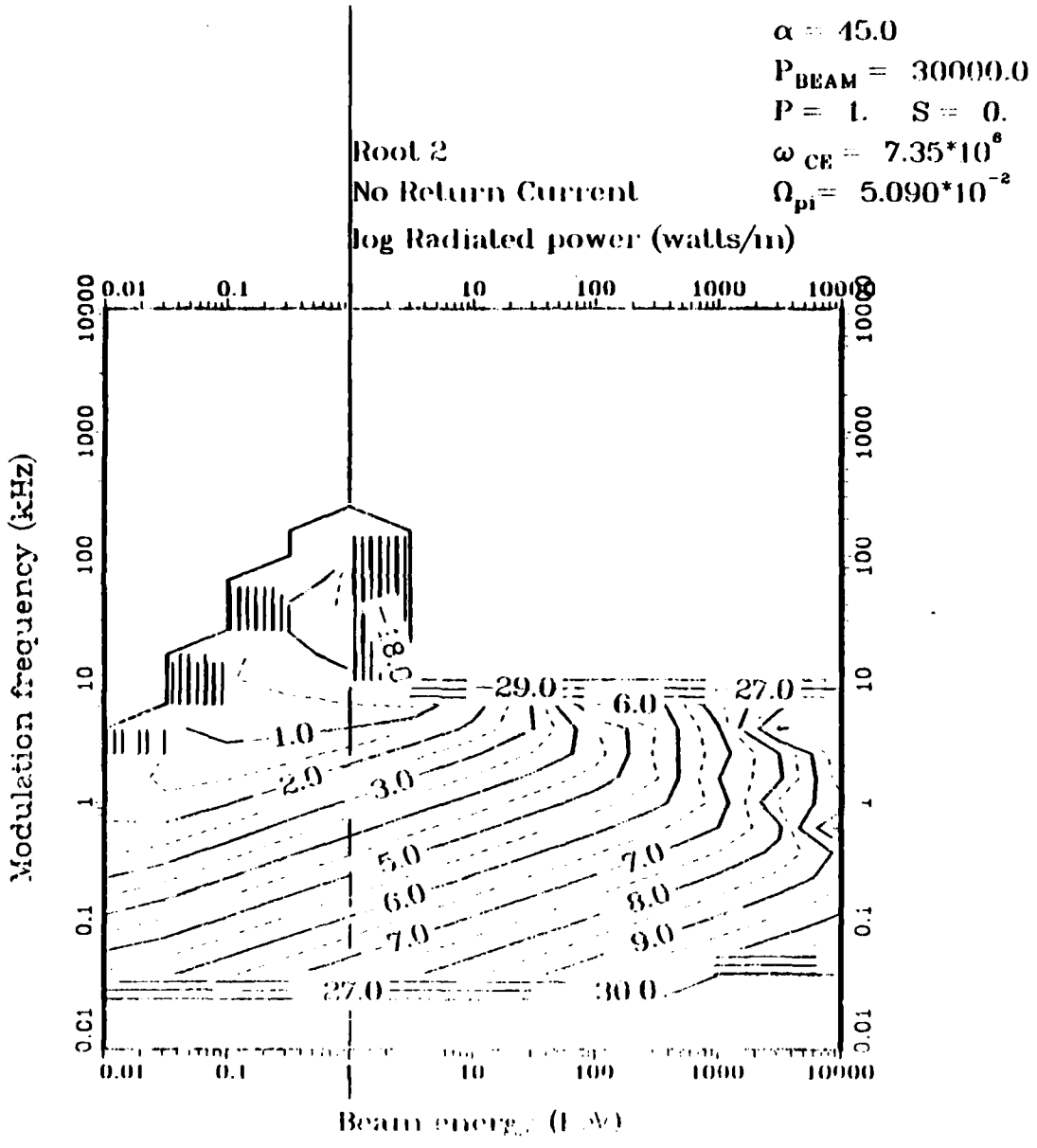

Fig. 20--Contours of daytime radiated power at 300 km for 45 deg pitch angle (root 2, future gun).

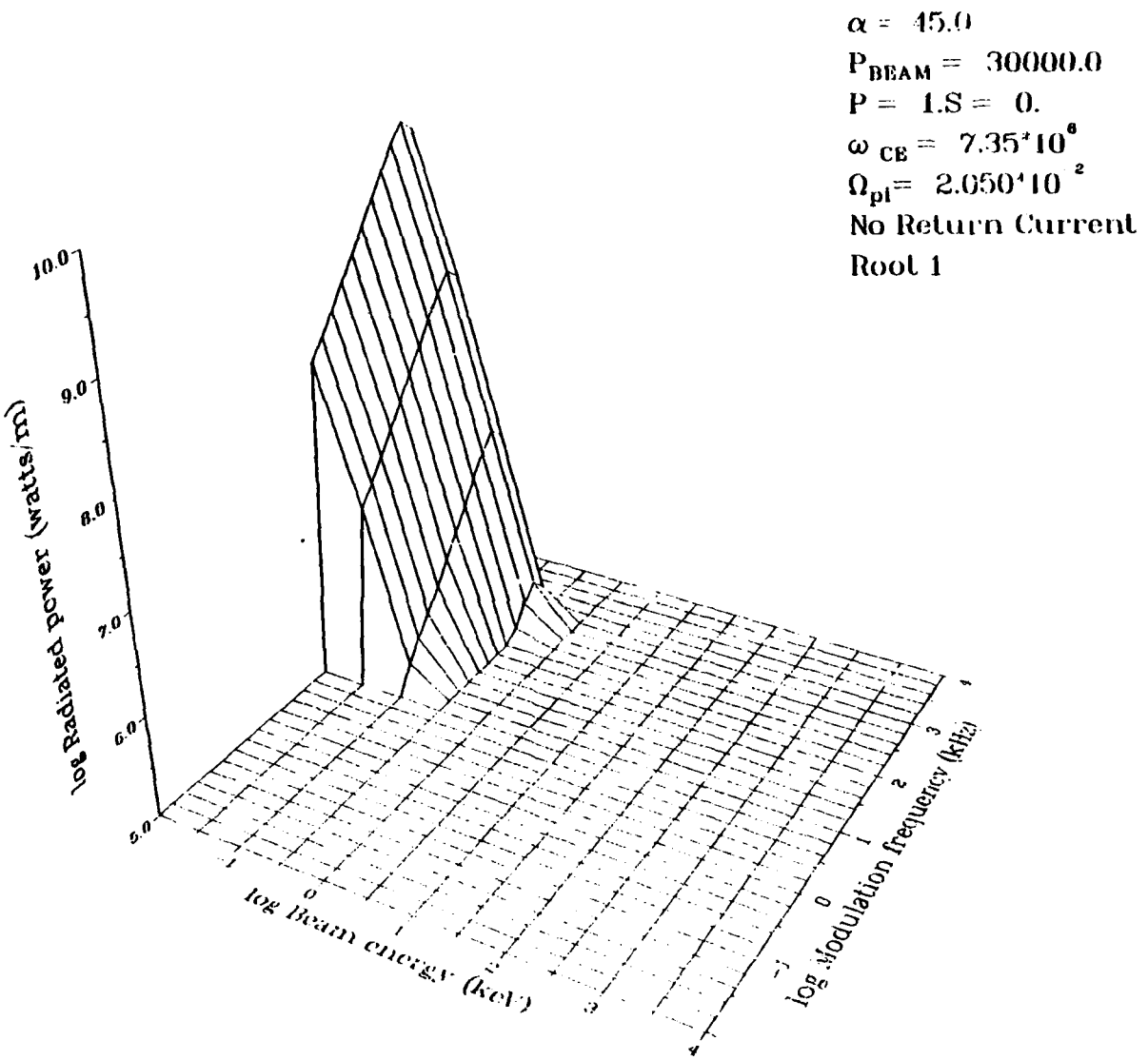

Fig. 21--Nighttime radiated power at 300 km for 45 deg pitch angle (root 1, future gun).

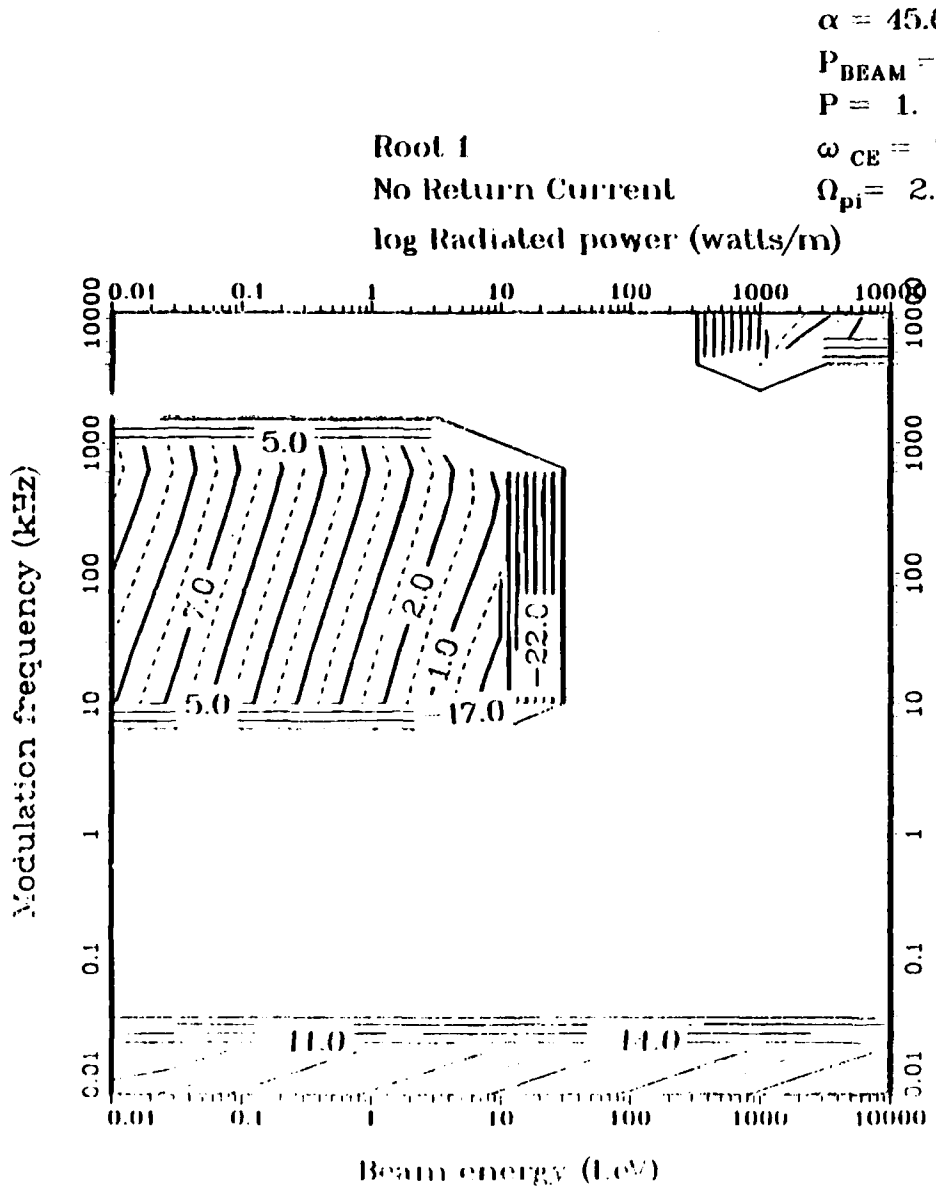

Fig. 22--Contours of nighttime radiated power at 300 km for 45 deg pitch angle (root 1, future gun).

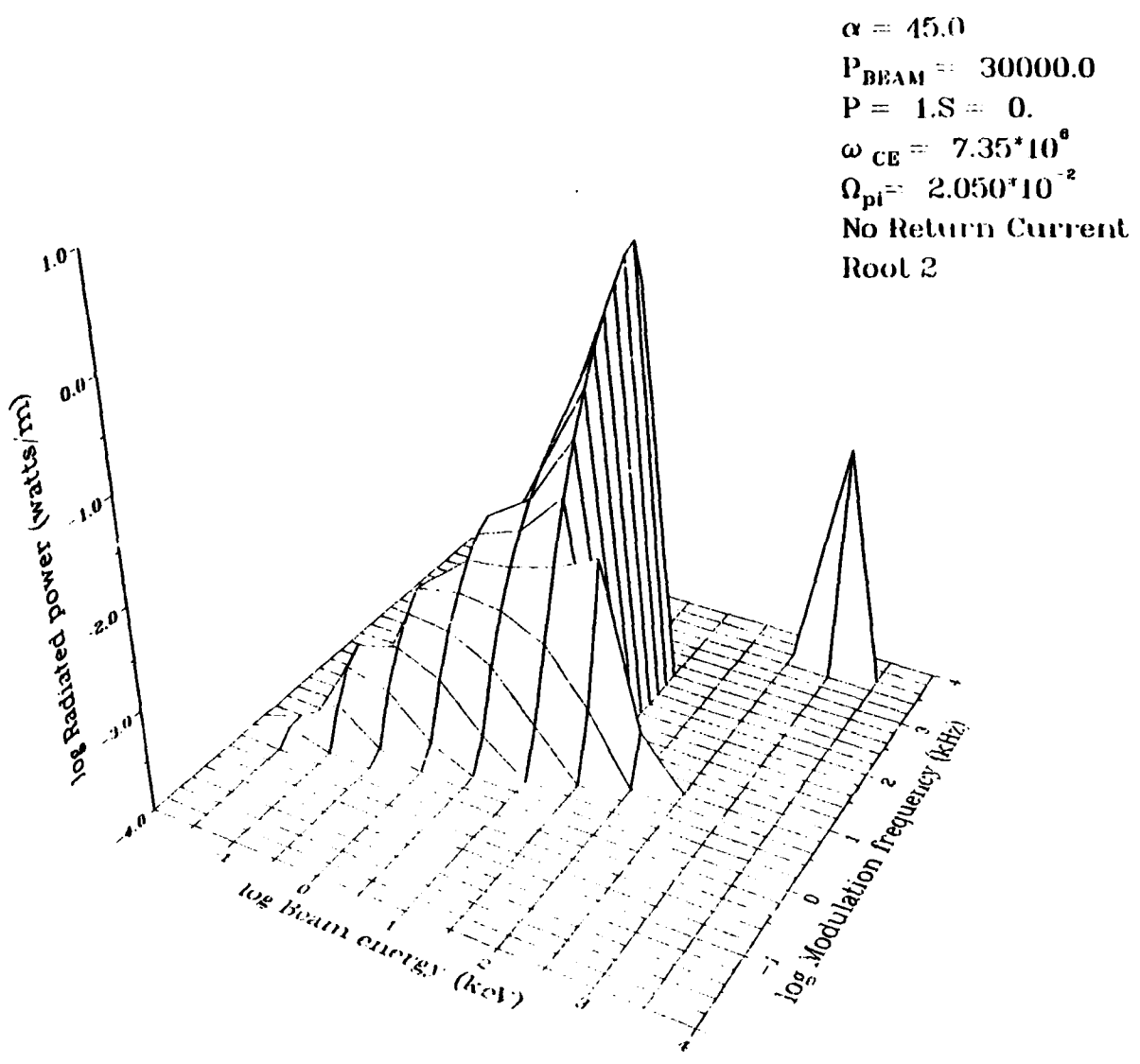

Fig. 23--Nighttime radiated power at 300 km for 45 deg pitch angle (root 2, future gun).

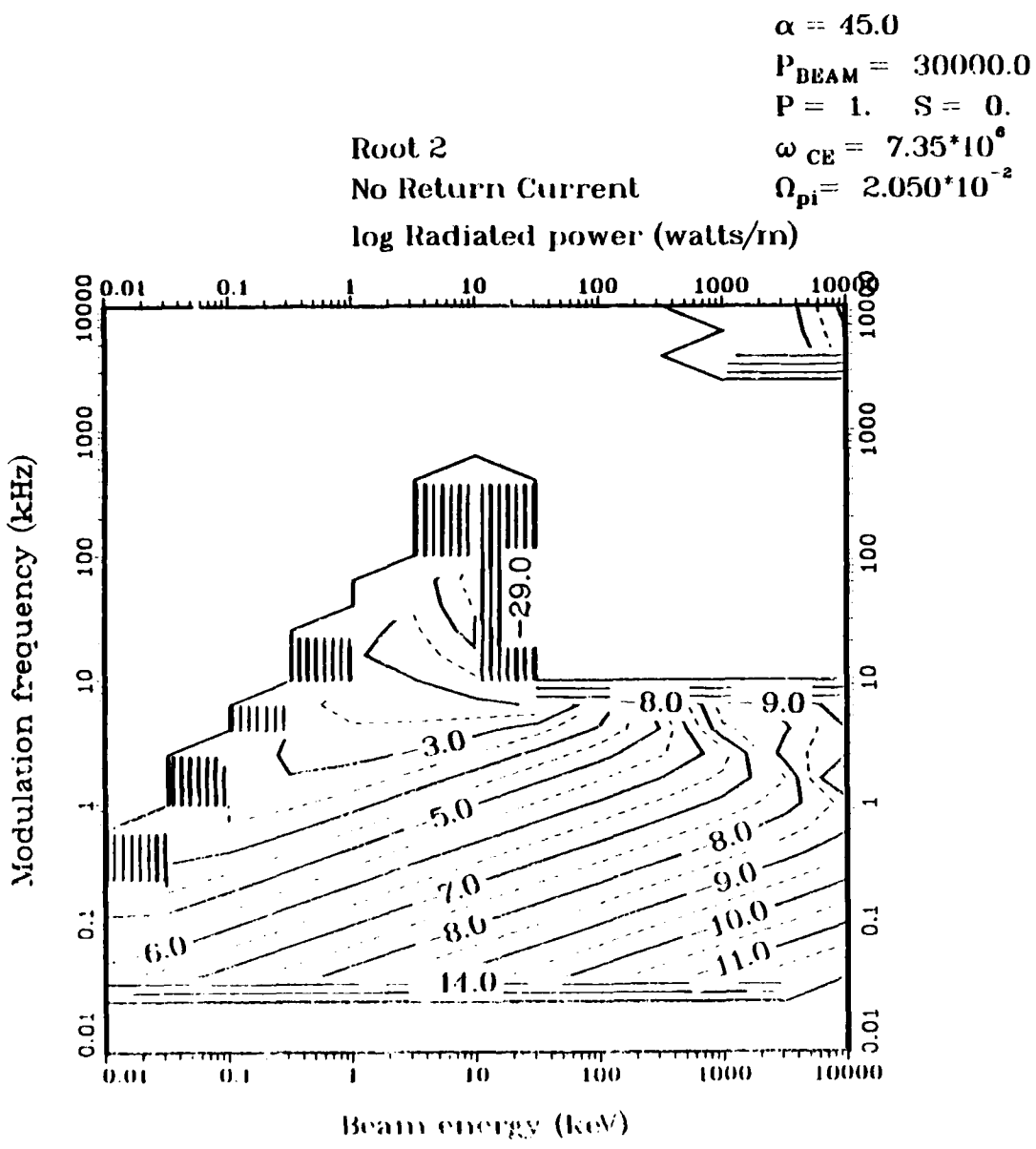

Fig. 24--Contours of nighttime radiated power at 300 km for 45 deg pitch angle (root 2, future gun).

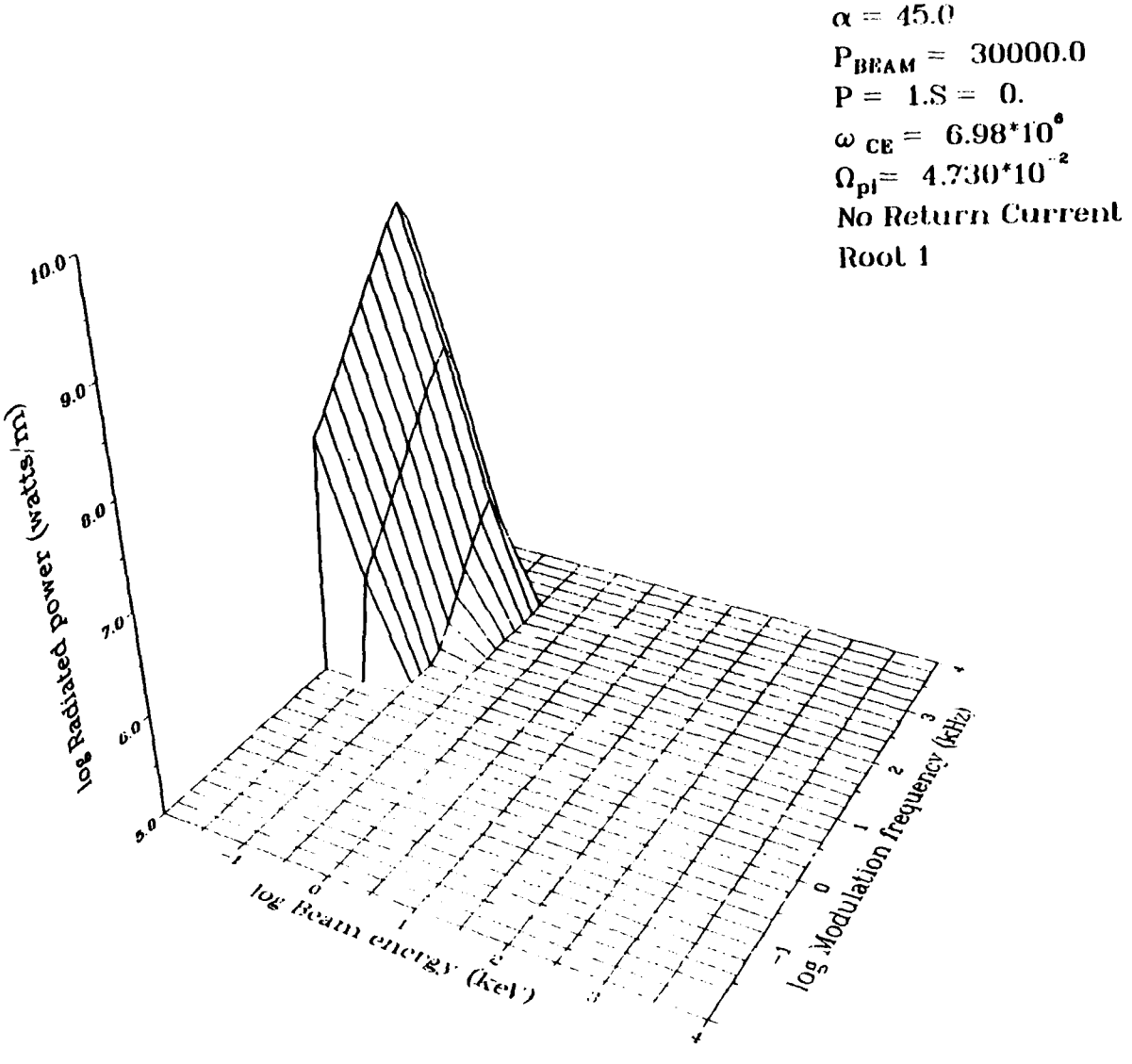

Fig. 25--Daytime radiated power at 400 km for 45 deg pitch angle (root 1, future gun).

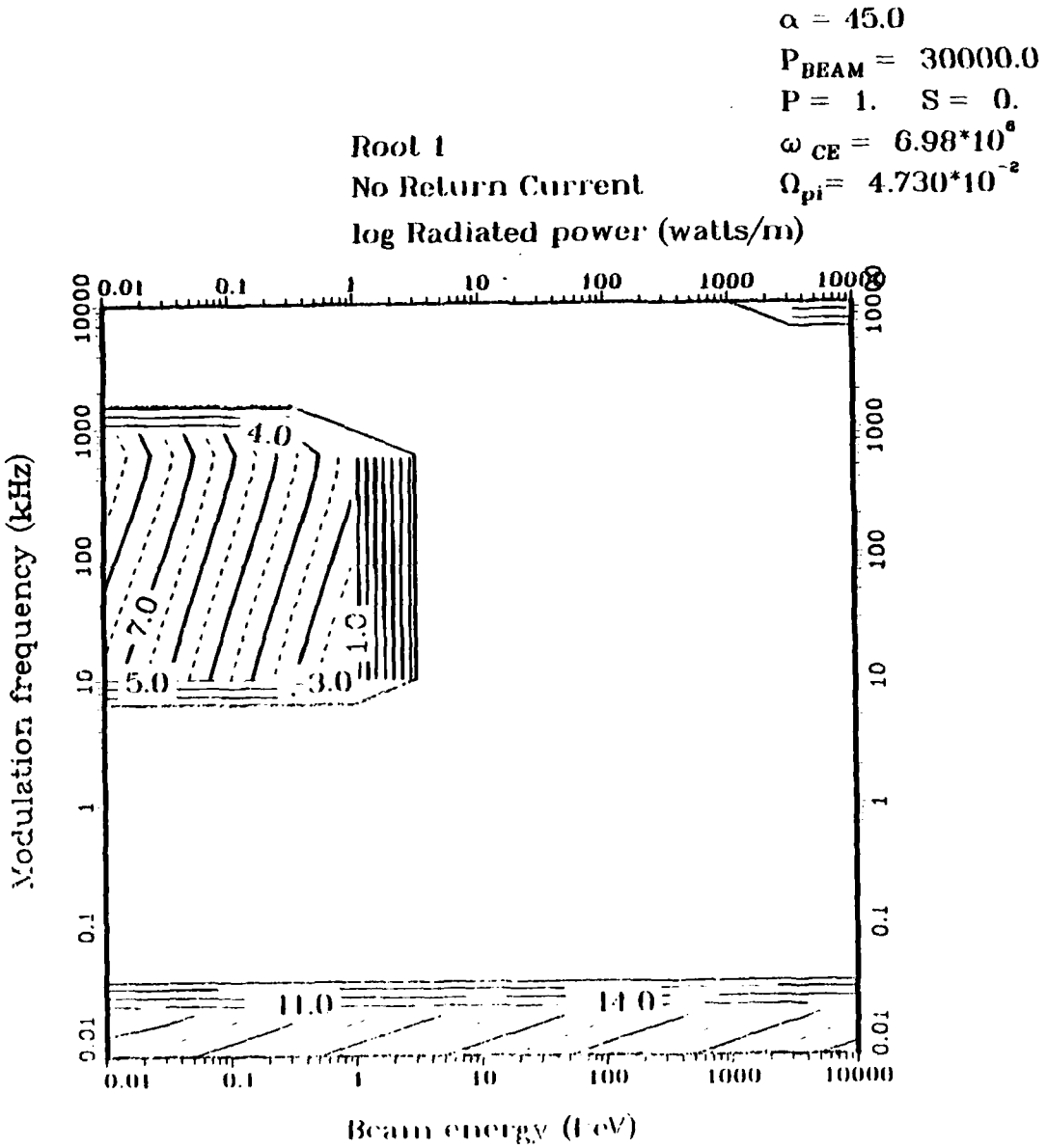

Fig. 26--Contours of daytime radiated power at 400 km for 45 deg pitch angle (root 1, future gun).

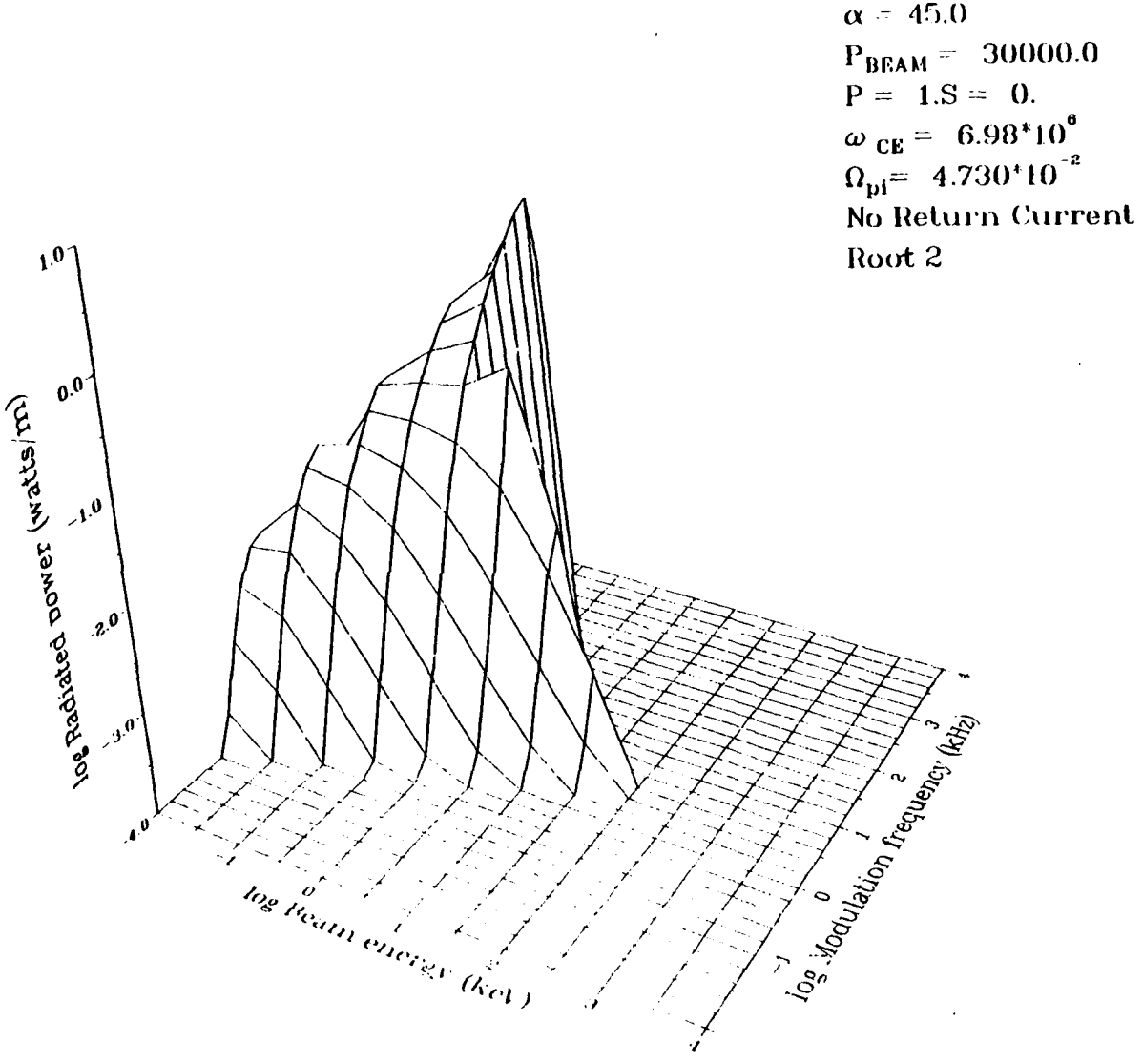

Fig. 27--Daytime radiated power at 400 km for 45 deg pitch angle (root 2, future gun).

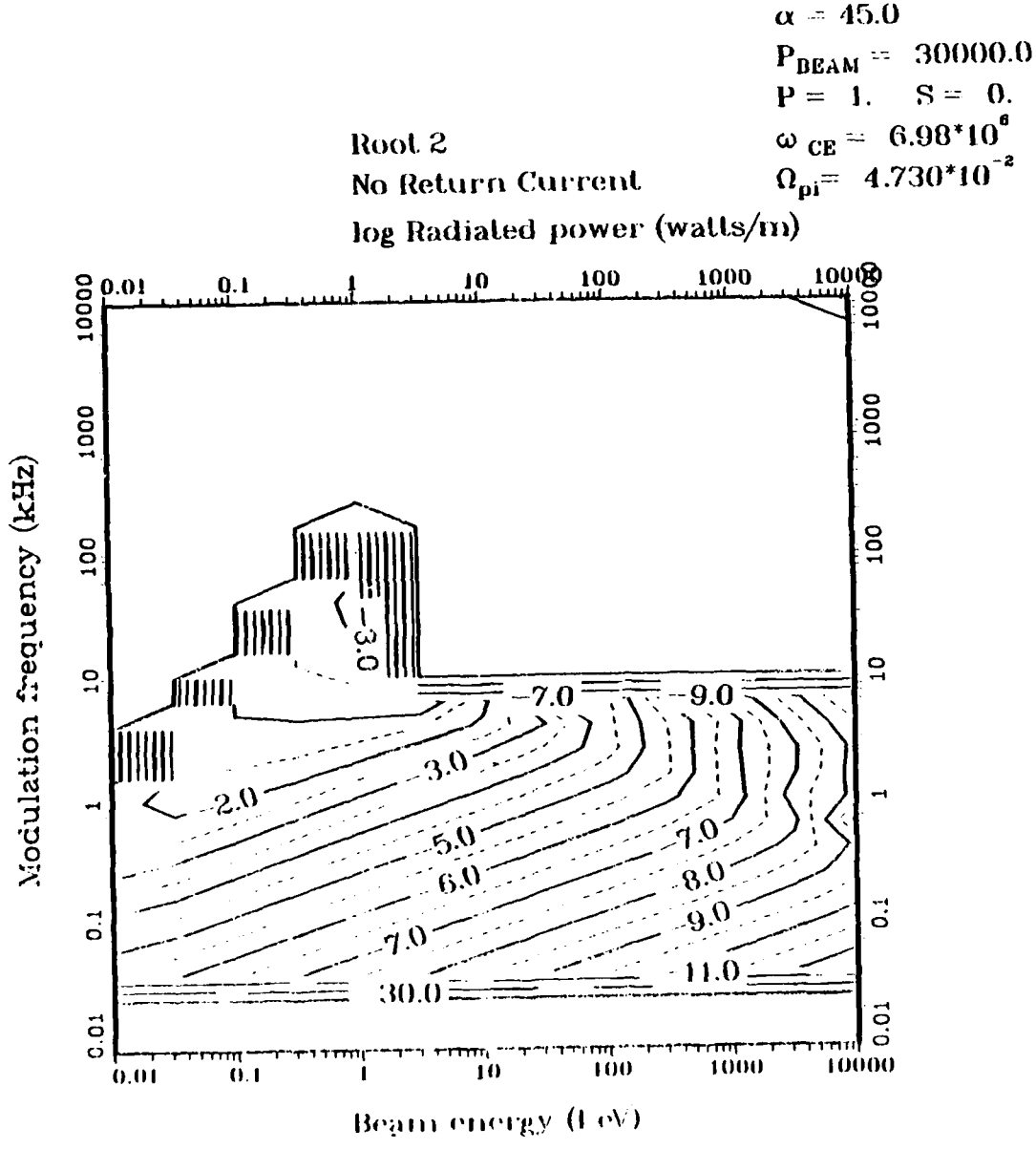

Fig. 28--Contours of daytime radiated power at 400 km for 45 deg pitch angle (root 2, future gun).

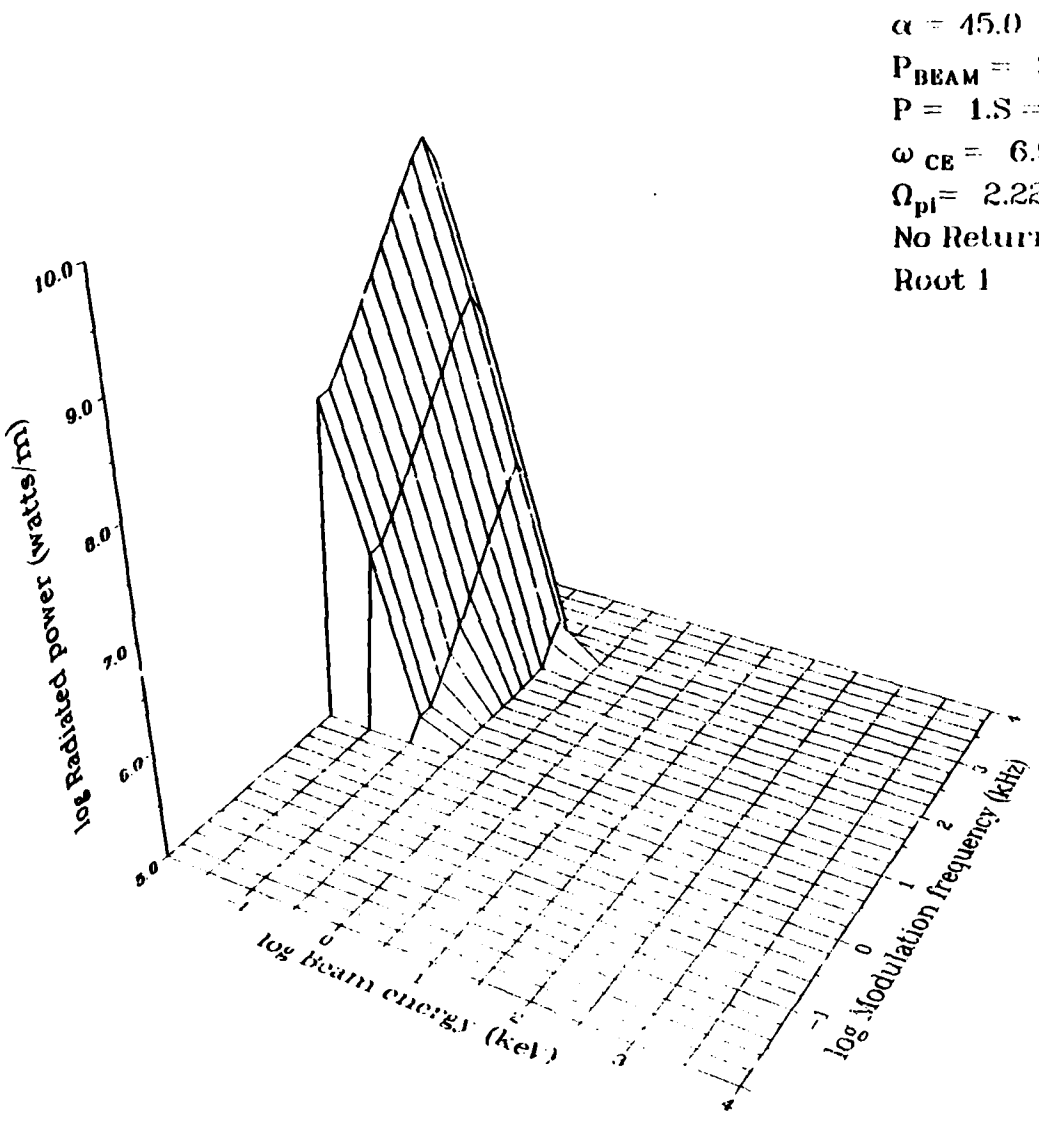

Fig. 29--Nighttime radiated power at 400 km for 45 deg pitch angle (root 1, future gun).

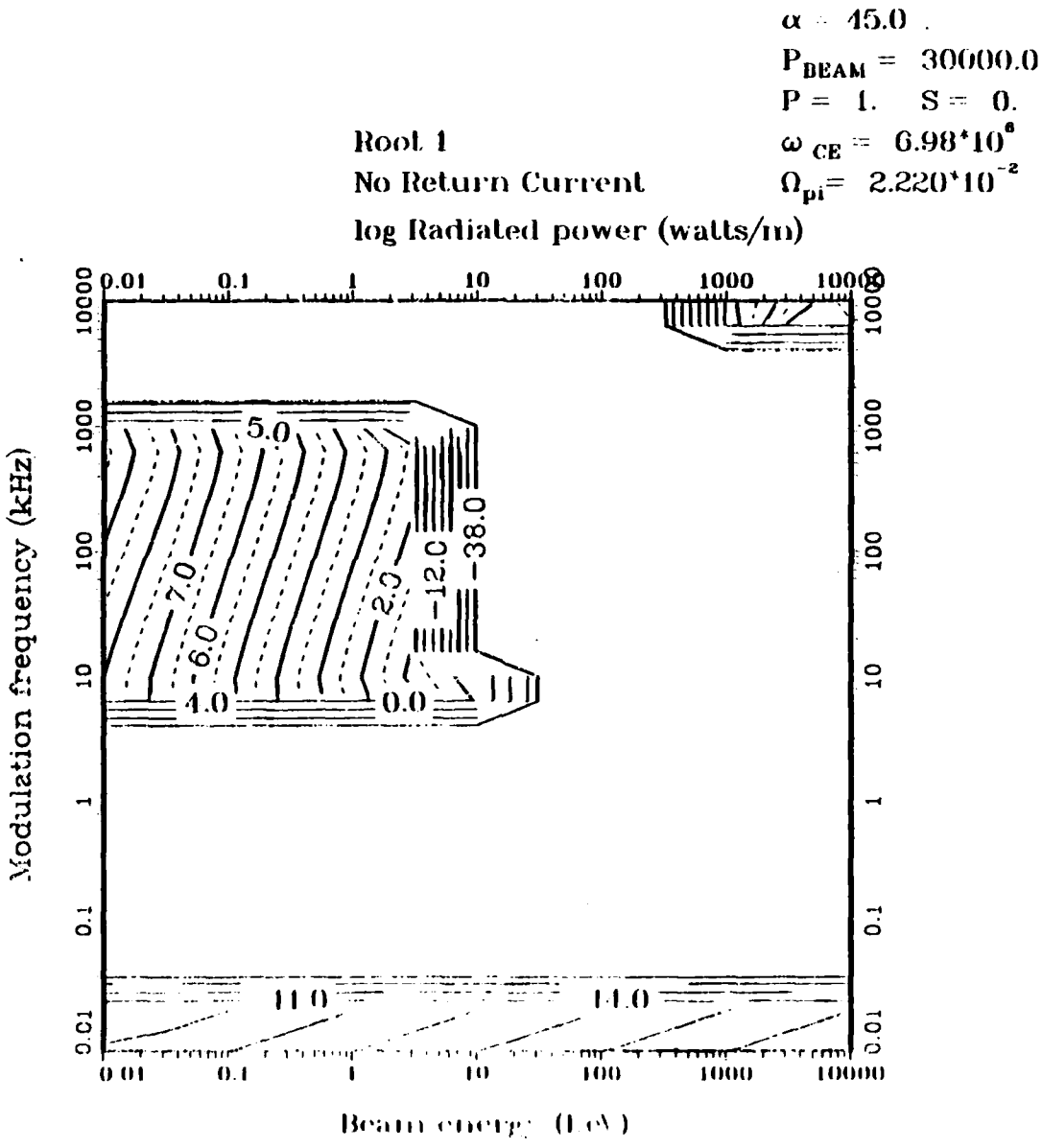

Fig. 30--Contours of nighttime radiated power at 400 km for 45 deg pitch angle (root 1, future gun).

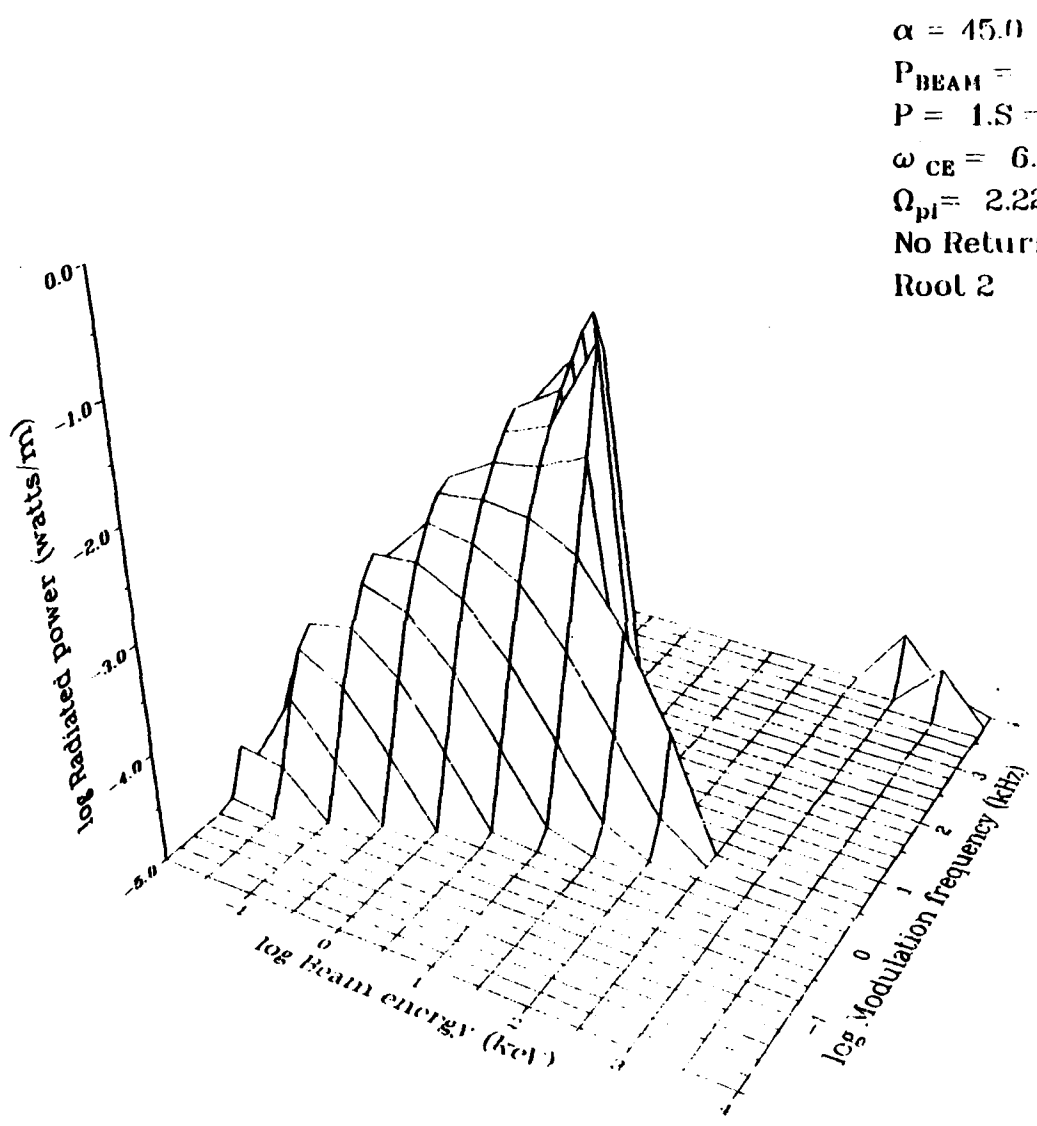

Fig. 31--Nighttime radiated power at 400 km for 45 deg pitch angle (root 2, future gun).

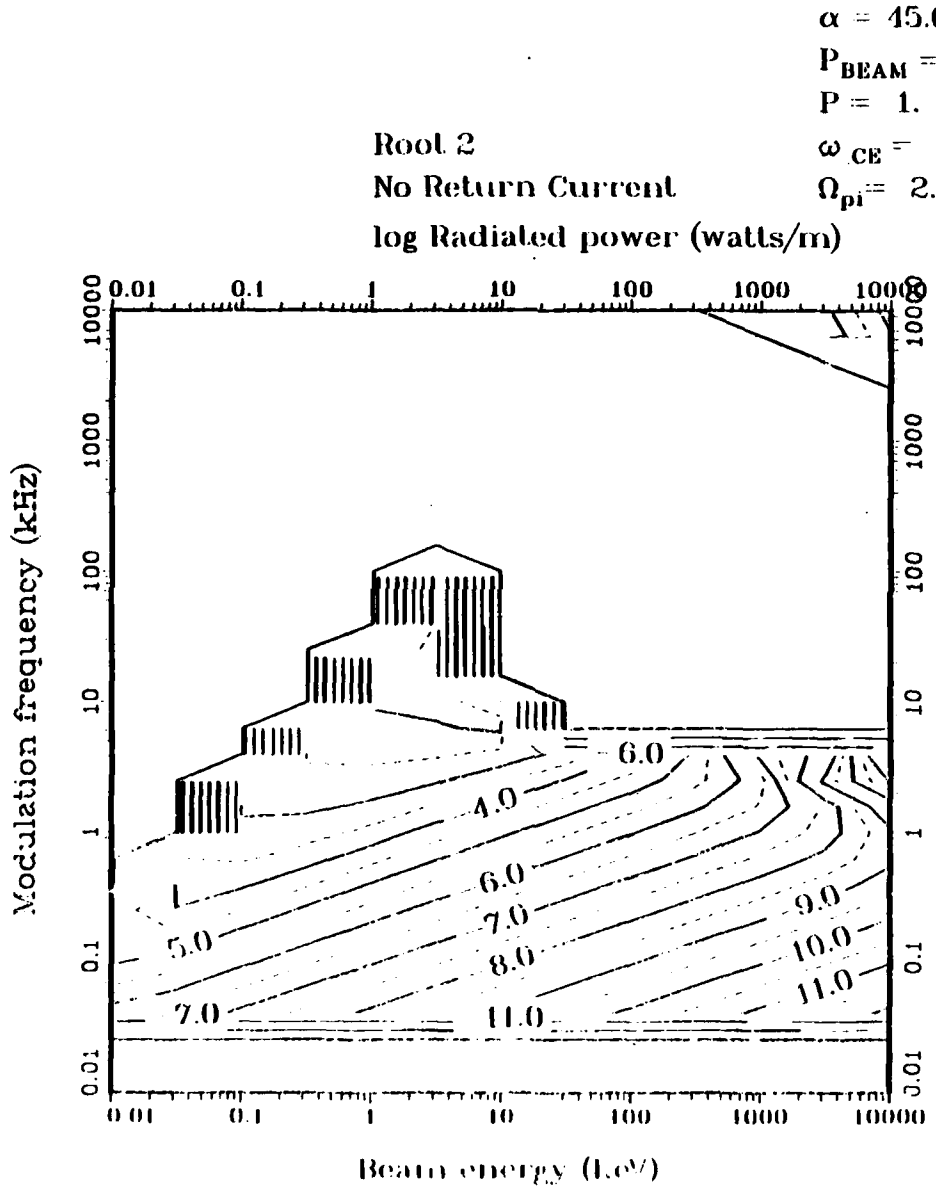

Fig. 32--Contours of nighttime radiated power at 400 km for 45 deg pitch angle (root 2, future gun).

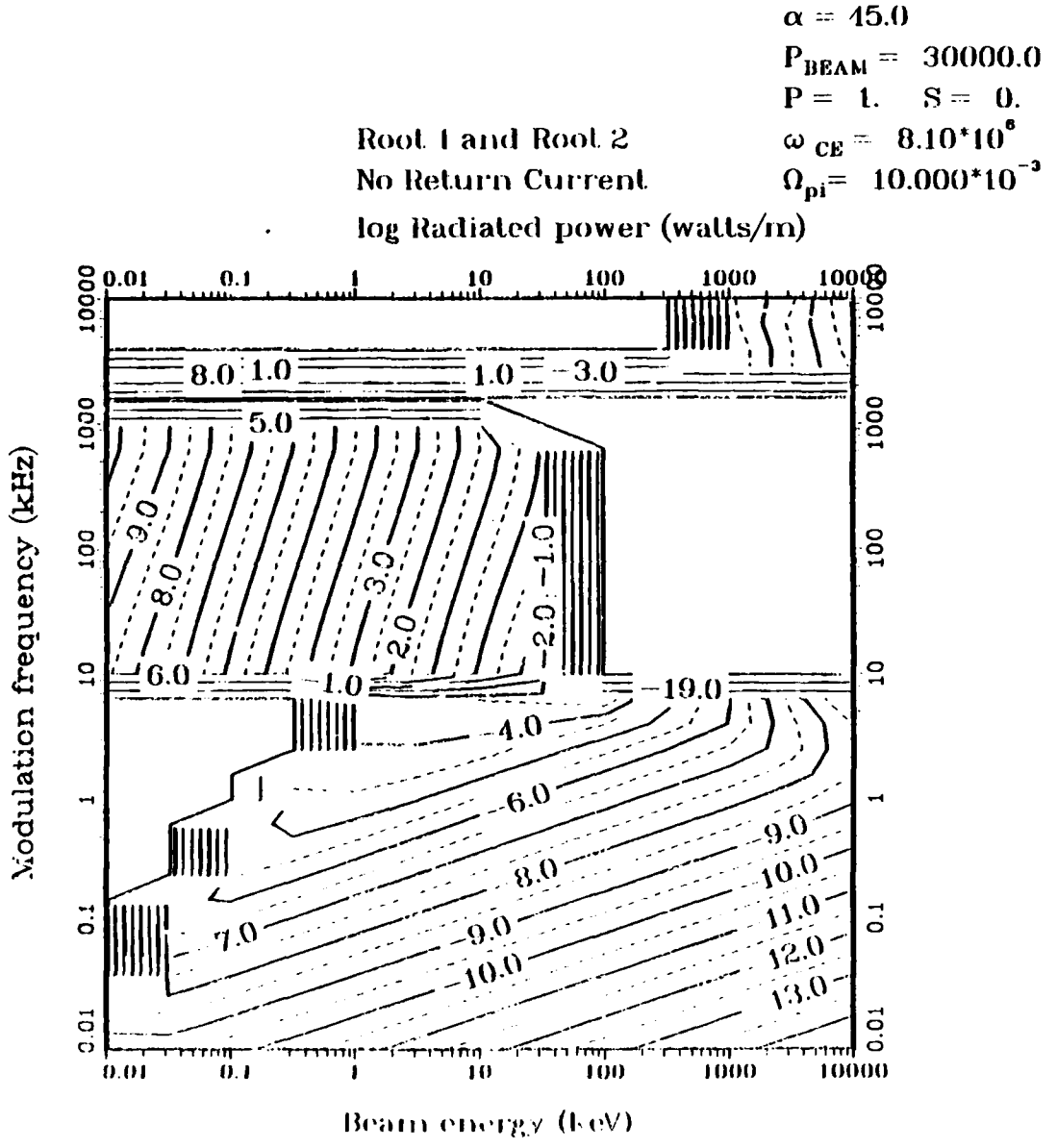

Fig. 33--Contours of total daytime radiated power at 100 km for 45 deg pitch angle (future gun).

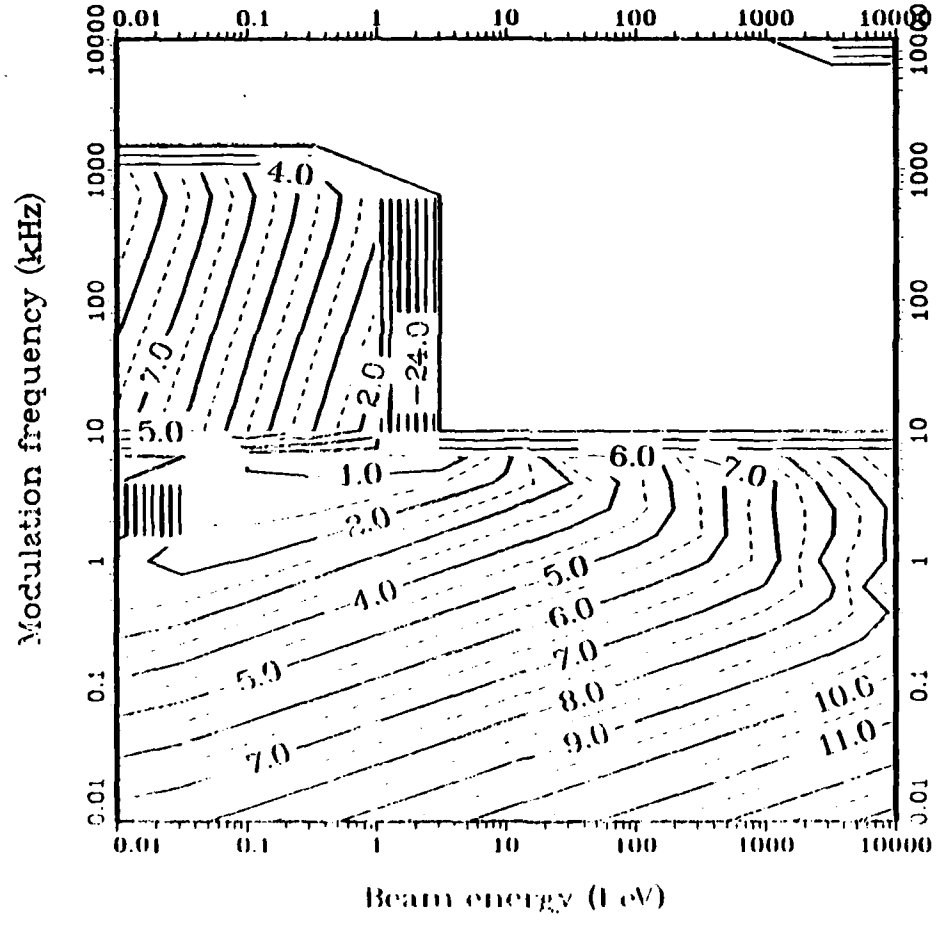

Fig. 34--Contours of total daytime radiated power at 400 km for 45 deg pitch angle (future gun).

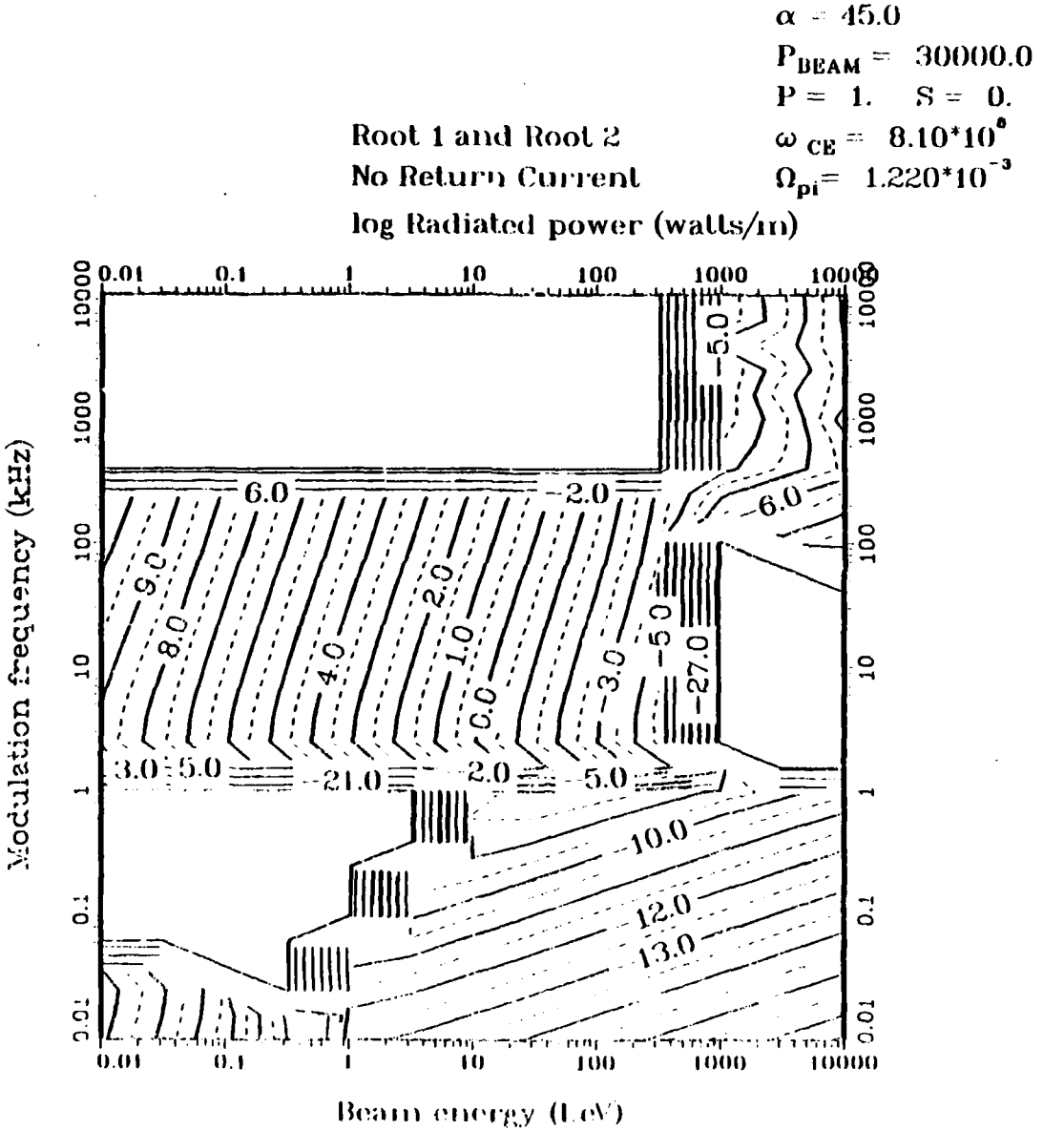

Fig. 35--Contours of total nighttime radiated power at 100 km for 45 deg pitch angle (future gun).

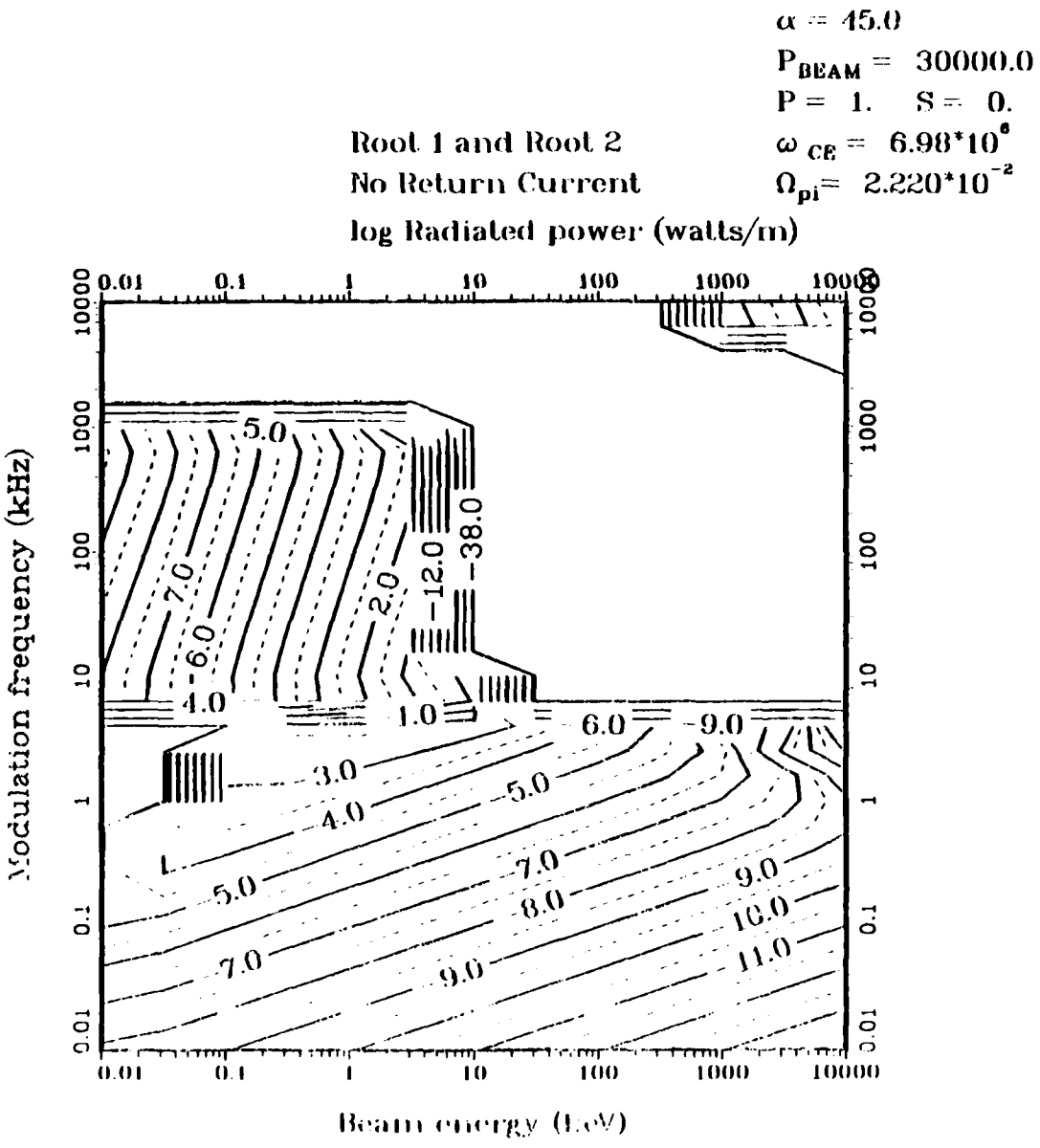

Fig. 36--Contours of total nighttime radiated power at 400 km for 45 deg pitch angle (future gun).

shifts in frequency, which are somewhat less significant.) The values for radiated power remain more or less constant on the structures as they move, although the radiated power at a given frequency and beam energy may change drastically.

The radiated power goes mainly into root 1 on the central plateau between 1 MHz and 1 to 200 kHz, depending on beam energy. The values range from 10^2 W/m, near the high energy edge of the plateau, to 10^9 W/m at low energies. The power into root 1 below about 50 Hz is much lower, typically 10^{-5} to 10^{-12} W/m. The radiated power into root 2 is much lower than into root 1 almost everywhere--typical values range from 10^{-4} to 10^{-16} W/m below 100 kHz. In part of that region, however, power goes into root 2 only. Above 1.5 MHz for daytime emission, root 2 dominates, particularly at low altitudes and for beam energies less than 10 keV.

VALUES OF INDEX OF REFRACTION AT RESONANCE

Detailed computer printouts show that the index of refraction at resonance usually decreases as the beam energy increases and as the angle of the wave normal moves away from 90 deg. At 100 km, the index of refraction is a maximum of about 10^4 at 10 eV on the low-frequency side of the central plateau of root 1, and decreases to 300 at the high-frequency side. At the high beam energy end, the index of refraction is about 500 on the low-frequency side, and about 6 on the high-frequency side. The results at 400 km for daytime emission are similar, but the variation at the high energy end is from 3000 at the low-frequency side to 300 at the high. Figures 37 and 38 show an intermediate case--altitude 200 km. The nighttime values are similar.

Figure 38 shows that the peak values for root 2, around 2 MHz for daytime emission at low altitudes, vary from about 600 at 10 eV to 1 at relativistic energies. The printouts also show that values for root 1 at low frequencies (as in Fig. 37) are around 300 at 100 km and 1000 at 400 km for daytime emission; for nighttime emission the values range from 10^5 at 10 eV to 40 at relativistic energies and at low altitudes, and fall around 600 at all energies at 400 km.

$\alpha = 45.0$
$P_{BEAM} = 30000.0$
$P = 1. \quad S = 0.$
$\omega_{CE} = 7.73*10^{6}$
$\Omega_{pi} = 2.860*10^{-2}$

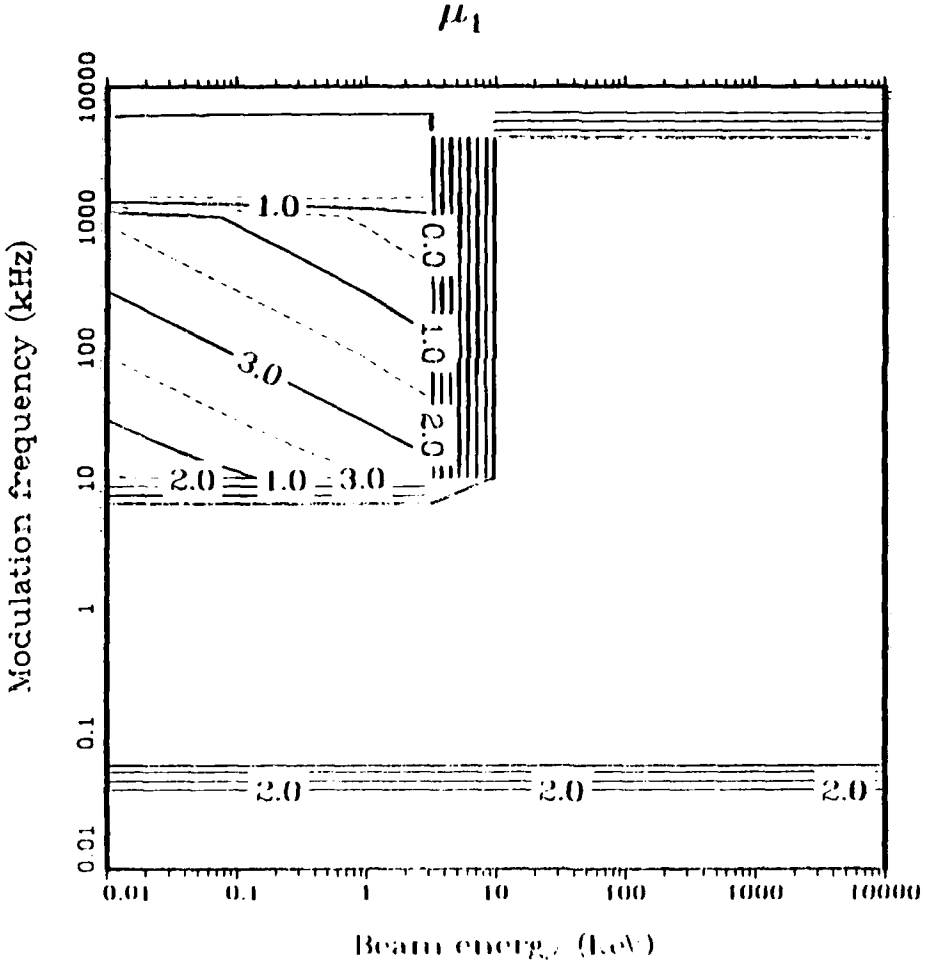

Fig. 37--Resonant value of index of refraction for daytime emission at 200 km (root 1, future gun).

α = 45.0
P_{BEAM} = 30000.0
P = 1. S = 0.
ω_{CE} = $7.73*10^{6}$
Ω_{pi} = $2.860*10^{-2}$

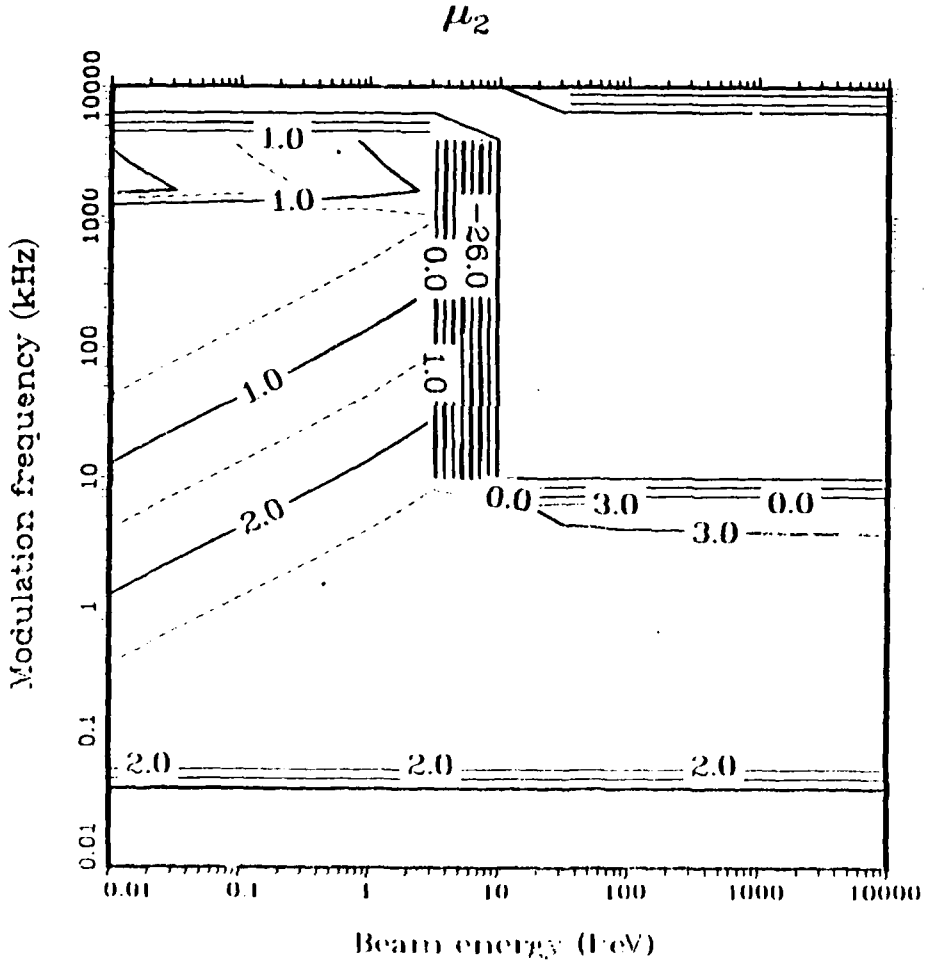

Fig. 38--Resonant value of index of refraction for daytime emission at 200 km (root 2, future gun).

WAVE-NORMAL AND RAY ANGLES

We have not prepared figures showing wave normal and ray angles. However, detailed computer printouts establish that the angle of the k vector (wave-normal angle) and the ray angle vary enormously over the parameter space, although the variation with altitude and time of day is not as marked as that for the index of refraction. At the low-energy end of the root 1 central plateau, the k vector ranges from 89.6 deg at the low-frequency side to 34 deg at the high-frequency edge. The corresponding ray angles are 179.6 and 124 deg. At the high-energy end, the k vector angle ranges from 89 deg at the low-frequency edge to 42 deg at the high-frequency edge. The corresponding ray angles are about 180 and 114 deg.

The wave-normal angle at very low frequencies is close to 90 deg at relativistic energies with a ray angle also close to 90 deg. At lower energies, the wave-normal angle falls to between 20 and 30 deg at low altitudes for daytime emission, with a ray angle between 10 and 30 deg. For nighttime emission at low altitude and daytime emission at high altitude, the ray angle is close to 180 deg for root 1 and 90 deg for root 2. For the peak in root 2 at low altitude and 2 MHz frequency, the wave-normal angle varies from 66 deg at low energy to 71 deg at high energy with a corresponding variation in ray angle from 156 to 149 deg.

In summary, the beam may send out electromagnetic waves in many directions depending on beam energy and modulation frequency; similarly, the radiation energy may flow in many directions. Frequencies below 100 Hz and beam energies below 10 keV are the only regions in which the directions of the wave normal and the ray are almost equal. Nighttime emission at low altitude and daytime emission at high altitude are exceptions as noted above. Rules for emission into higher harmonics, which are not presented here, appear to be much more complicated.

EFFECT OF VARYING PITCH ANGLES

Figures 39 through 46 show the effect of varying the pitch angle on both day and night emission at 200 km. A comparison of these plots with those for emission at 45 deg (Figs. 9 through 16), demonstrates

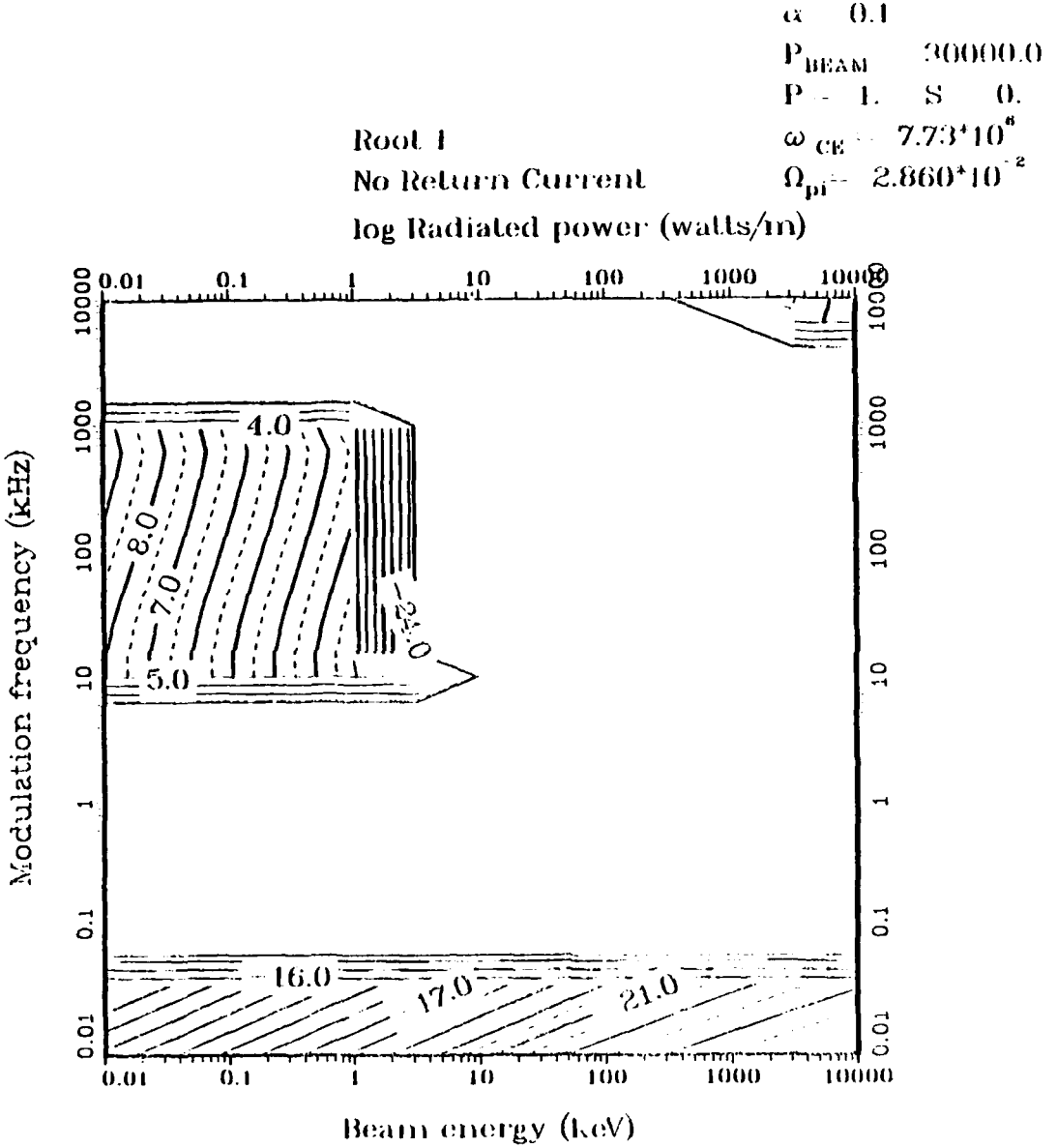

Fig. 39--Contours of daytime radiated power at 200 km for 0.1 deg pitch angle (root 1, future gun).

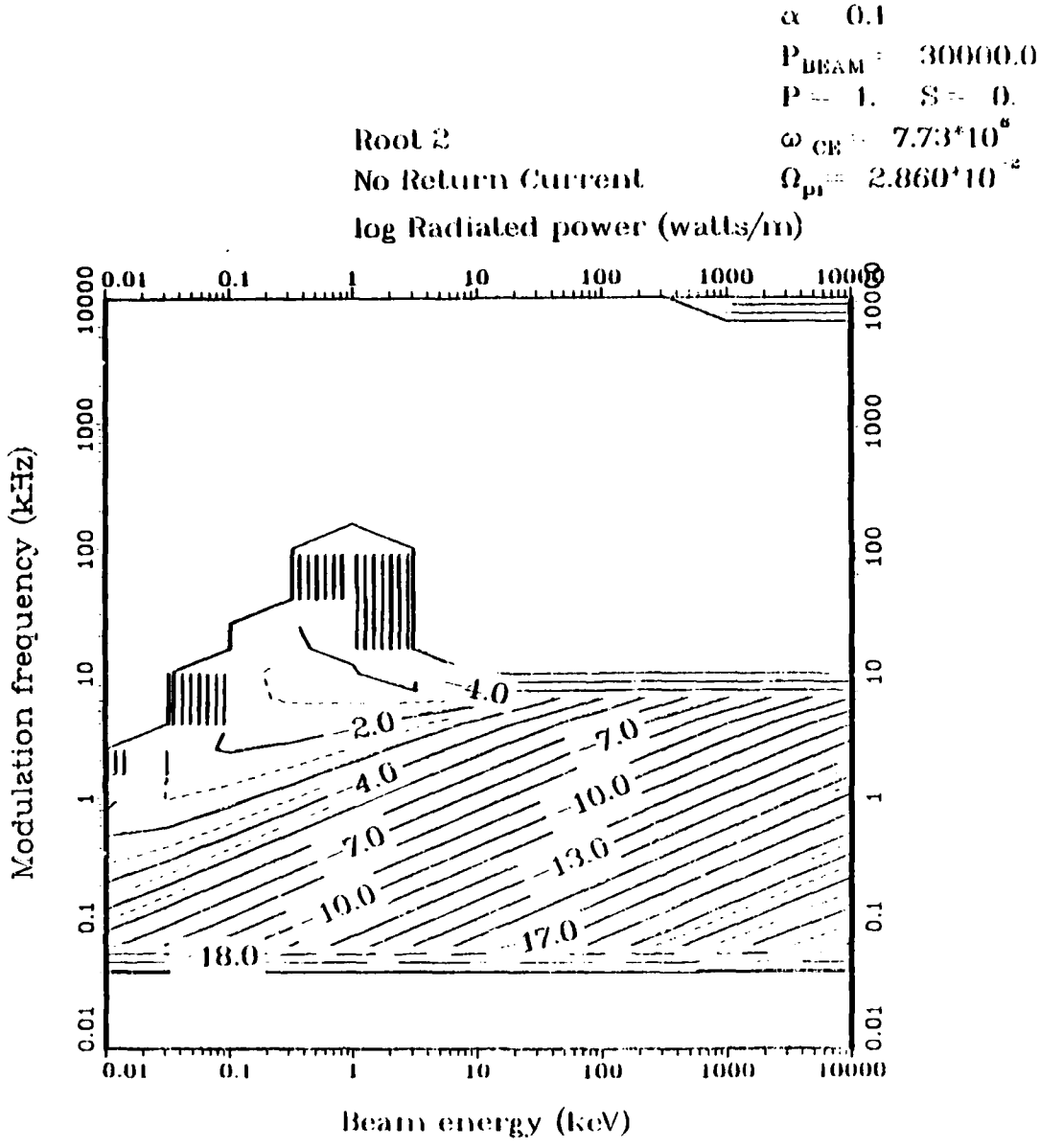

Fig. 40--Contours of daytime radiated power at 200 km for 0.1 deg pitch angle (root 2, future gun).

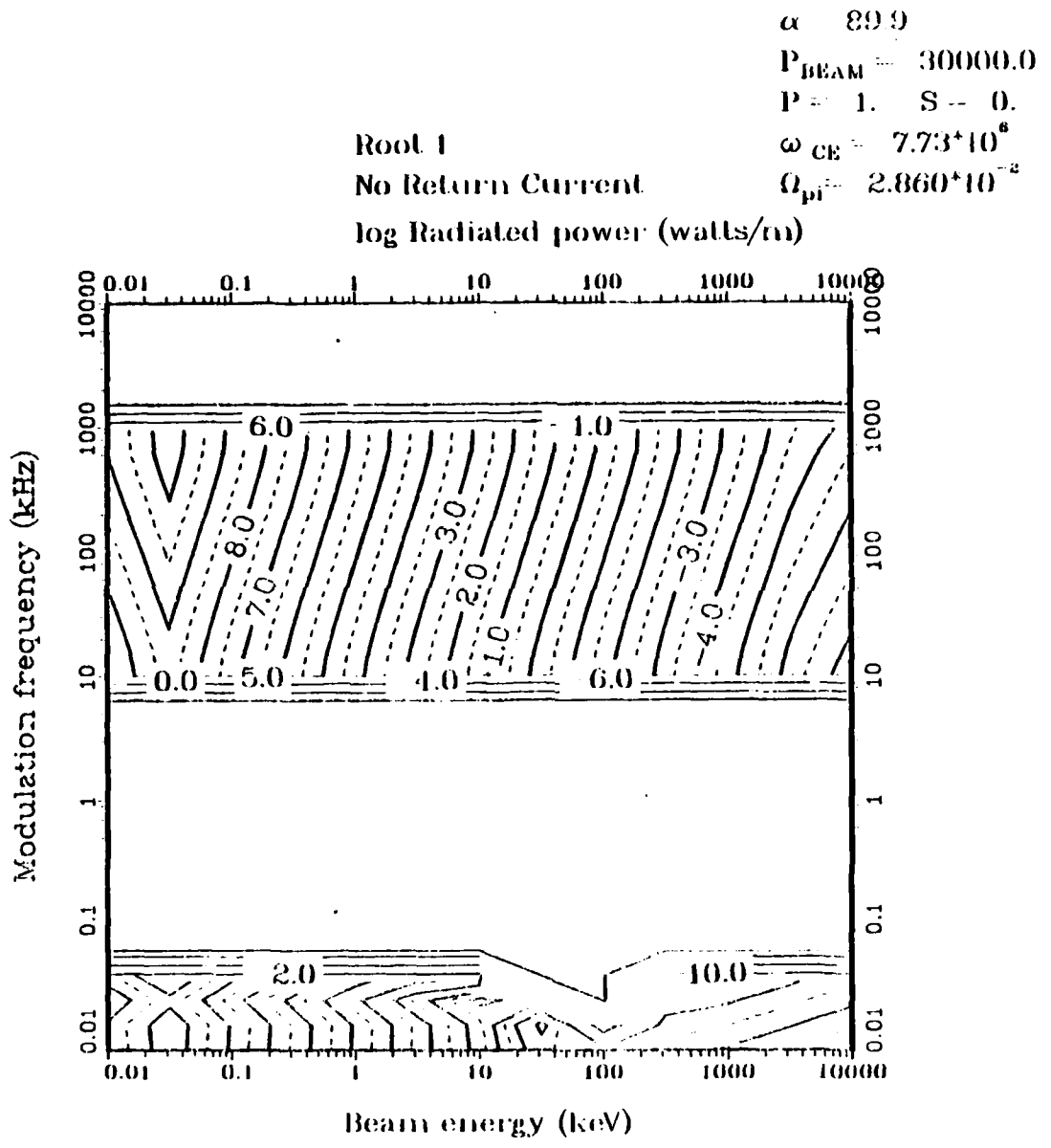

Fig. 41--Contours of daytime radiated power at 200 km for 89.9 deg pitch angle (root 1, future gun).

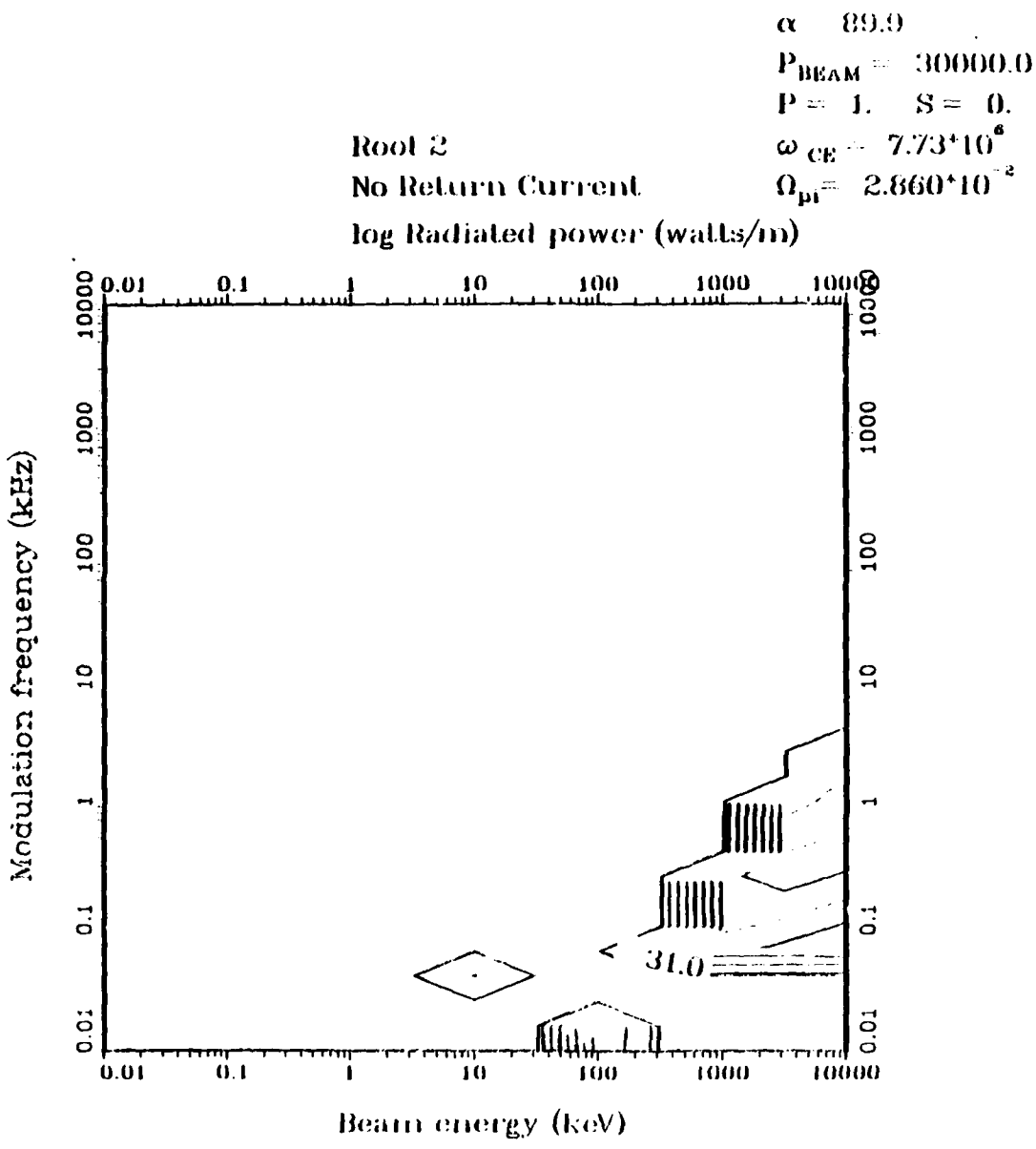

Fig. 42--Contours of daytime radiated power at 200 km for 89.9 deg pitch angle (root 2, future gun).

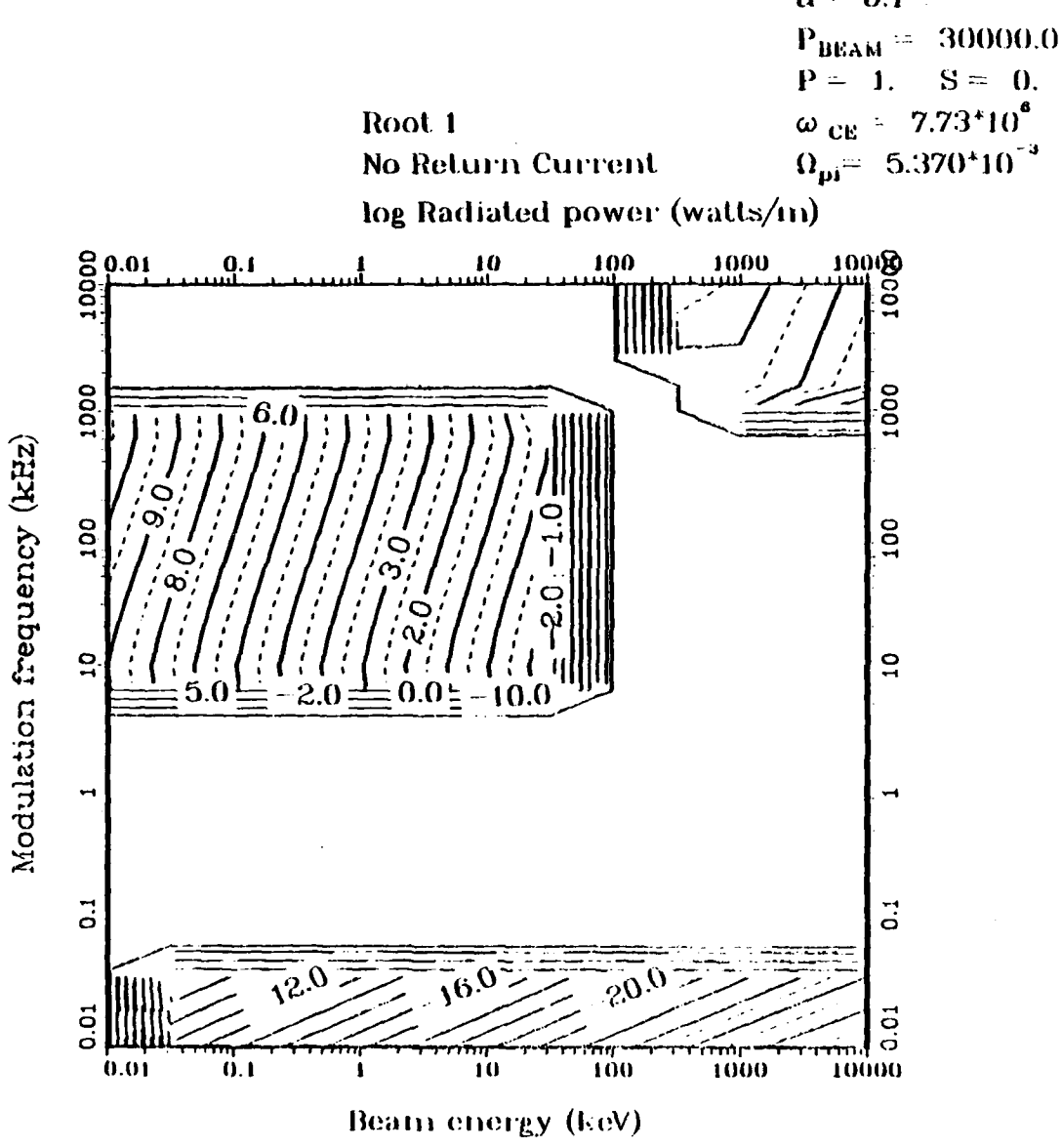

Fig. 43--Contours of nighttime radiated power at 200 km for 0.1 deg pitch angle (root 1, future gun).

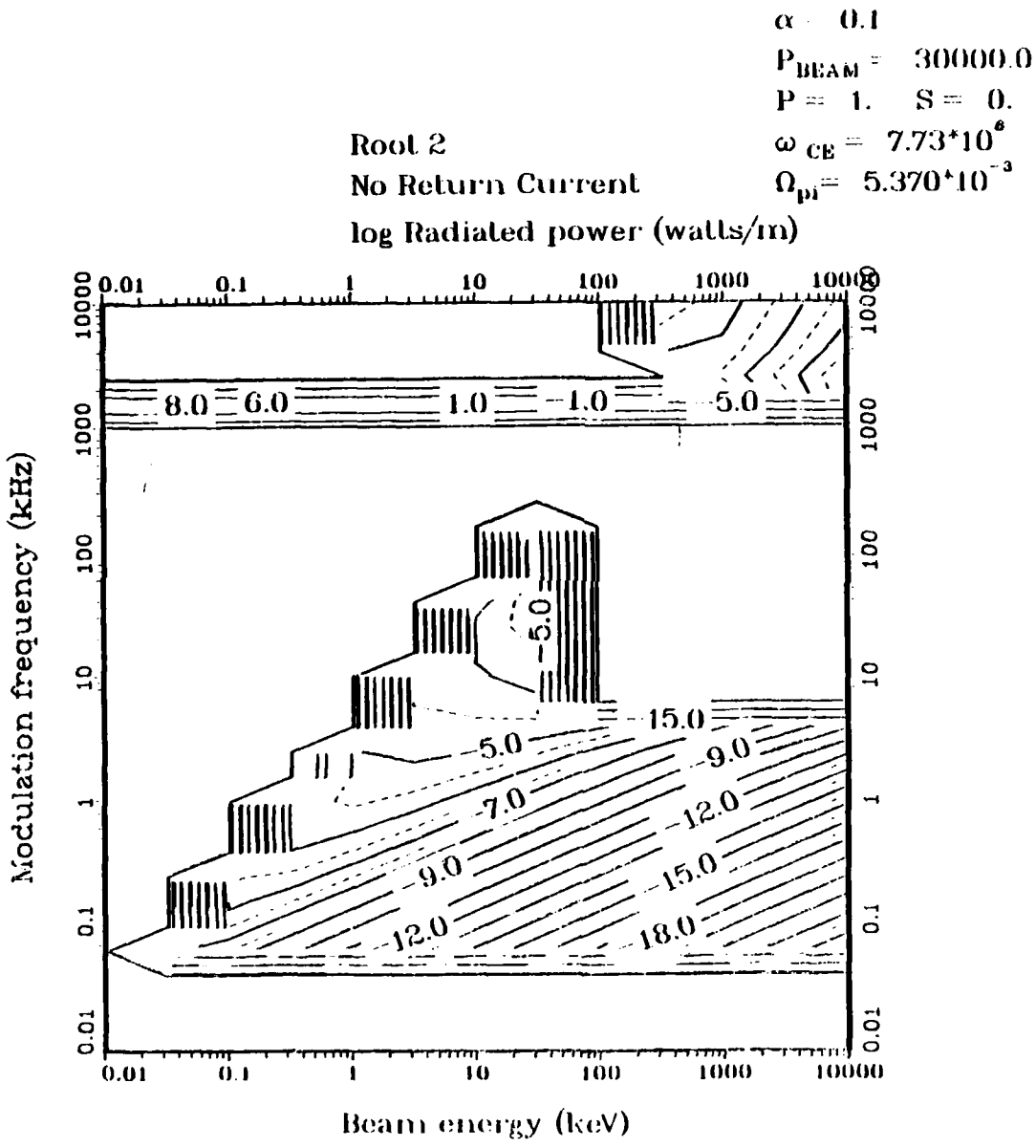

Fig. 44--Contours of nighttime radiated power at 200 km for 0.1 deg pitch angle (root 2, future gun).

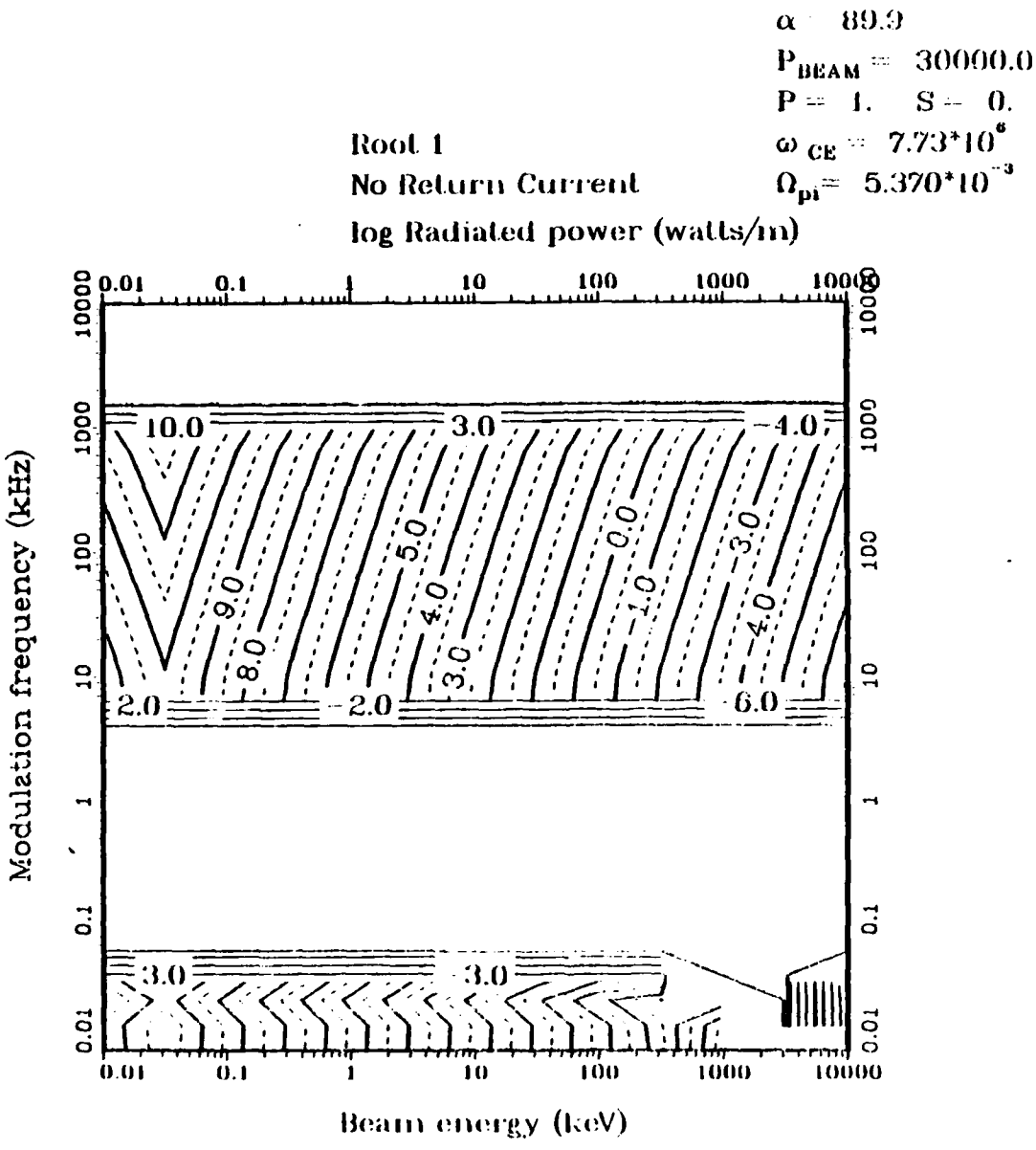

Fig. 45--Contours of nighttime radiated power at 200 km for 89.9 deg pitch angle (root 1, future gun).

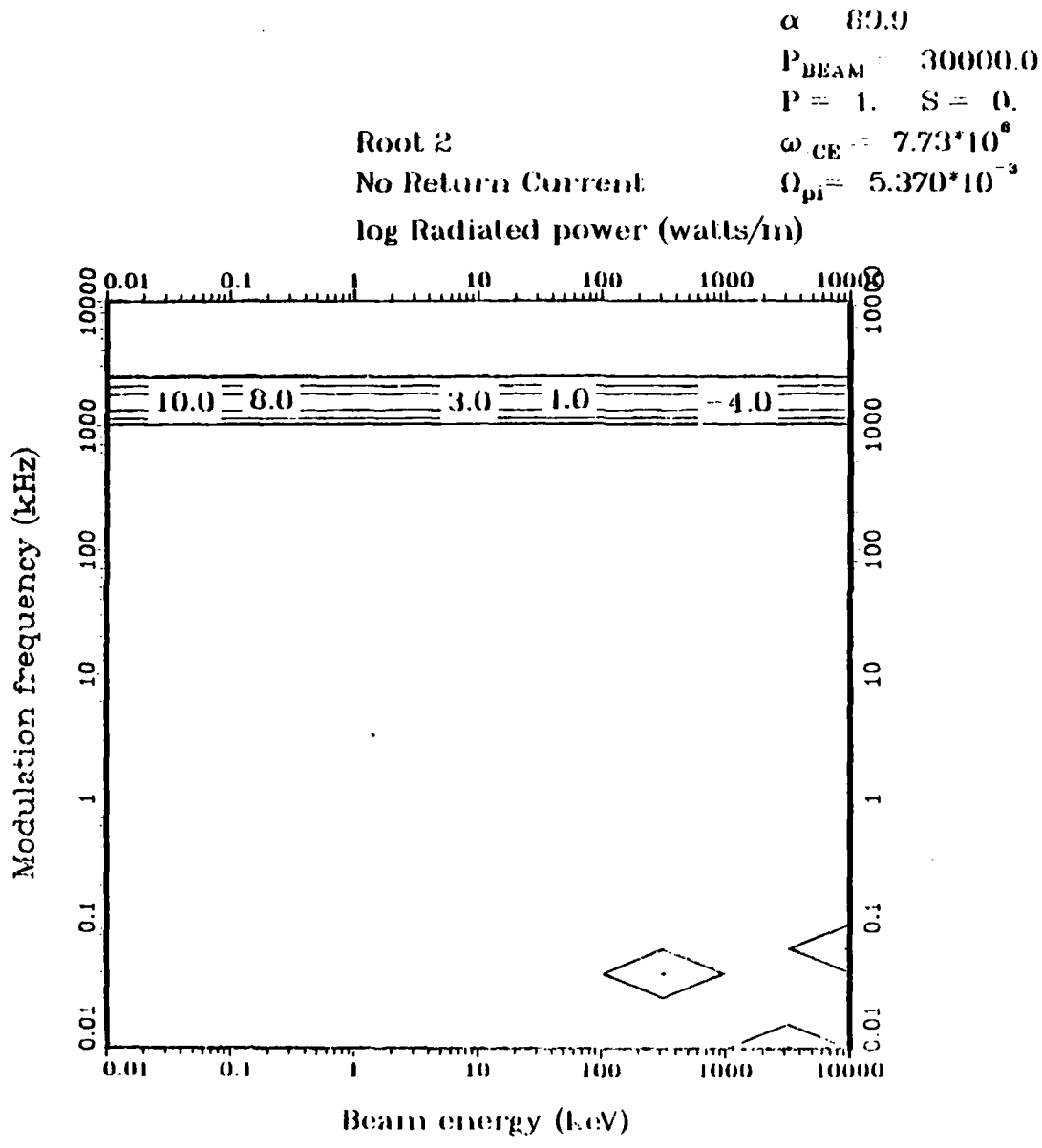

Fig. 46--Contours of nighttime radiated power at 200 km for 89.9 deg pitch angle (root 2, future gun).

that changing the pitch angle does not greatly affect the peak values of the structure in the radiated power, but increasing the pitch angle moves and stretches out the structures toward higher beam energies. Thus beams of higher energies (greater than 1 kV) may not radiate at zero pitch angle, but will radiate at pitch angles near 90 deg.

CHARACTERISTICS OF CYCLOTRON MODES

Figures 47 and 48 show the power radiated into the regular (s = 1) cyclotron mode for the daytime ionosphere. Figures 49 and 50 show the power into the anomalous (s = -1) cyclotron mode. Figures 51 through 54 represent the corresponding nighttime ionosphere. The assumed pitch angle in all these figures is 45 deg. The plots show that very little power goes into root 2, except for the nighttime case above 1 MHz. In that region, the power levels for regular cyclotron emission are about the same as for Cerenkov emission.

Figure 55 shows contours of the index of refraction at resonance for regular cyclotron emission using root 1 during the daytime. Near 1 MHz, the index of refraction varies from 900 at 10 eV to about 3 at 10 keV. Near 10 kHz, it ranges from 200 at the low energy end to about 20 at 10 keV. Inside the rectangular region thus defined, the power levels for regular cyclotron emission are about 2 orders of magnitude less than for Cerenkov emission.

For anomalous cyclotron emission into root 1, the power levels on the central plateau are also about 2 orders of magnitude less than for Cerenkov emission. The plateau is stretched out to higher energies at reduced power. Values for the index of refraction are comparable to the case of regular cyclotron emission.

The power levels at frequencies less than 60 Hz are much larger than those for Cerenkov emission. However, the resonant index of refraction is also much larger--about 10^{10}. As the wave travels from the ionosphere to the ground it enters a region where the index of refraction is one, and therefore it has a high probability of total internal reflection. Apparently, the cyclotron modes will be important for ionosphere to ground communication only for frequencies above several hundred kilohertz at moderate electron beam energies, or above 10 kHz for near-relativistic electron beams.

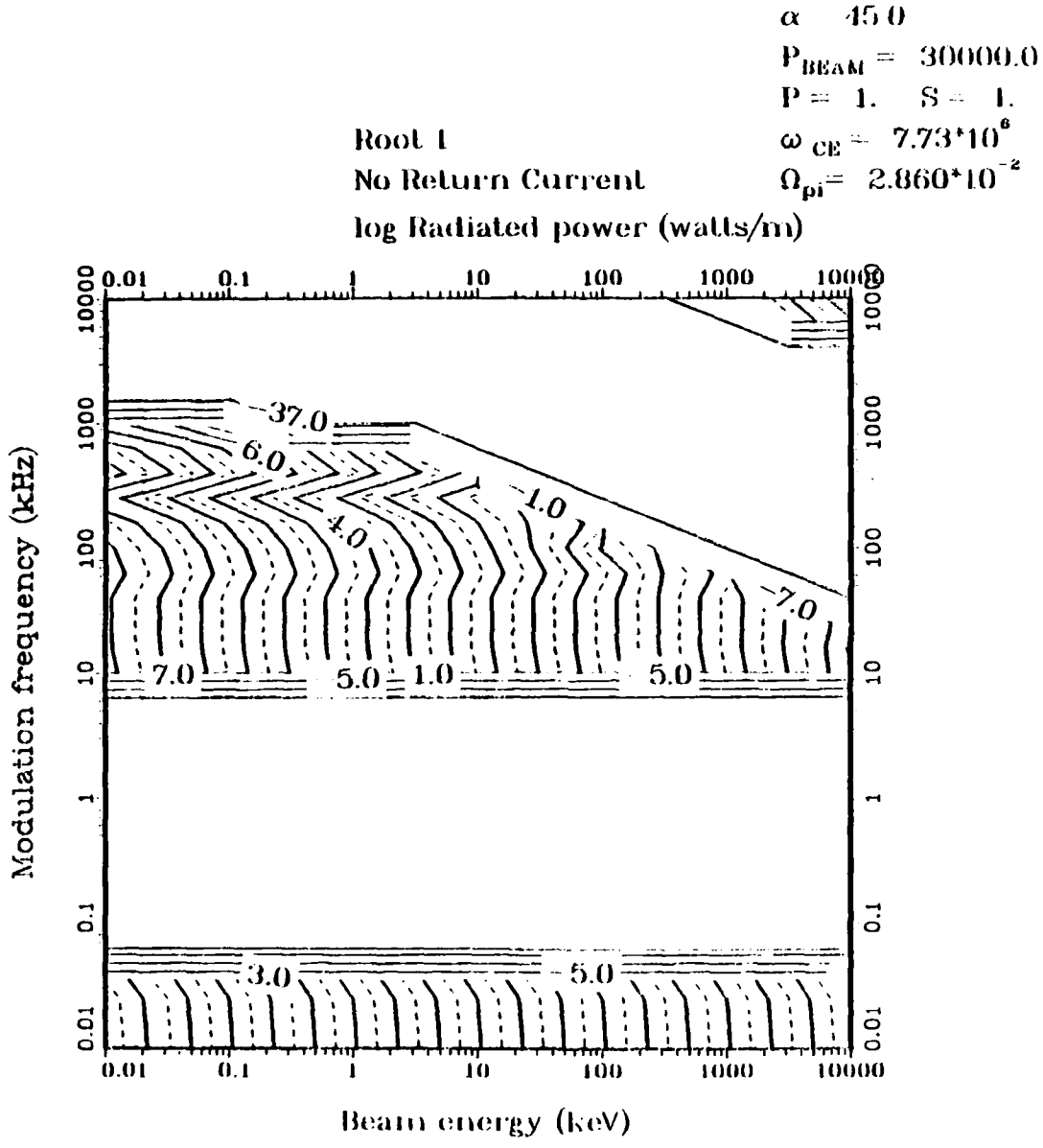

Fig. 47--Power into regular cyclotron mode for daytime ionosphere at 200 km (root 1, future gun).

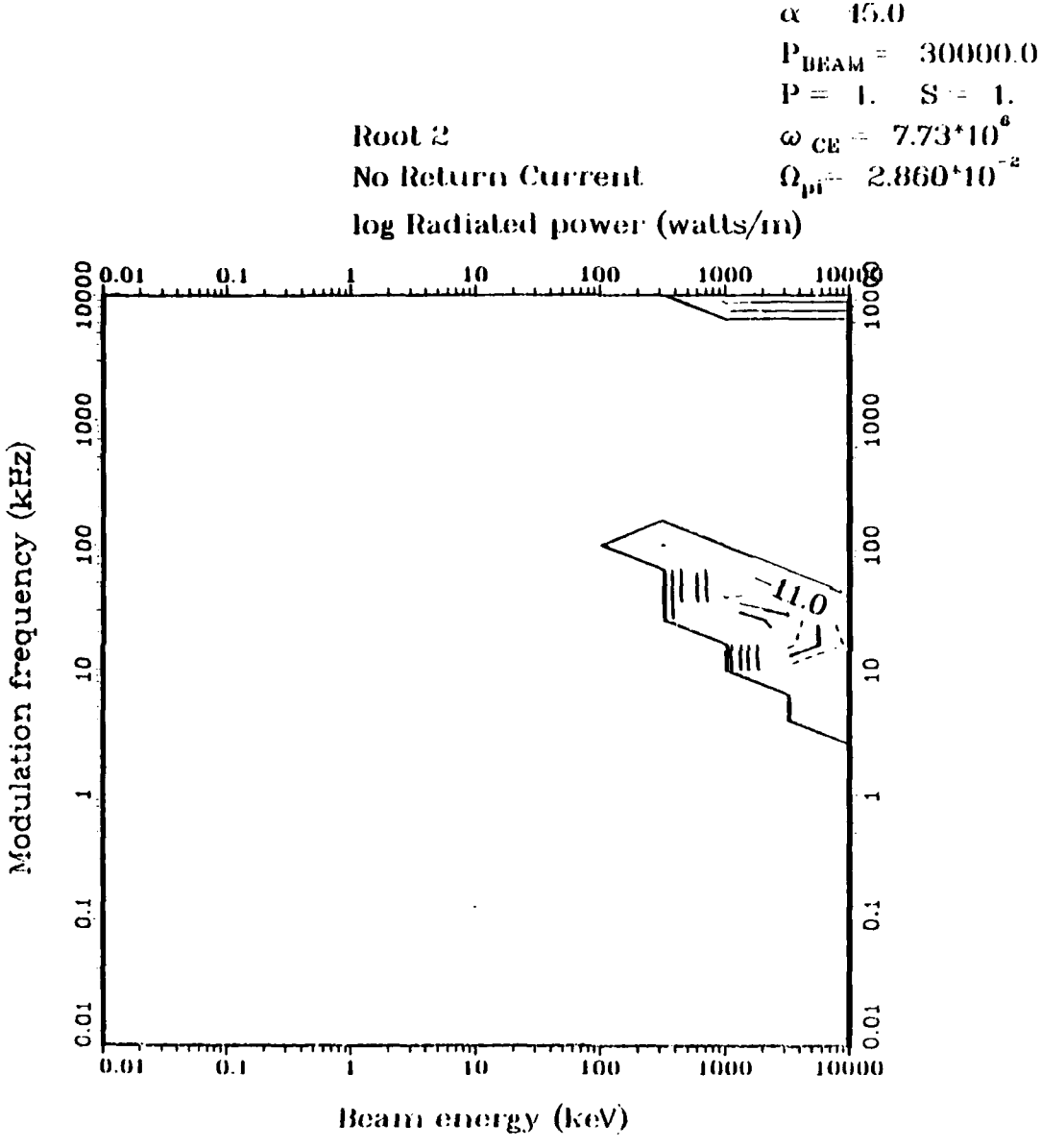

Fig. 48--Power into regular cyclotron mode for daytime ionosphere at 200 km (root 2, future gun).

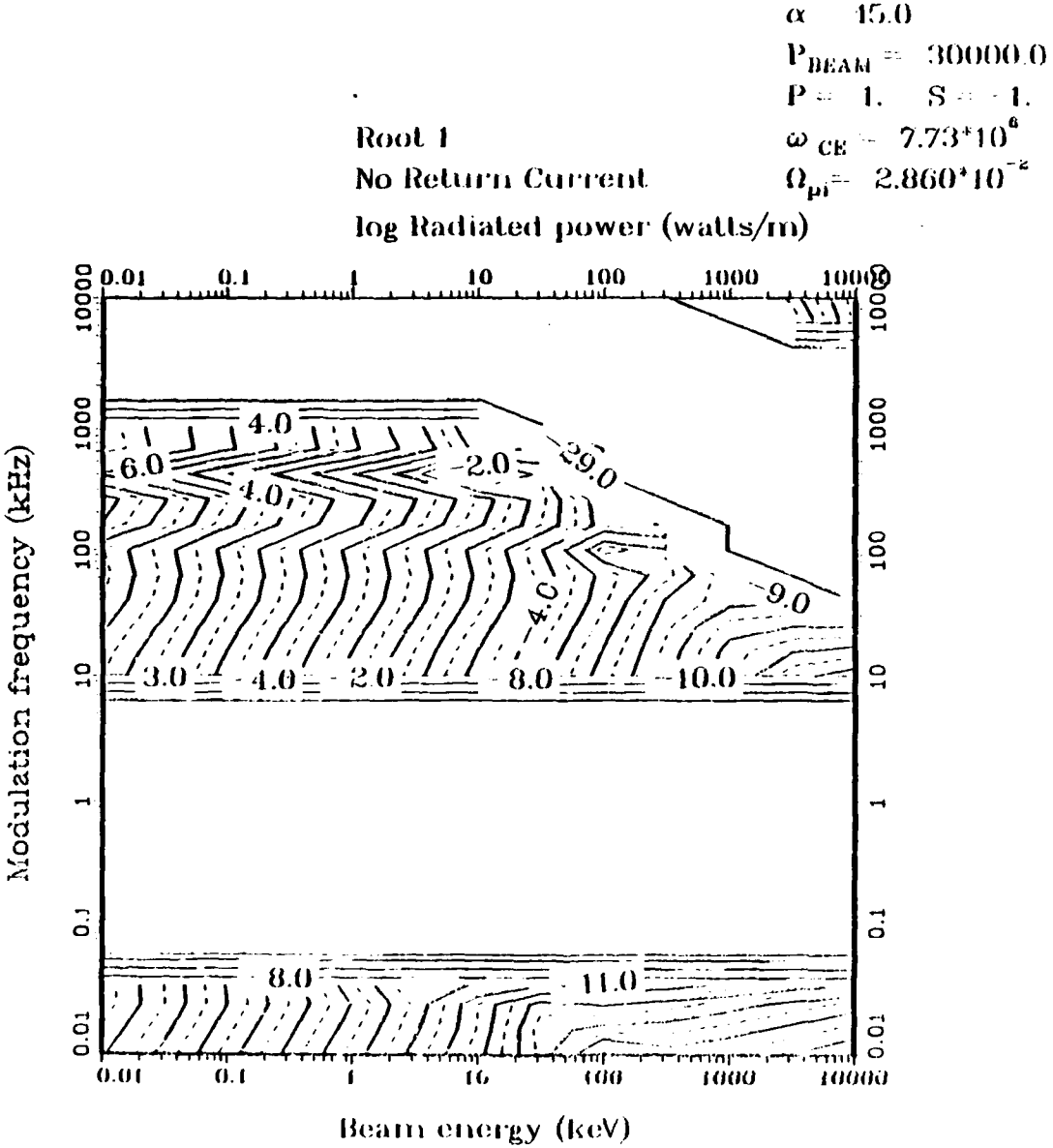

Fig. 49--Power into anomalous cyclotron mode for daytime ionosphere at 200 km (root 1, future gun).

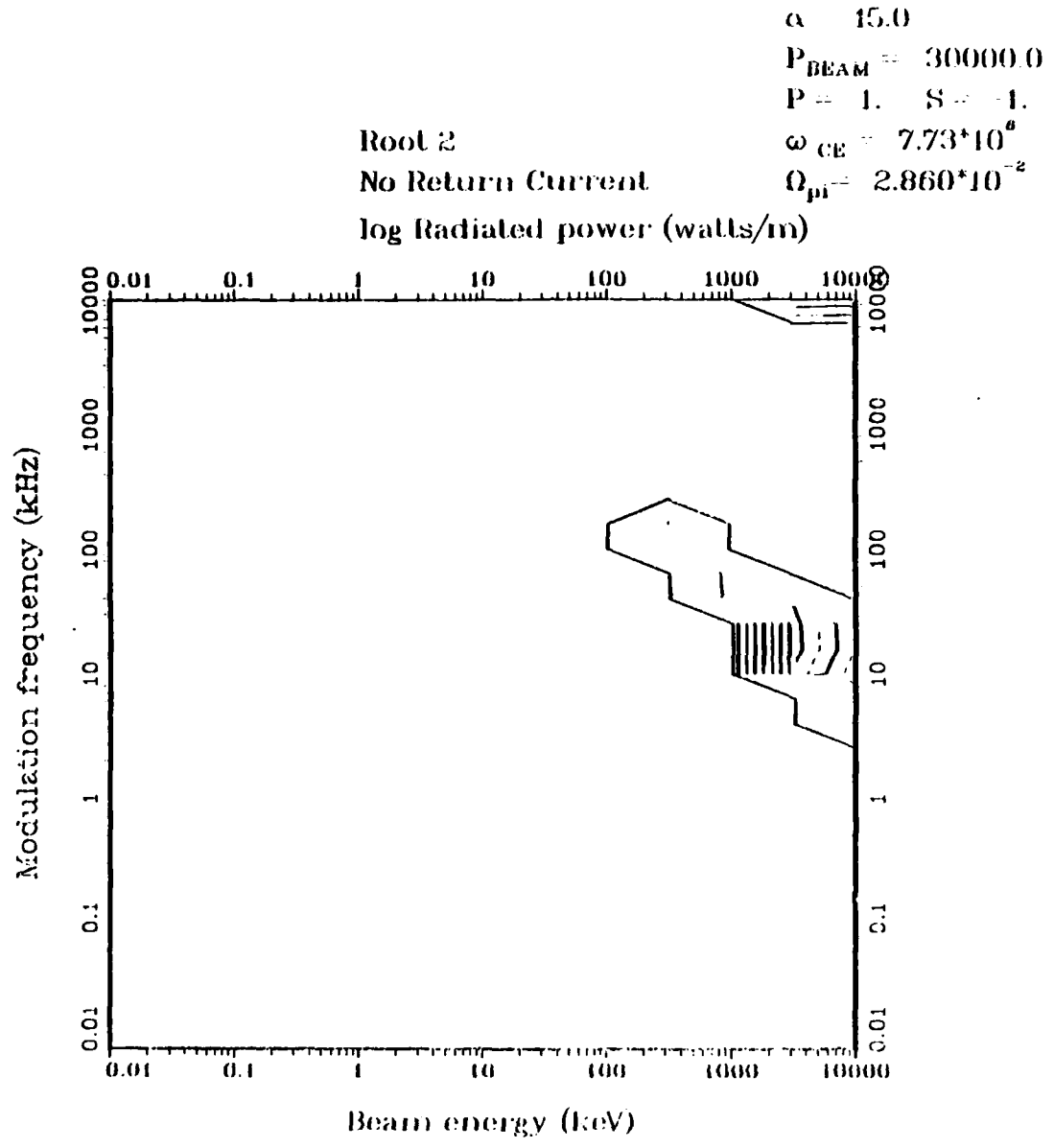

Fig. 50--Power into anomalous cyclotron mode for daytime ionosphere at 200 km (root 2, future gun).

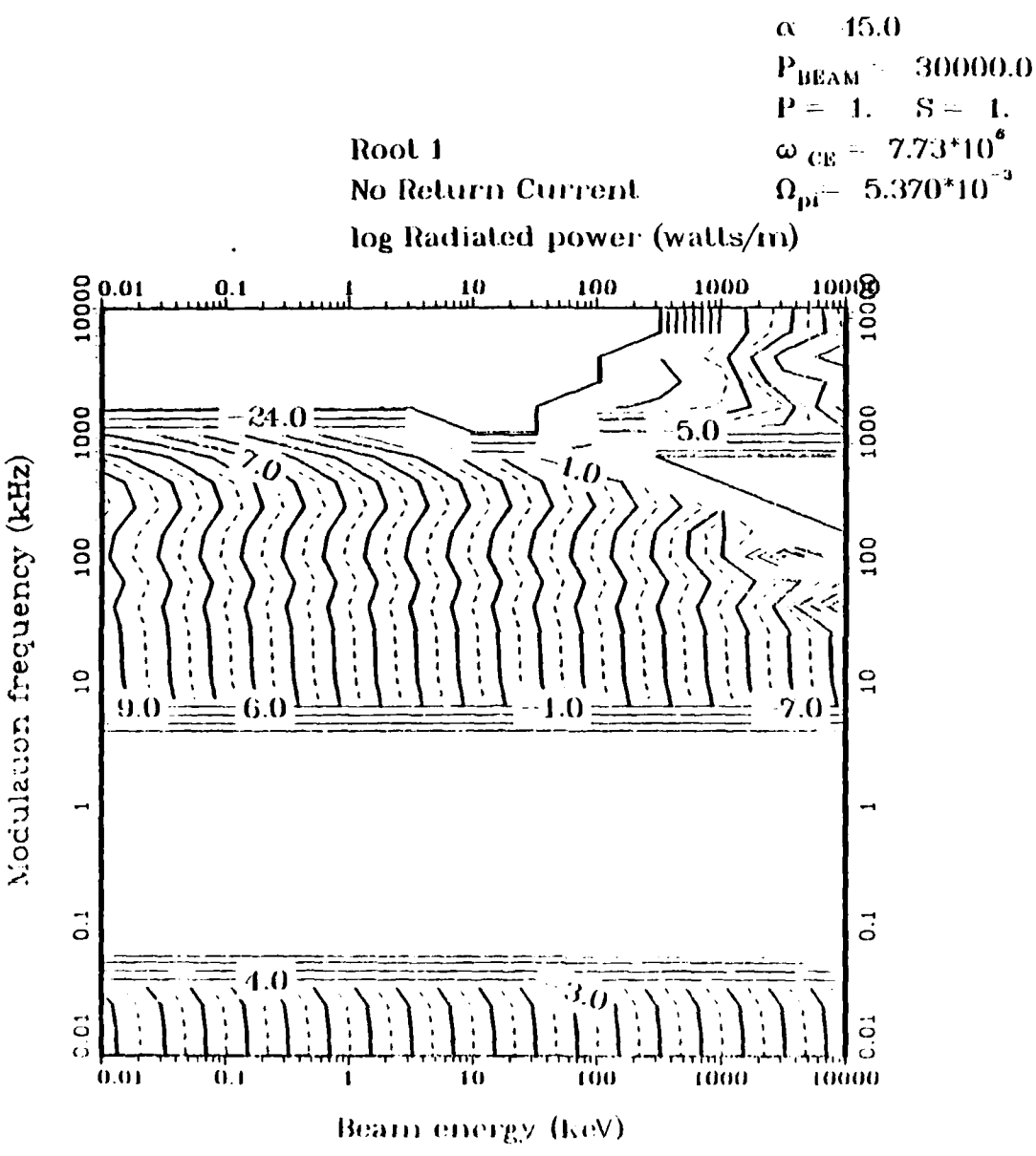

Fig. 51--Power into regular cyclotron mode for nighttime ionosphere at 200 km (root 1, future gun).

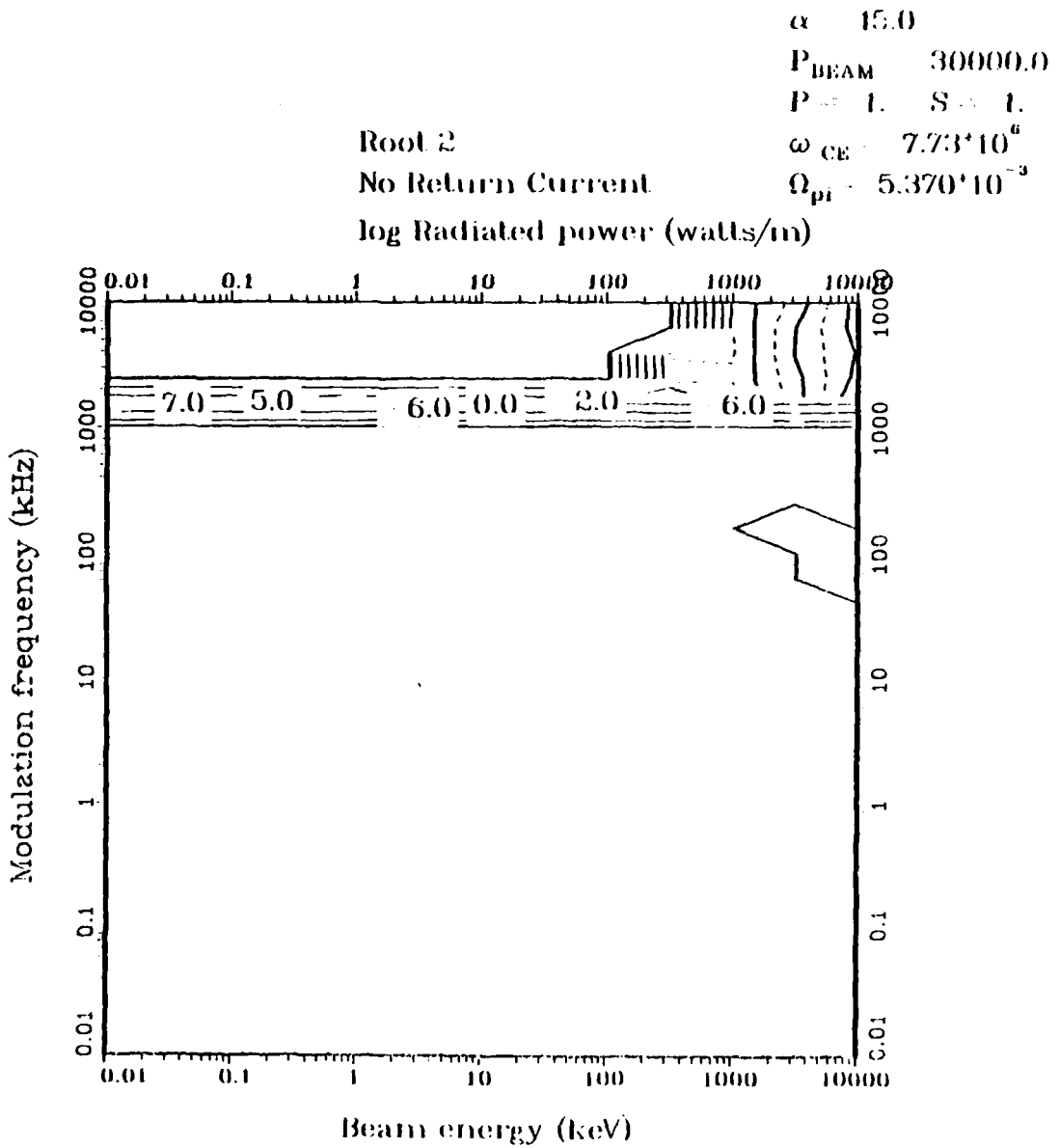

Fig. 52--Power into regular cyclotron mode for nighttime ionosphere at 200 km (root 2, future gun).

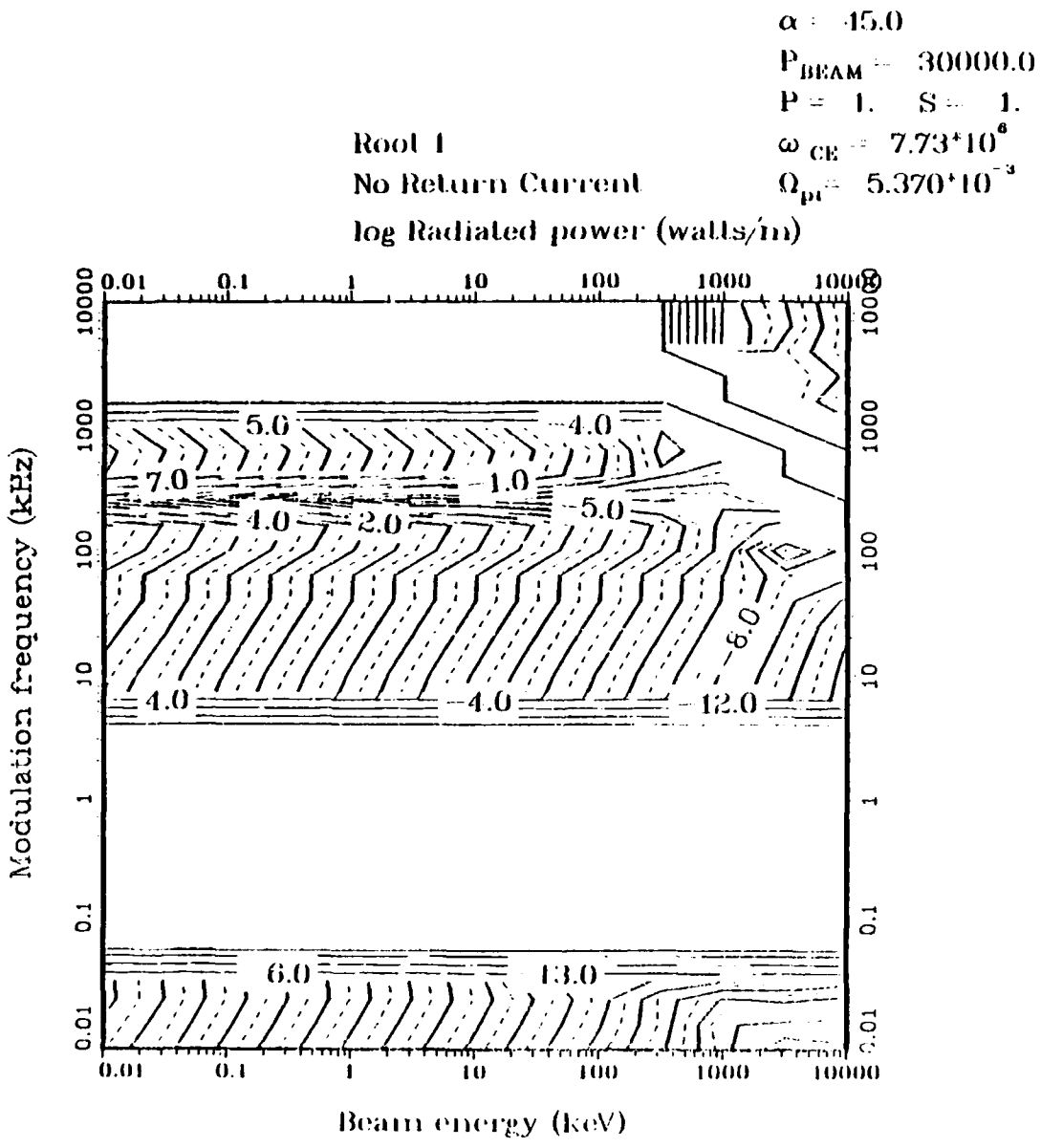

Fig. 53--Power into anomalous cyclotron mode for nighttime ionosphere at 200 km (root 1, future gun).

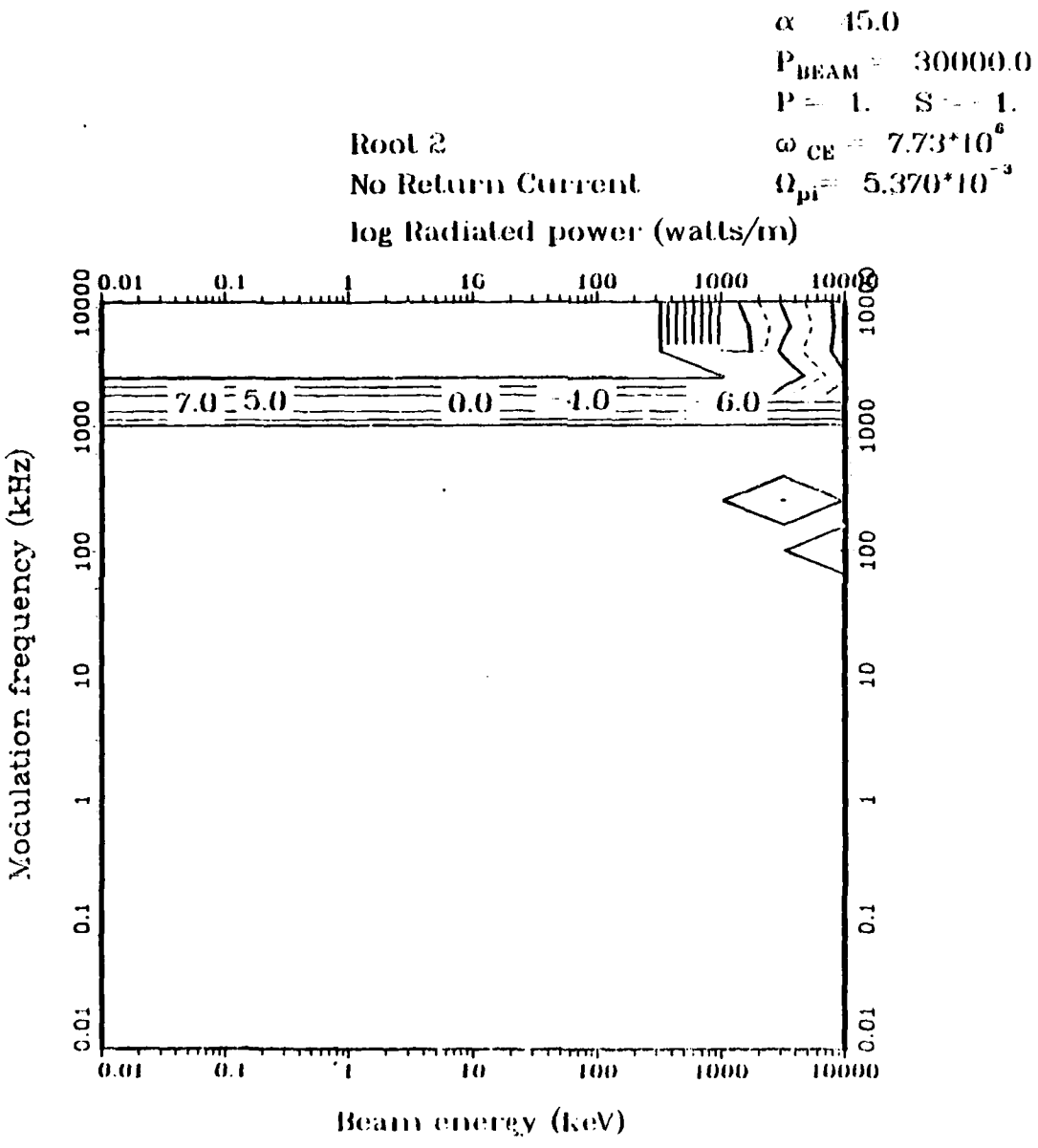

Fig. 54--Power into anomalous cyclotron mode for nighttime ionosphere at 200 km (root 2, future gun).

α = 45.0
P_{BEAM} = 30000.0
P = 1. S = 1.
ω_{CE} = $7.73*10^{6}$
Ω_{Pi} = $2.860*10^{-2}$

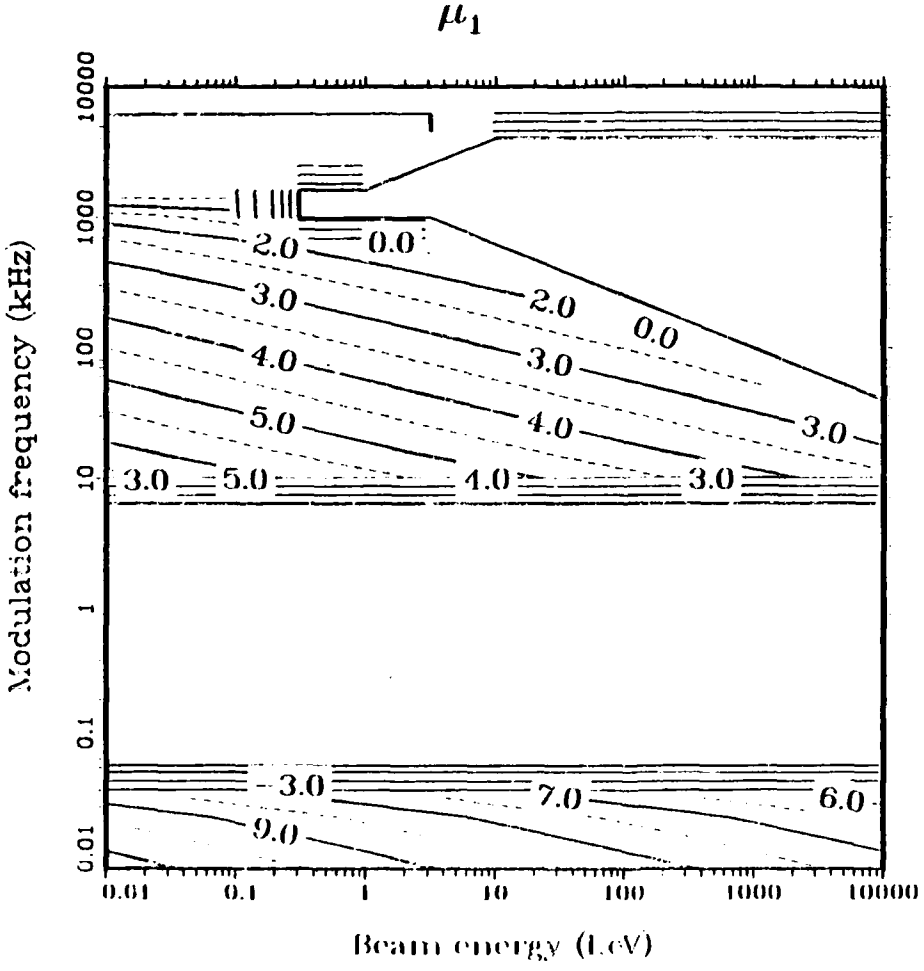

Fig. 55--Resonant value of index of refraction for regular cyclotron mode at 200 km during daytime (root 1, future gun).

EFFECT OF RETURN CURRENT

Presently, no adequate theory predicts the distribution of current that returns to a rocket or spacecraft to neutralize the positive charge built up as an electron beam leaves an electron gun. Harker[6] has suggested that a worst-case estimate of the effect on the radiation could be modeled within the framework of his theory by supposing that the parallel components of the emitted current are completely canceled by the return current. The expression for the radiated power [Eqs. (3) and (4)] is then evaluated using only the terms that involve the perpendicular component of the velocity. As might be imagined, the radiated power is drastically reduced for pitch angles close to 0 deg. At 45 deg (as Figs. 56 and 57 show), for emission into the nighttime ionosphere at 200 km, the root 1 levels are reduced by 9 orders of magnitude on the central plateau but by less than a factor of 2 below 60 Hz. These figures should be compared with those for no return current--Figs. 14 and 16. The power levels on root 2 are reduced by 1 order of magnitude in the central region and by 5 or 6 orders of magnitude above 1 MHz. Daytime results are similar.

Although this is a worst-case estimate in the context of Harker's[6] theory, it is not based on a self-consistent calculation of the electric fields built up around a spacecraft or rocket or within the electron beam itself. To our knowledge, such a calculation has not been done. Some researchers believe that any return current will involve electrons moving at much lower velocities along various trajectories and very little cancellation of the parallel current will occur. (See, for example, Lavergnat and Lehner.[7])

The collisional slowing and broadening of the electron beam is related to the return current. At 100 km, the collisional effects may be severe, yielding a radiated power lower than that given in this report. A detailed radiation emission and propagation calculation should include electron collisions for beam injection at low altitudes.

CONSTANT BEAM CURRENT

In all the calculations presented here, the power in the electron beam was a constant 30 kW. A subset of the parameter study was also

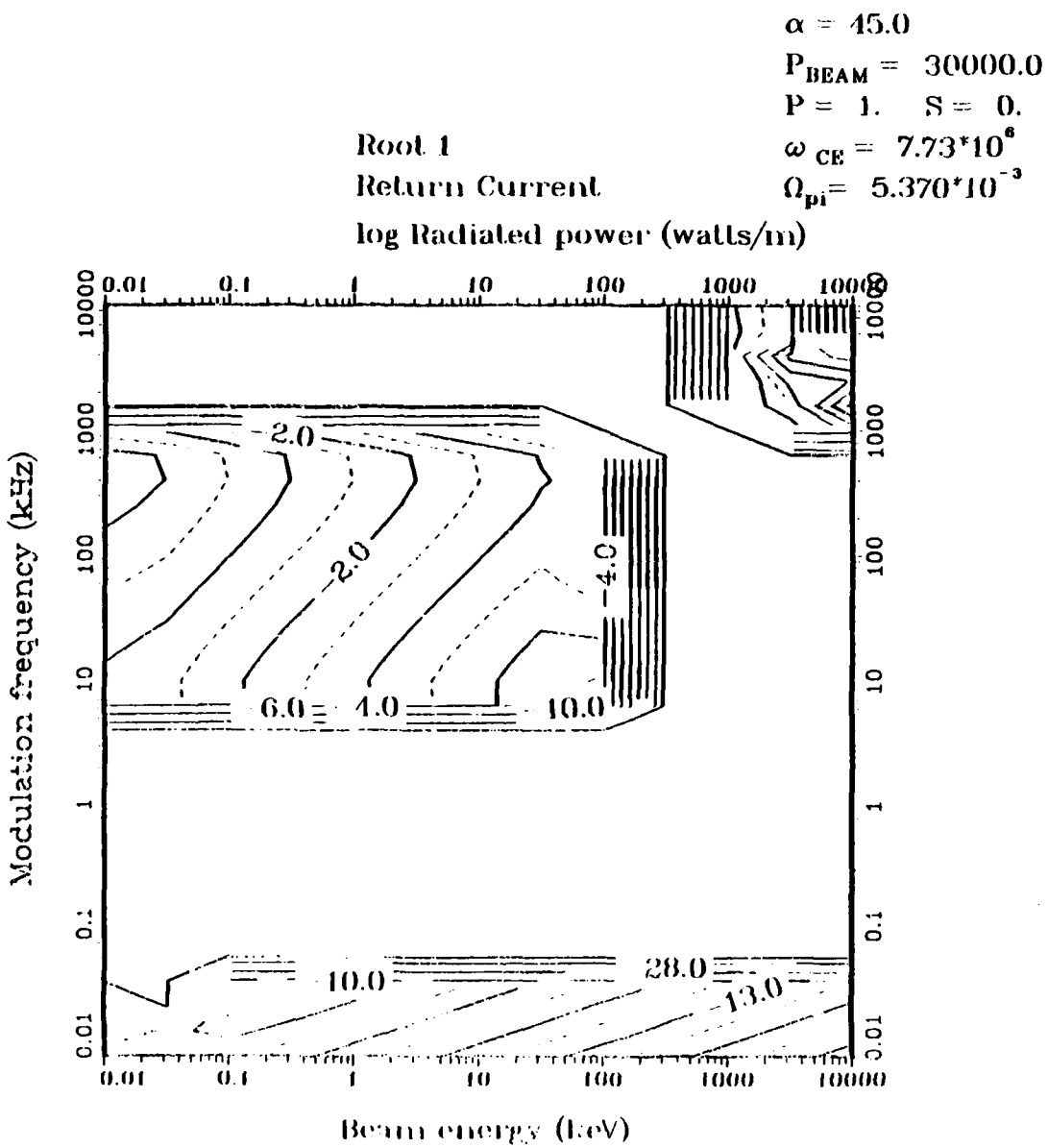

Fig. 56--Nighttime radiated power calculated with only perpendicular velocity terms (root 1).

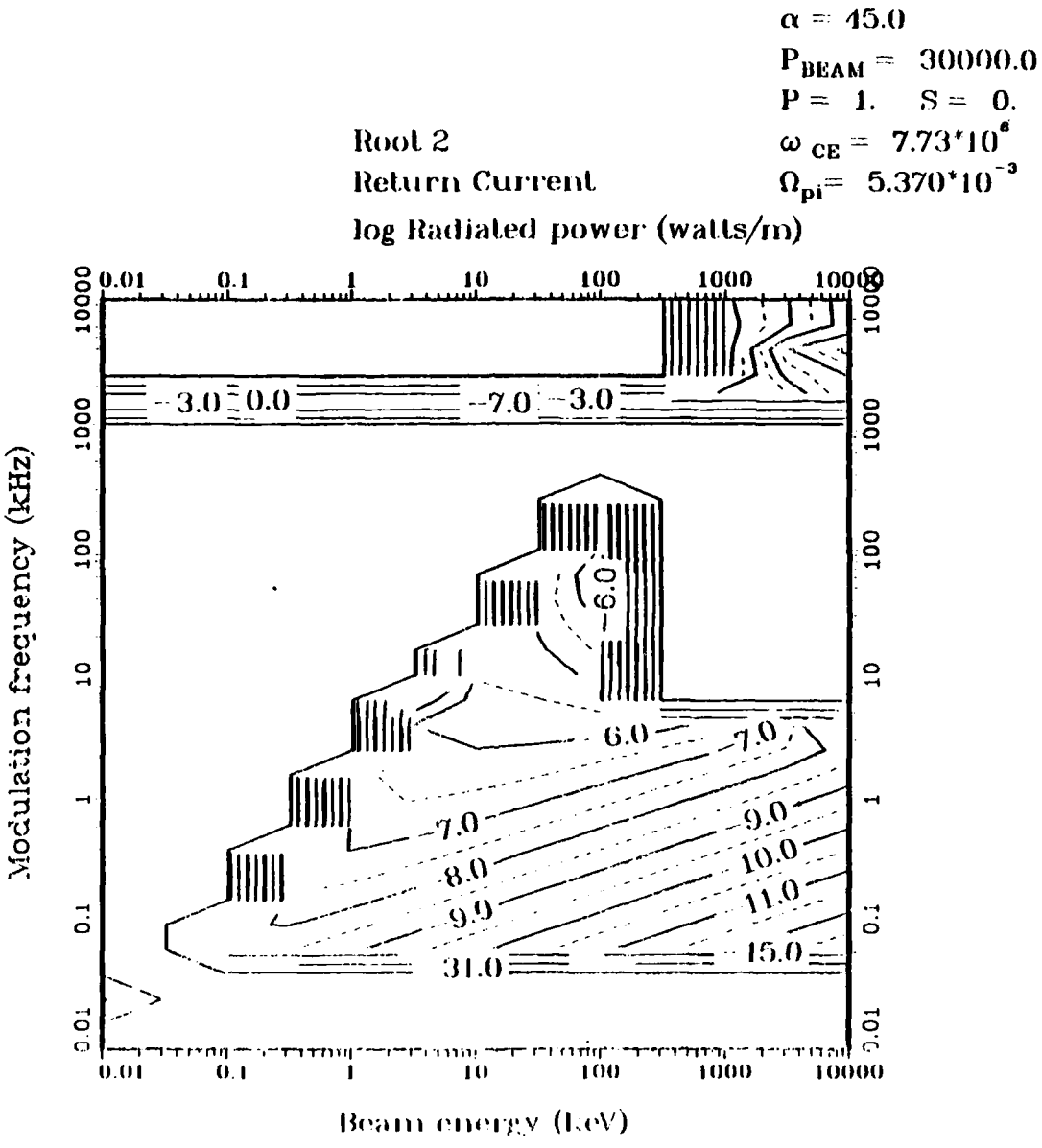

Fig. 57--Nighttime radiated power calculated with only perpendicular velocity terms (root 2).

performed for constant beam current at 100 A. Figures 58 through 61 show the results for Cerenkov emission with a pitch angle of 45 deg into the nighttime ionosphere at 200 km. In Figs. 58 through 61, the beam power is 30 kW at beam energy of 0.3 keV. The beam power is, of course, higher or lower than 30 kW at higher or lower energies, respectively. The peak radiated power at higher energies is, therefore, higher than that shown in Figs. 13 through 16, and lower at lower energies, for emission at constant beam power. The constant current calculation has an additional feature--it gives the sum of the radiated power into the frequencies and first five odd harmonics. For that reason the forbidden region for root 1 below 1 kHz appears to be narrower than the calculations at constant beam power would indicate and an additional allowed band is seen in root 2 above 100 kHz. The higher harmonics in the square wave electron beam current evidently excited allowed electromagnetic modes although the fundamental was in a forbidden region. (Note that the plots show the beam modulation frequency, not the radiation frequency, which in the band from 100 to 4 kHz, is above 1 MHz.)

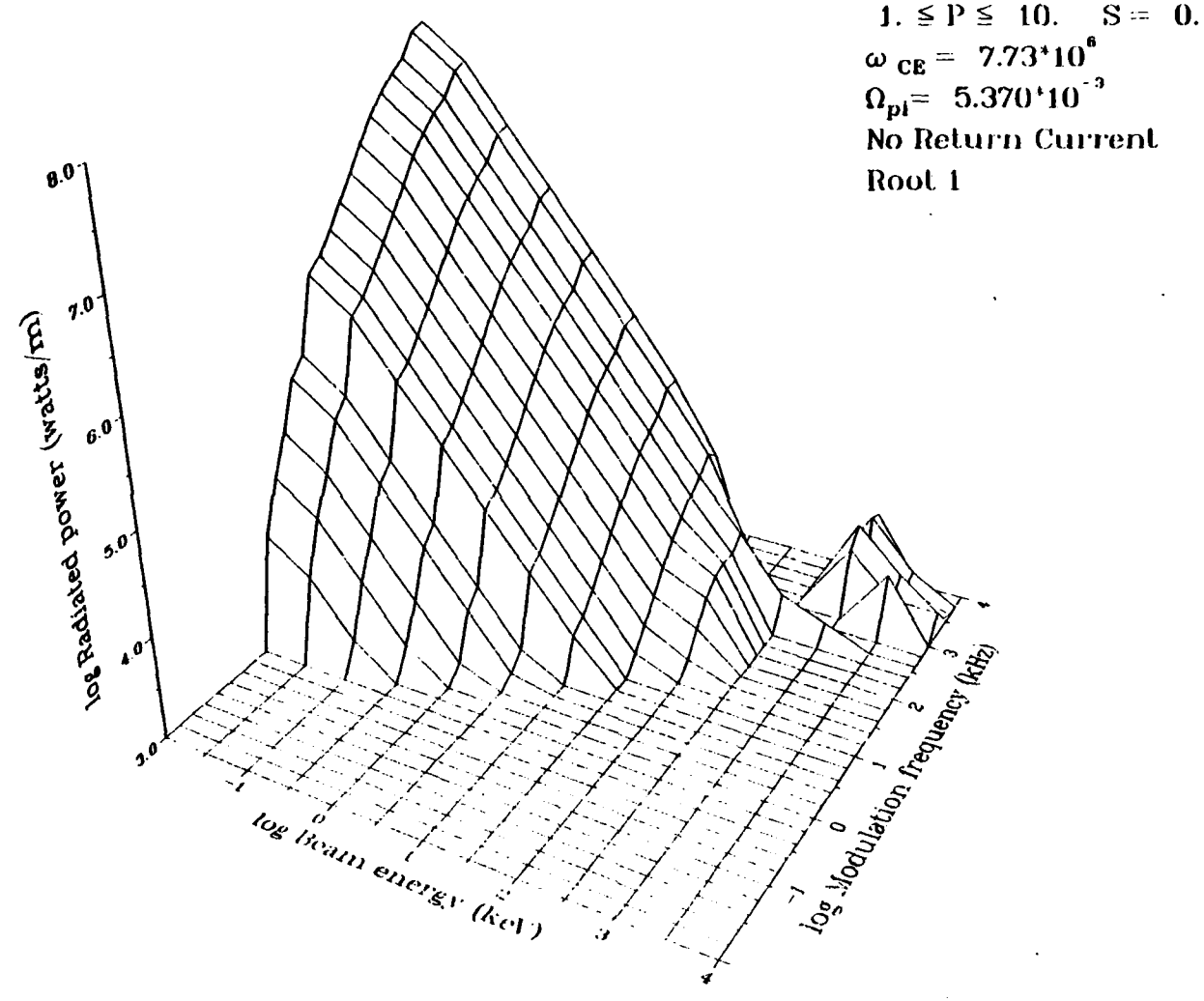

Fig. 58--Nighttime radiated power at 200 km for 45 deg pitch angle and beam current 100 A (root 1, future gun).

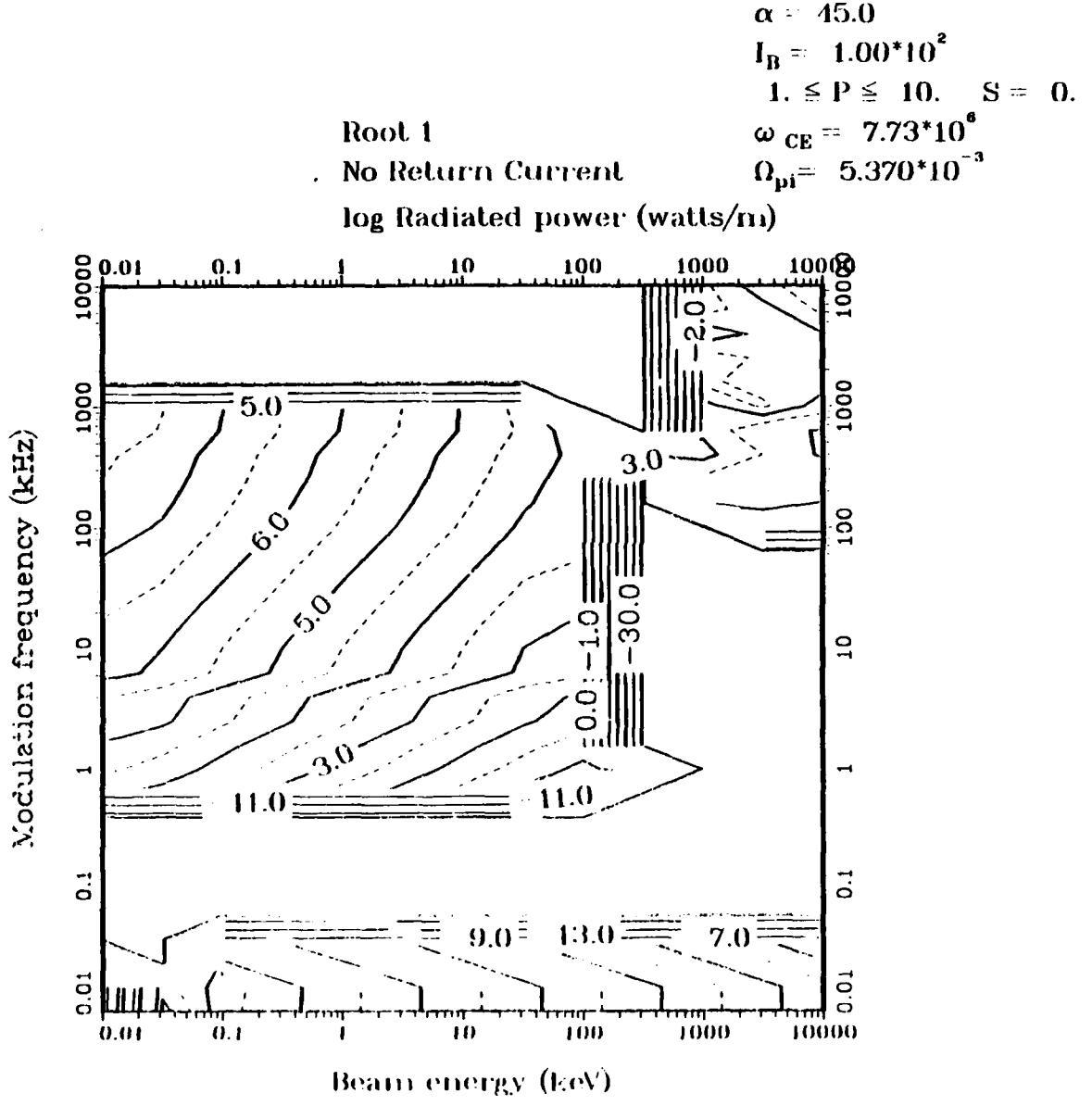

Fig. 59--Contours of nighttime radiated power at 200 km for 45 deg pitch angle and beam current 100 A (root 1, future gun).

α = 45.0
I_B = $1.00*10^2$
1. ≤ P ≤ 10. S = 0.
ω_{CE} = $7.73*10^6$
Ω_{pi} = $5.370*10^{-3}$
No Return Current
Root 2

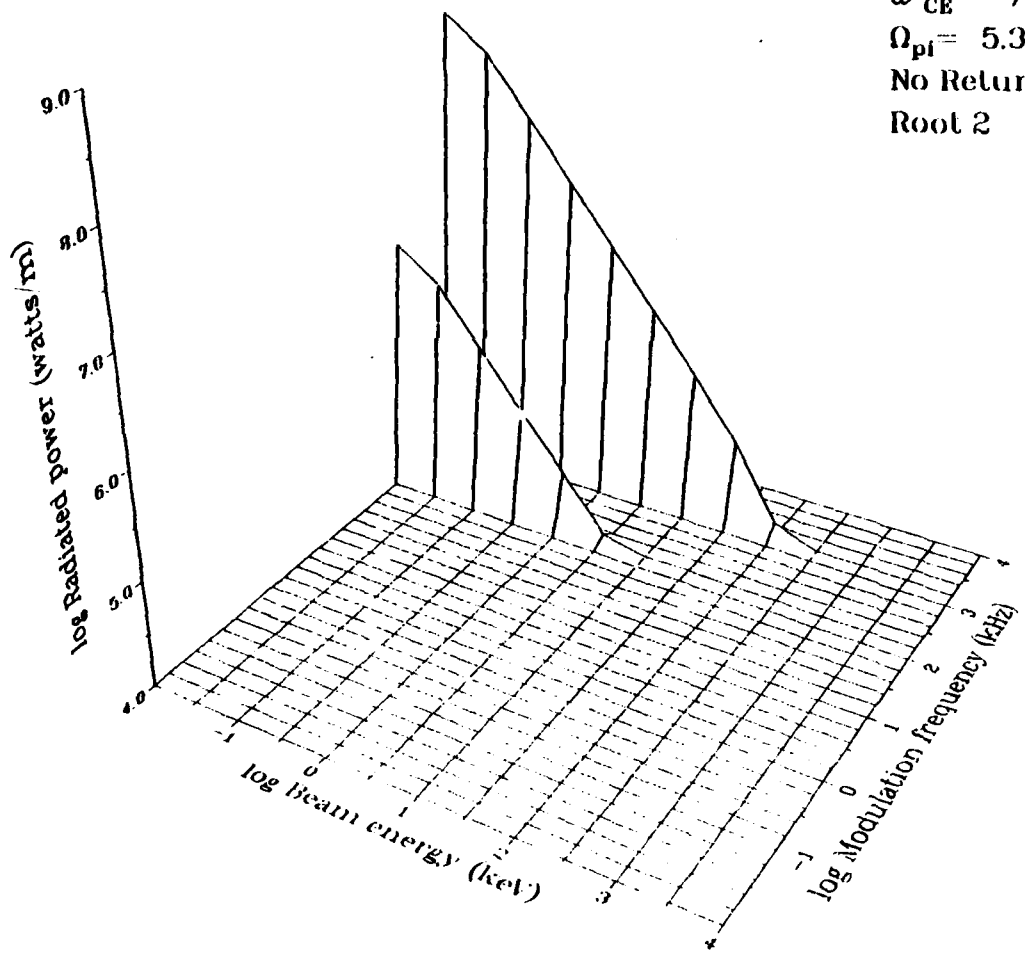

Fig. 60--Nighttime radiated power at 200 km for 45 deg pitch angle and beam current 100 A (root 2, future gun).

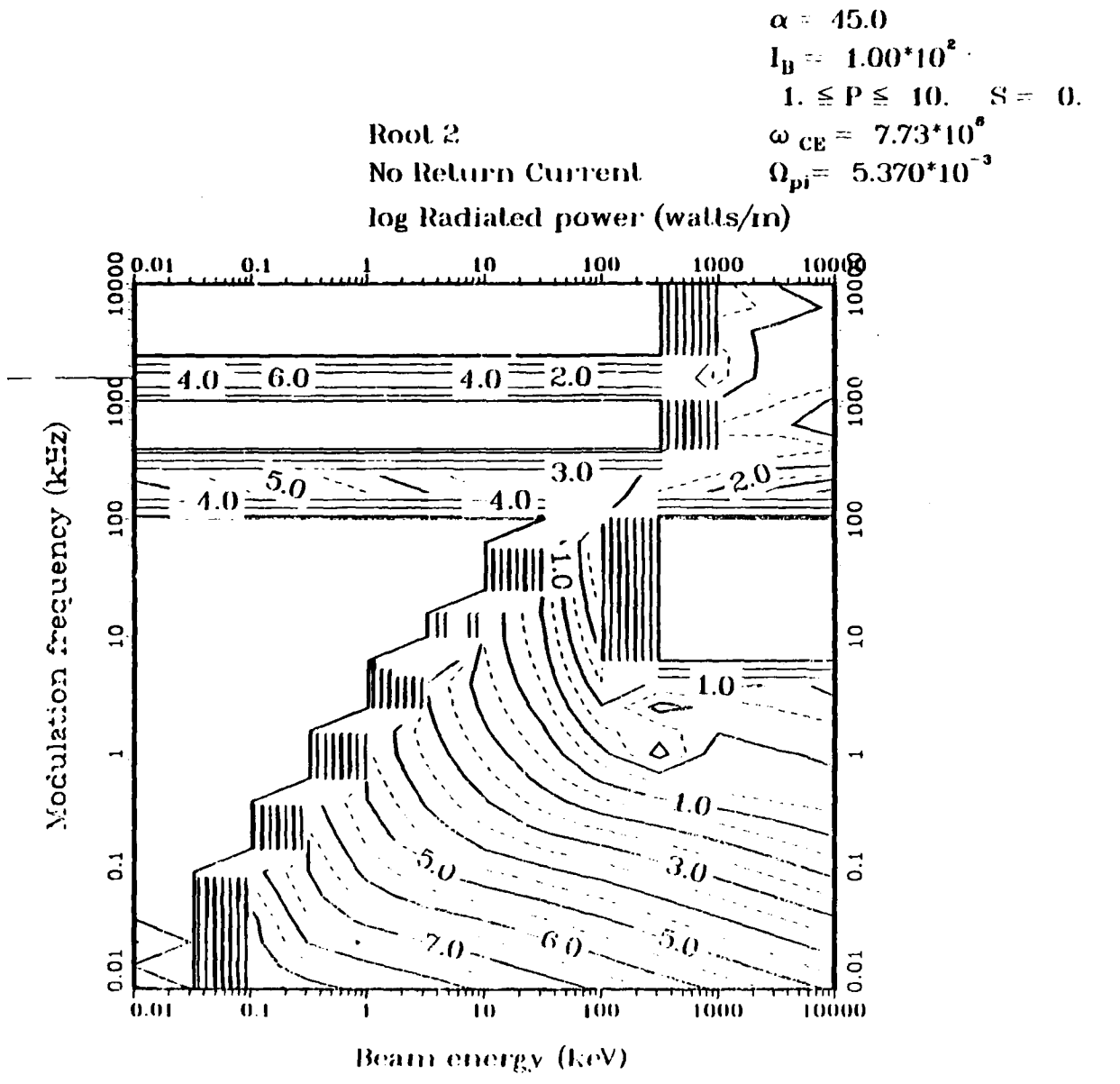

Fig. 61--Contours of nighttime radiated power at 200 km for 45 deg pitch angle and beam current 100 A (root 2, future gun).

IV. BERT-I

Plans call for the BERT-I rocket to be launched at night from White Sands, New Mexico and to travel in a northerly direction reaching an apogee of 230 km. An electron beam will be ejected perpendicular to the rocket axis, and the rocket will be spinning during the ejection. If the rocket is traveling due north during the beam ejection, pitch angles from about 25 to 155 deg will be swept out.

The electron gun can eject currents of 0.02, 0.2, 2.0, and 20 mA at energies of 0.5, 1, and 2 keV.[8] It may be possible to modulate the beam using a square wave up to a frequency of 1 kHz. One kilohertz is below the central plateau for root 1 emission, so to estimate the maximum possible power going into higher harmonics, the radiation up to the tenth harmonic is kept in the BERT-I calculation. Table 2 summarizes the ionospheric parameters assumed for the purpose of the calculation.

TABLE 2.

Ionospheric Parameters for BERT-I Calculation.

Electron Gyrofrequency (Hz)	Ion Gyro-frequency (Hz)	Time	Electron Plasma Frequency (Hz)	Ion Plasma Frequency (Hz)	Lower Hybrid Frequency (Hz)
1.36×10^6	46.1	Night	1.77×10^6	1.05×10^4	7.92×10^3

Plots were generated for pitch angles of 30, 60, and 89.9 deg. The extremes, 30 and 89.9 deg, are shown in Figs. 62 through 69. Two regions are of interest: one at frequencies lower than 50 Hz, the other near 1 kHz. Figures 62 through 69 show the power radiated into root 1 below 50 Hz. The values are quite small--between 10^{-17} and 10^{-16} W/m. The radiation into root 2 is somewhat higher in this region, and more power goes into higher harmonics than into the fundamental.

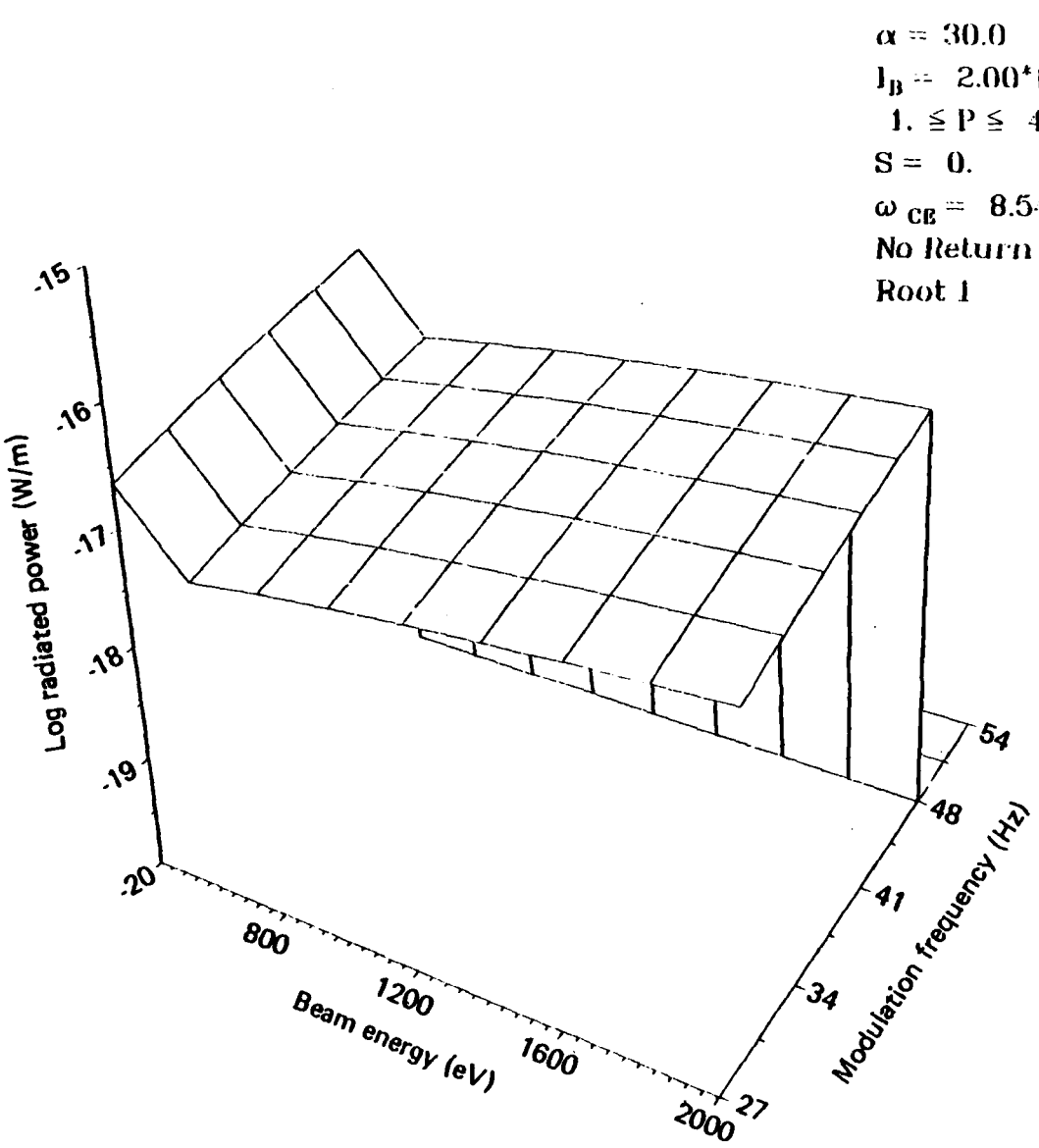

Fig. 62--Radiated power for BERT-I below 50 Hz, 30 deg pitch angle .

$\alpha = 30.0$

$I_B = 2.00 * 10^{-2}$

$1. \leq P \leq 40.$

$S = 0.$

$\omega_{CE} = 8.5450 * 10^{6}$

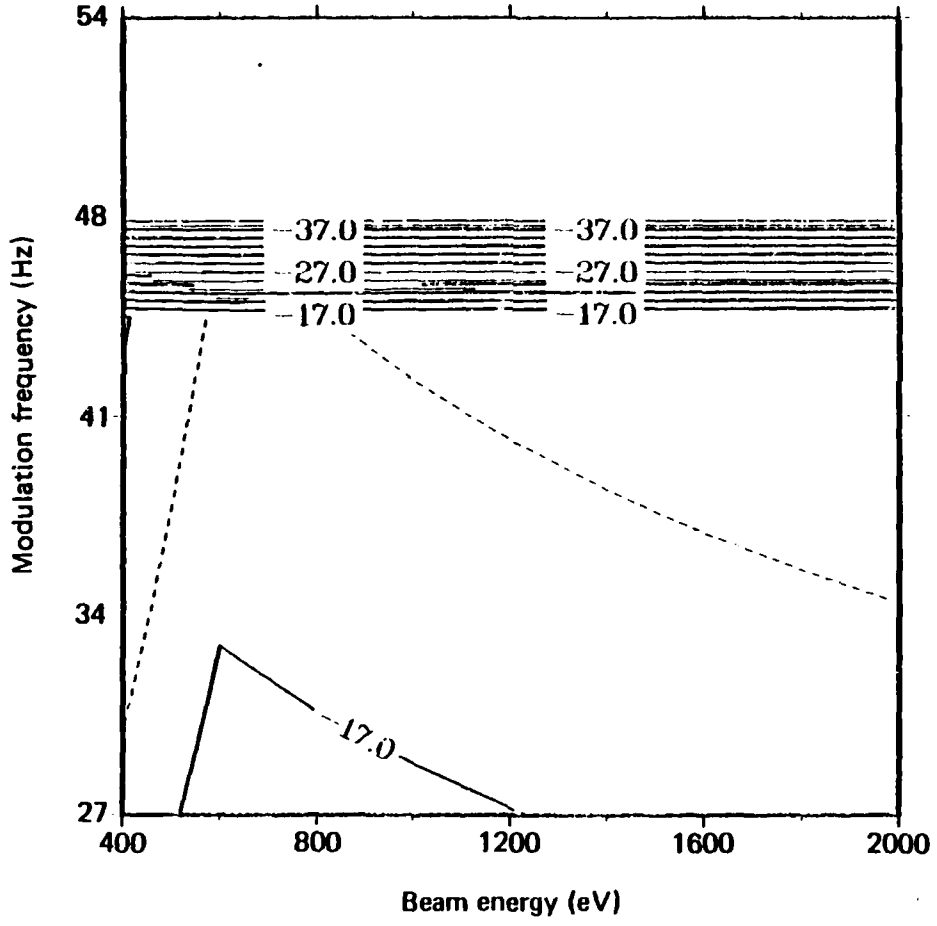

Fig. 63--Contours of radiated power for BERT-I below 50 Hz, 30 deg pitch angle.

AD-A157 810 EXPERIMENTS IN LONG-WAVELENGTH COMMUNICATION USING MODULATED ELECTRON BEA..(U) PACIFIC-SIERRA RESEARCH CORP LOS ANGELES CA L E JOHNSON AUG 85 PSR-1513 2/2

UNCLASSIFIED RADC-TR-85-133 DNA001-84-C-0288 F/G 20/7 NL

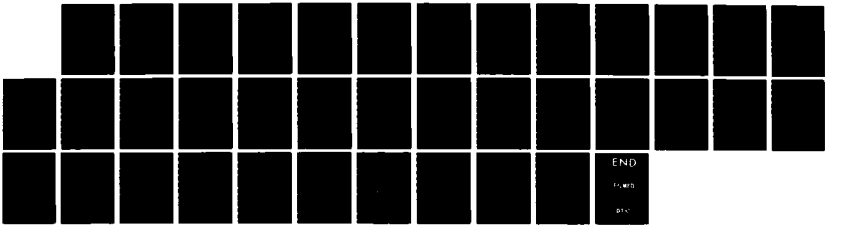

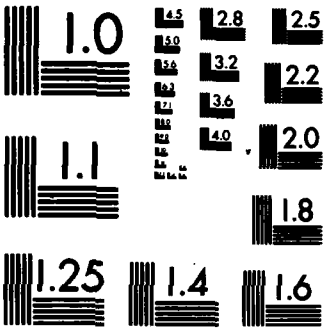

MICROCOPY RESOLUTION TEST CHART

)ARDS-1963-A

$\alpha = 89.9$
$I_B = 2.00*10^{-2}$
$1. \leq P \leq 40.$
$S = 0.$
$\omega_{CB} = 8.5450*10^{8}$
No Return Current
Root 1

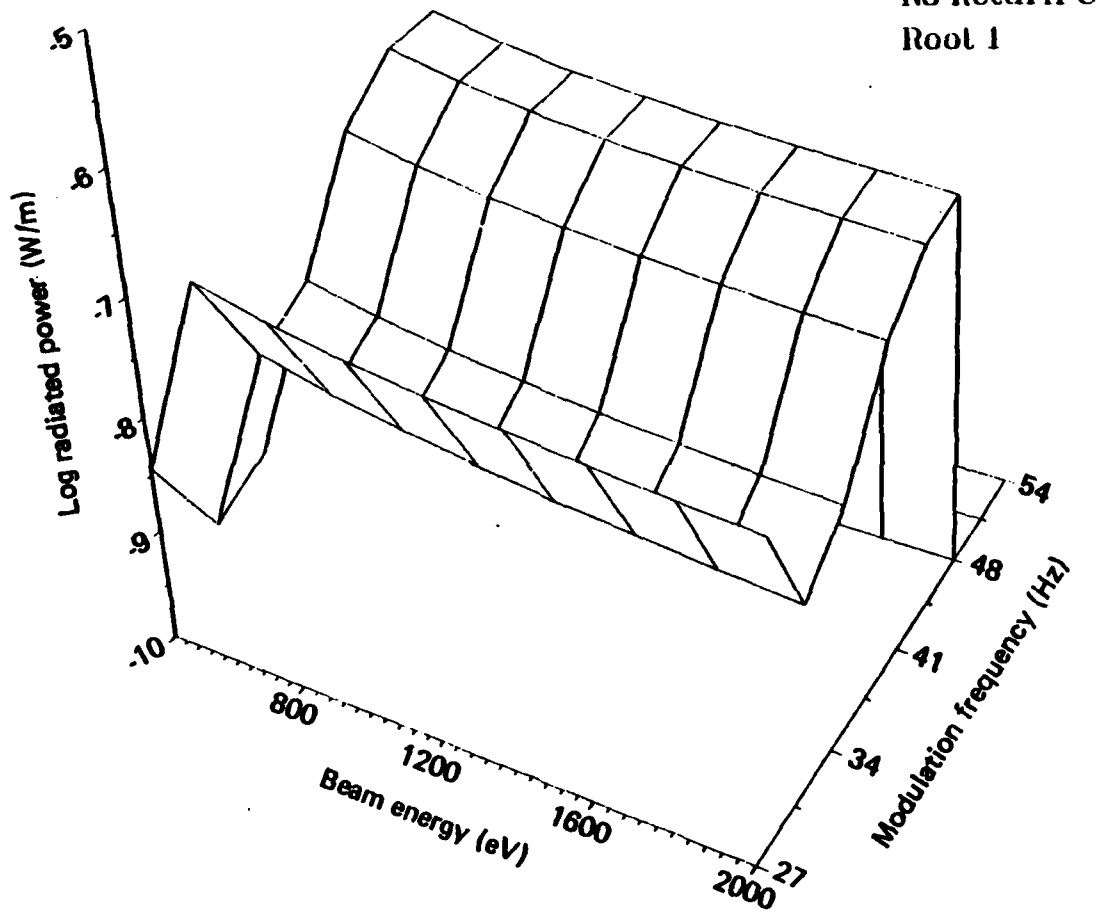

Fig. 64--Radiated power for BERT-I below 50 Hz, 89.9 deg pitch angle.

$\alpha = 89.9$
$I_B = 2.00*10^{-2}$
$1. \leq P \leq 40.$
$S = 0.$
$\omega_{CE} = 8.5450*10^{6}$

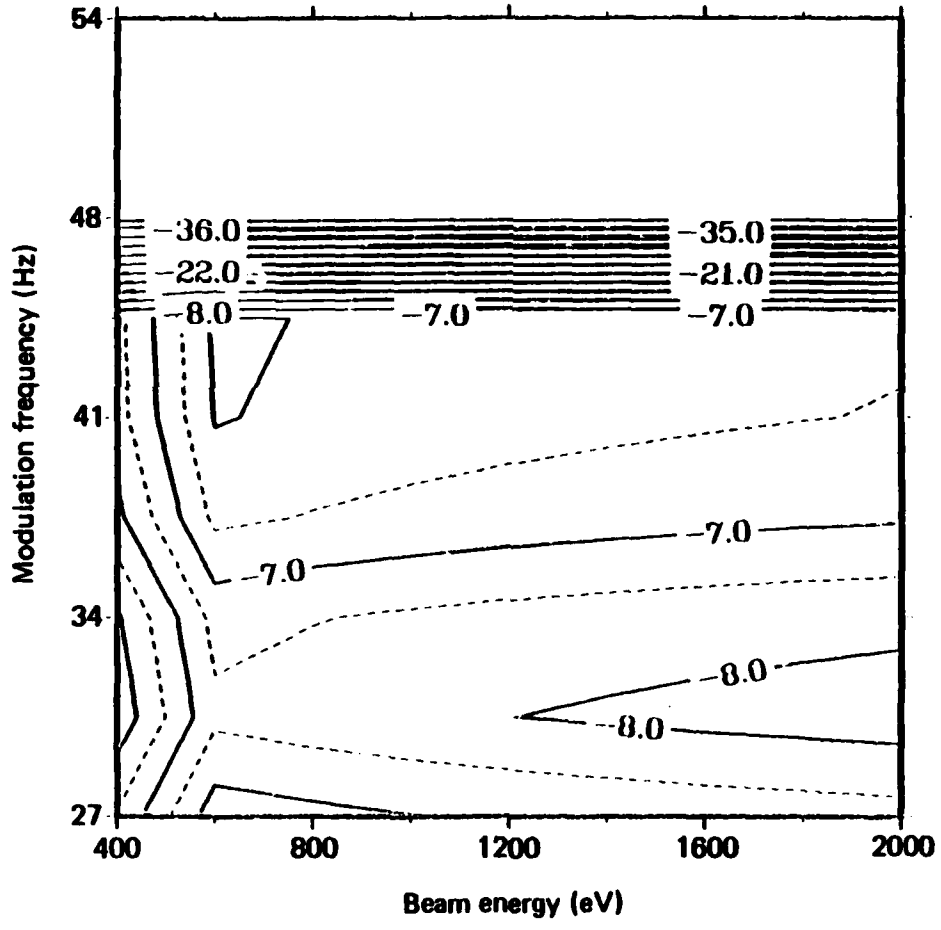

Fig. 65--Contours of radiated power for BERT-I below 50 Hz, 89.9 deg pitch angle .

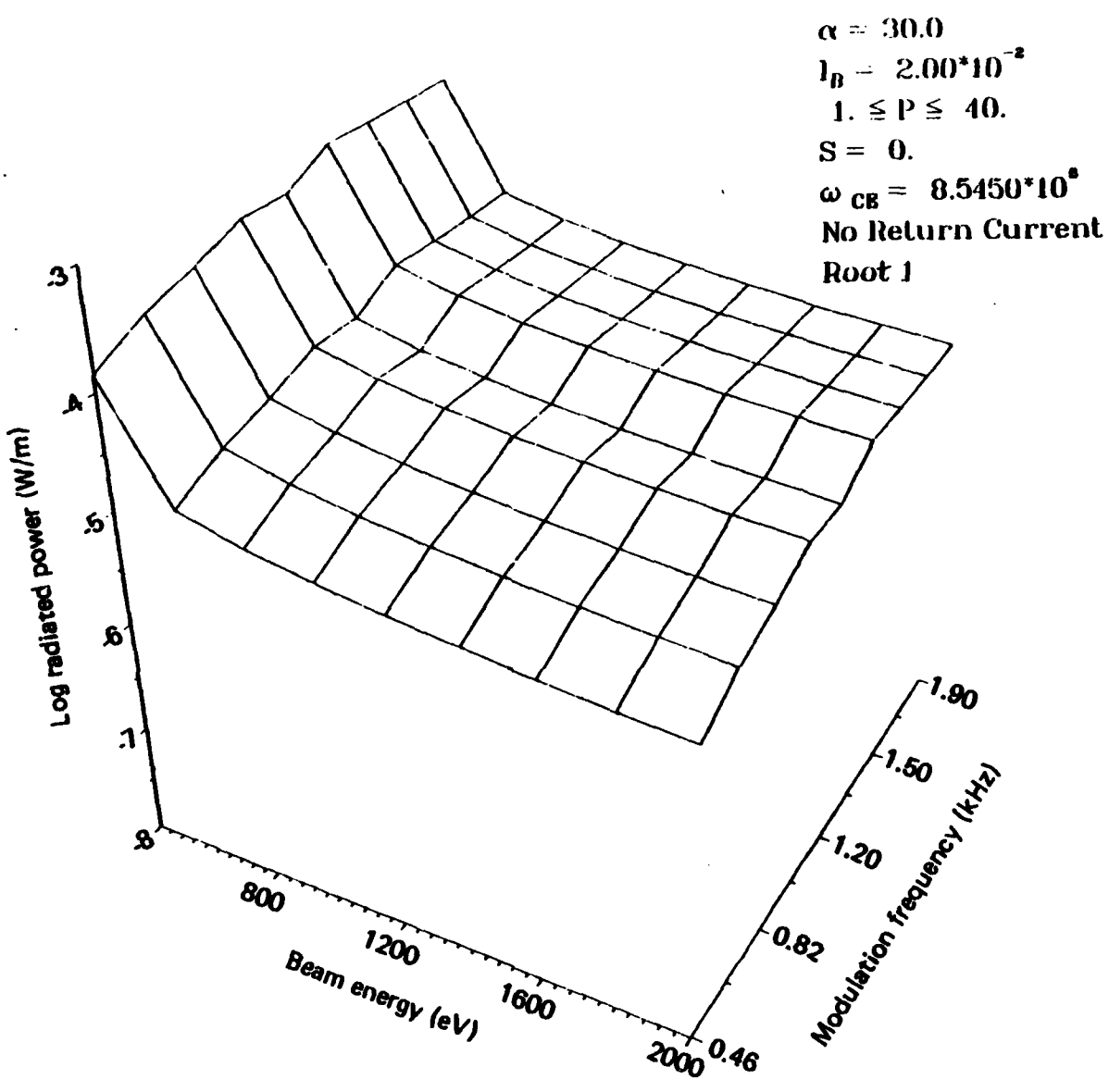

Fig. 66--Radiated power for BERT-I near 1 kHz, 30 deg pitch angle.

$\alpha = 30.0$
$I_0 = 2.00*10^{-2}$
$1. \leq P \leq 40.$
$S = 0.$
$\omega_{CE} = 8.5450*10^{6}$

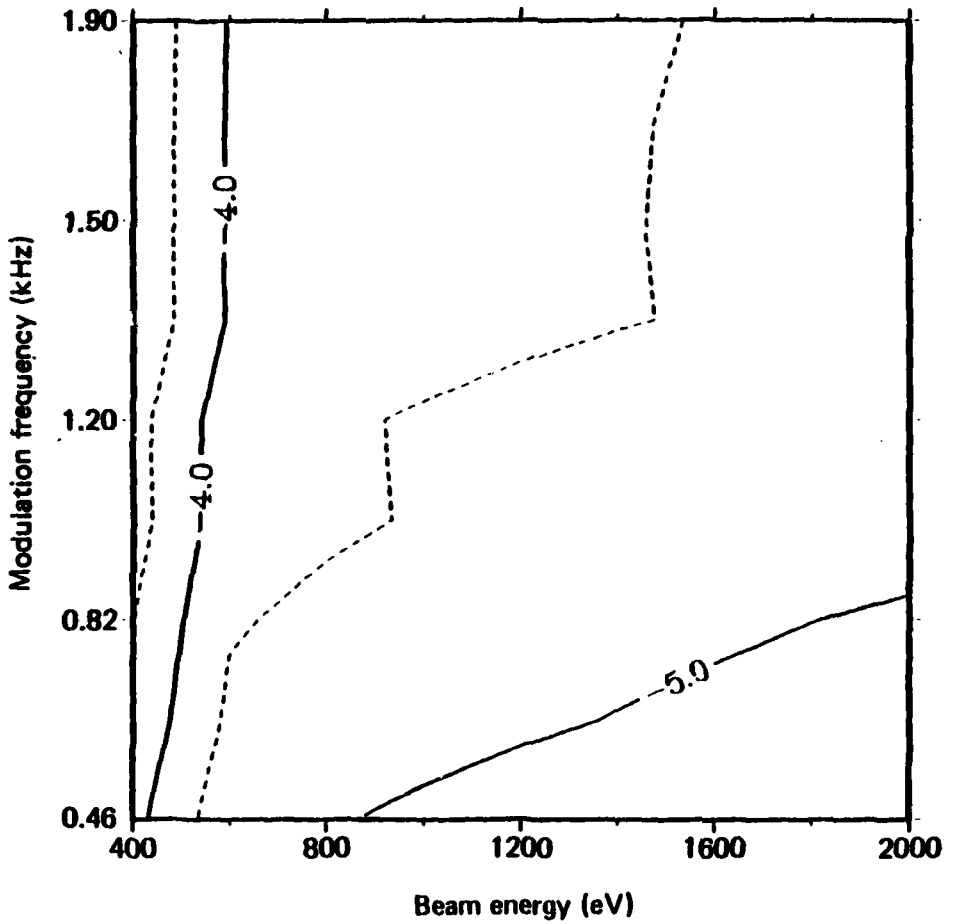

Fig. 67--Contours of radiated power for BERT-I near 1 kHz, 30 deg pitch angle .

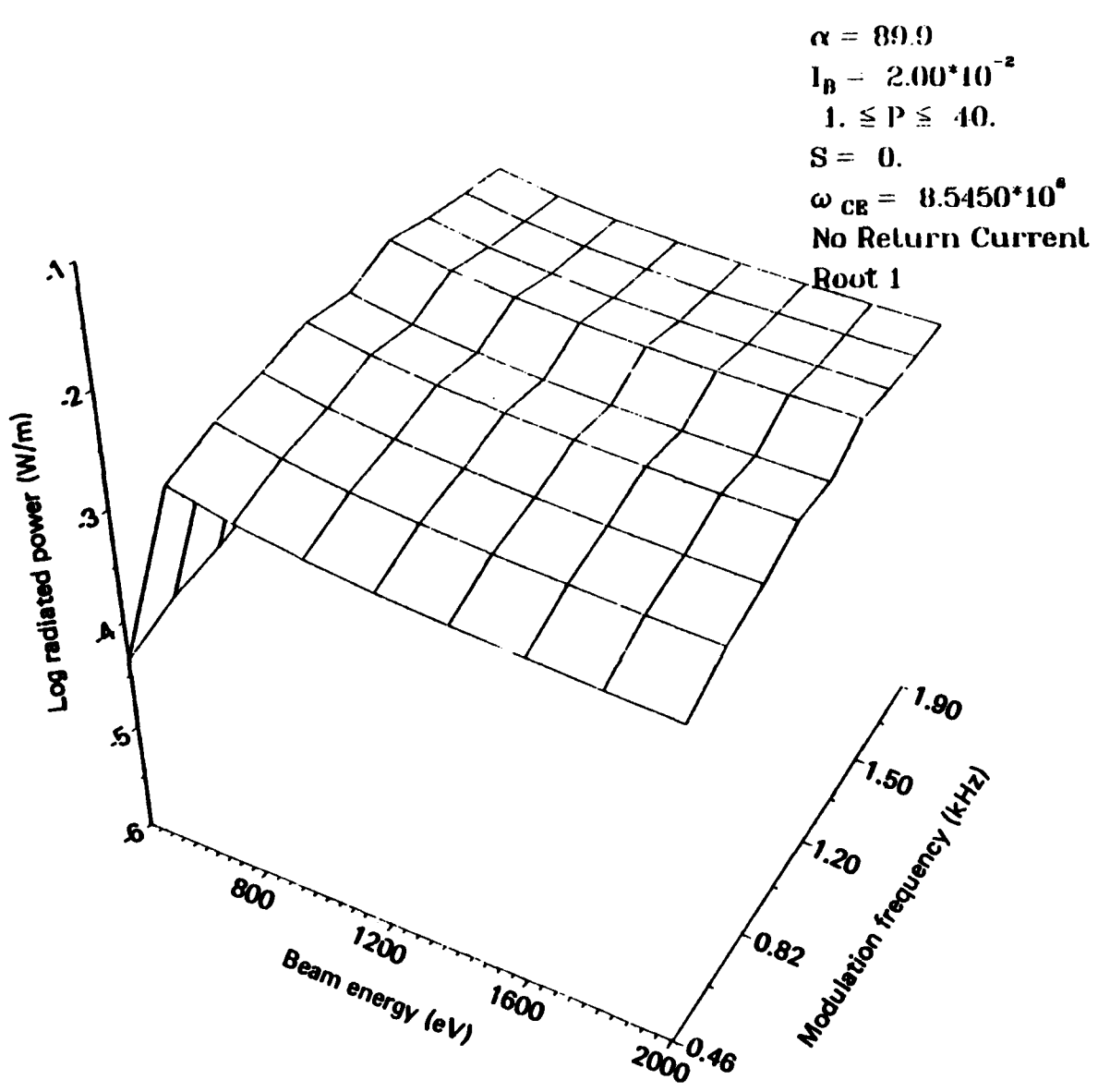

Fig. 68--Radiated power for BERT-I near 1 kHz, 89.9 deg pitch angle.

α = 89.9
I_B = $2.00*10^{-2}$
1. $\leq$ P $\leq$ 40.
S = 0.
ω_{CE} = $8.5450*10^{6}$

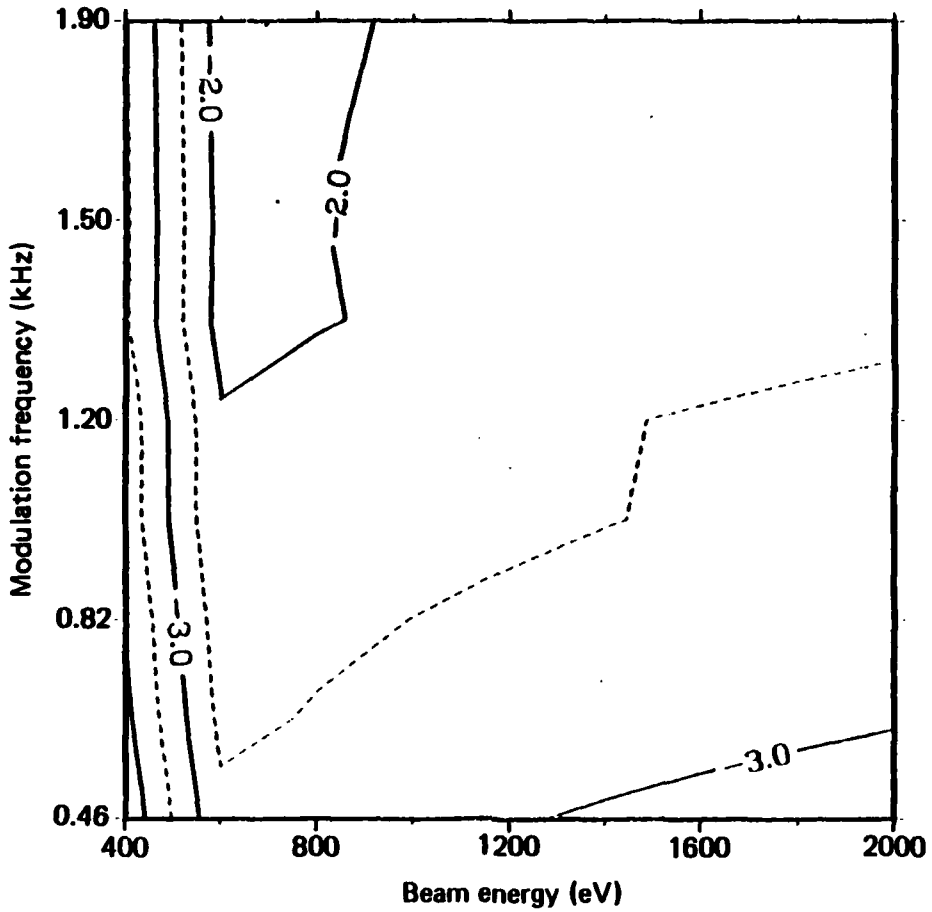

Fig. 69--Contours of radiated power for BERT-I near 1 kHz, 89.9 deg pitch angle .

Figures 66 through 69 show power into root 1 near 1 kHz. In that region no power at all goes into the fundamental; the fifth harmonic is the lowest frequency radiated. The power into root 2 is 6 orders of magnitude smaller than that into the fifth harmonic of root 1 and because it is so small it is not shown.

The figures confirm that the radiated power levels are small--on the order of 10^{-4} to 10^{-5} W/m. Analysis suggests that even so, the beam has high enough gain (in the ideal case described by Harker and Banks[1]) that radiation might be detectable at the ground. For that reason, an experiment utilizing the BERT-I beam might be successful; however, there is a high risk of failure.

V. VCAP/SPACELAB 2

Spacelab 2, earmarked for mid-1985, will be conducted at an altitude of 350 km. The inclination of its orbit will be 50 deg, which will take the spacecraft into high, middle, and low geomagnetic latitudes. Stanford University will use the VCAP electron gun aboard this flight and will launch beams at various pitch angles and modulation frequencies. The modulation will be square wave; the frequencies will range from a few hertz to several megahertz.[9] The gun currents will be fixed at 50 and 100 mA. The gun voltages may reach 1 kV. The duty cycle may also be varied.

Table 3 summarizes the ionospheric parameters PSR assumed in this study. The analysis was geared toward a specific position at midlatitude, above White Sands. A 50 percent duty cycle (equal on and off time) was assumed for the pulses and only radiation into the Cerenkov mode was calculated. The gun current was assumed to be 100 mA and the first 10 harmonics were summed. Pitch angles of 0.1, 30, 60, and 89.9 deg were run. Figures 70 through 76 and 77 through 84 show contours for daytime and nighttime emission, respectively.

The figures reveal power levels up to 0.1 W/m on the central plateau of root 1, much lower levels at ELF, and lower levels into root 2 (except above 1 MHz for nighttime emission). As in the case of the BERT-I calculation, the power goes into higher harmonics for modulation frequencies between 6 and 60 kHz.

TABLE 3.

Ionospheric Parameters for VCAP/Spacelab 2 Calculation.

Electron Gyrofrequency (Hz)	Ion Gyro-frequency (Hz)	Time	Electron Plasma Frequency (Hz)	Ion Plasma Frequency (Hz)	Lower Hybrid Frequency (Hz)
1.2×10^6	40.6	Day	9.42×10^6	5.51×10^4	6.98×10^3
		Night	4.75×10^6	2.77×10^4	

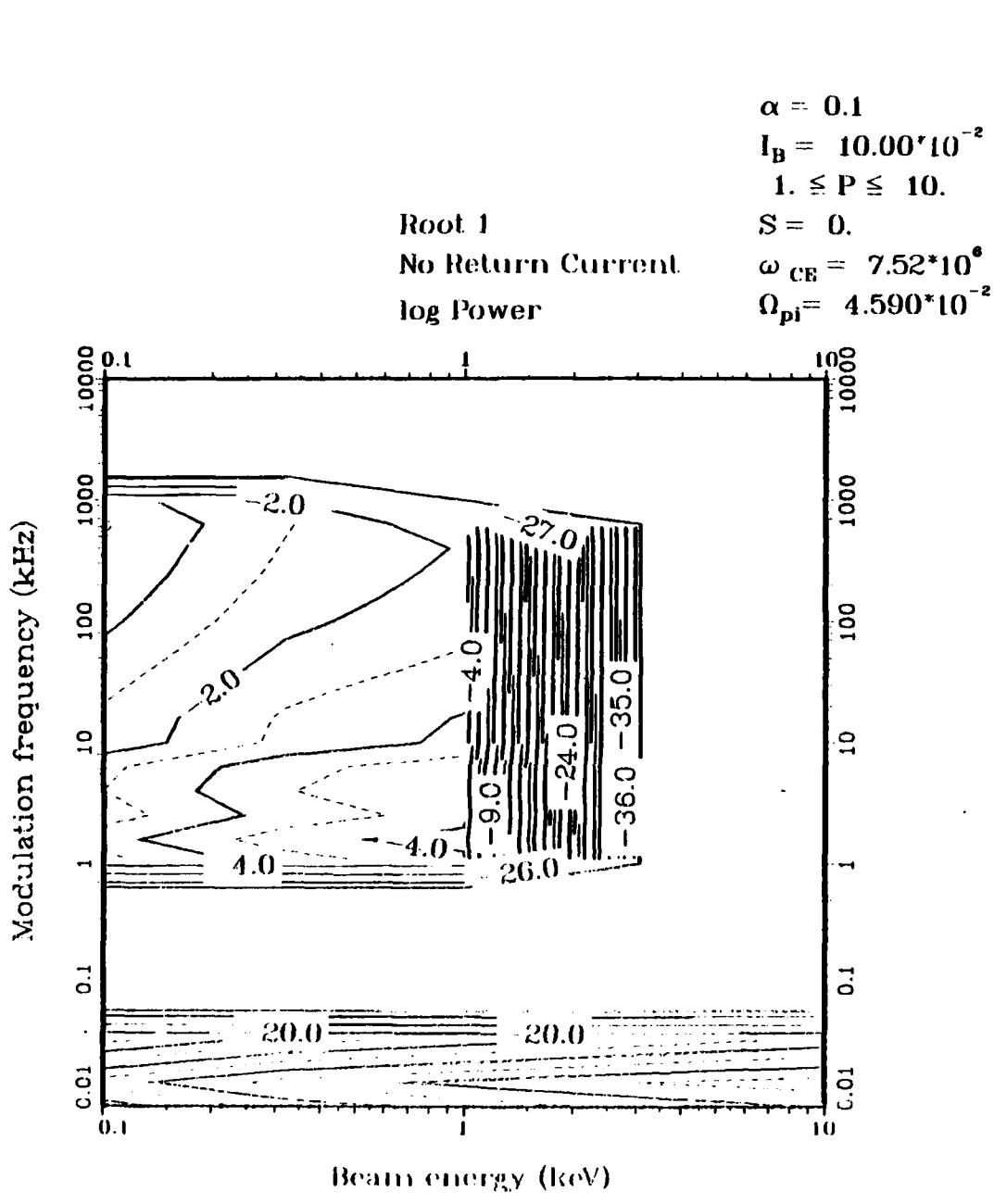

Fig. 70--Daytime radiated power (Cerenkov mode) for VCAP, pitch angle 0.1 deg (root 1).

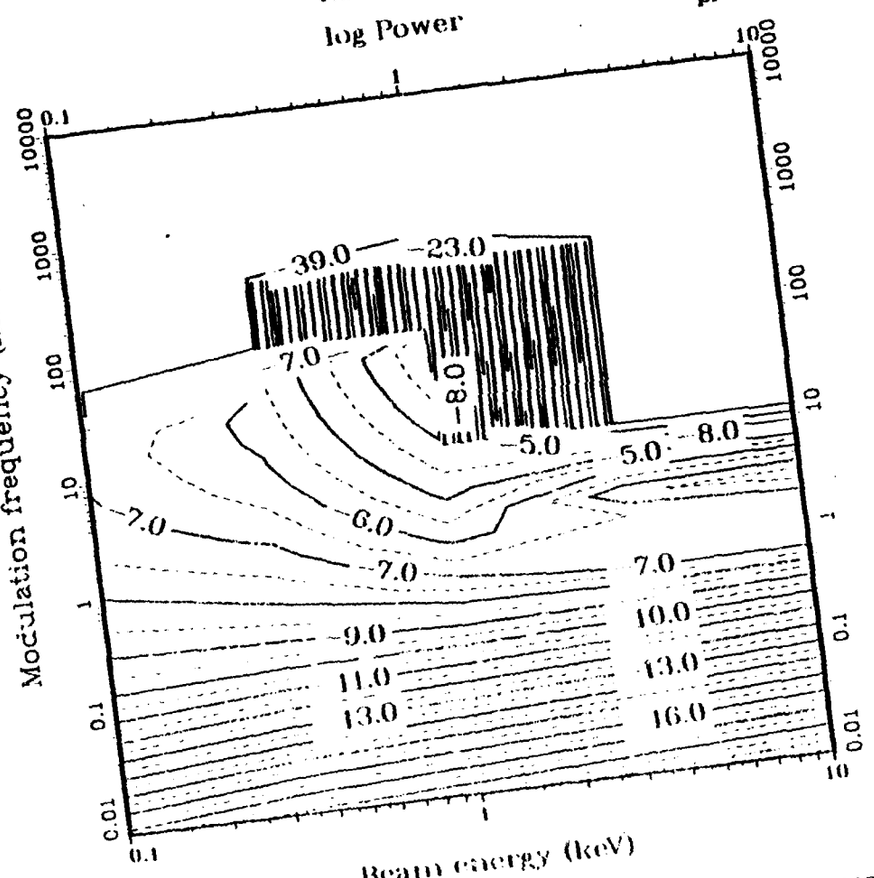

Fig. 71--Daytime radiated power (Cerenkov mode) for VCAP, pitch angle 0.1 deg (root 2).

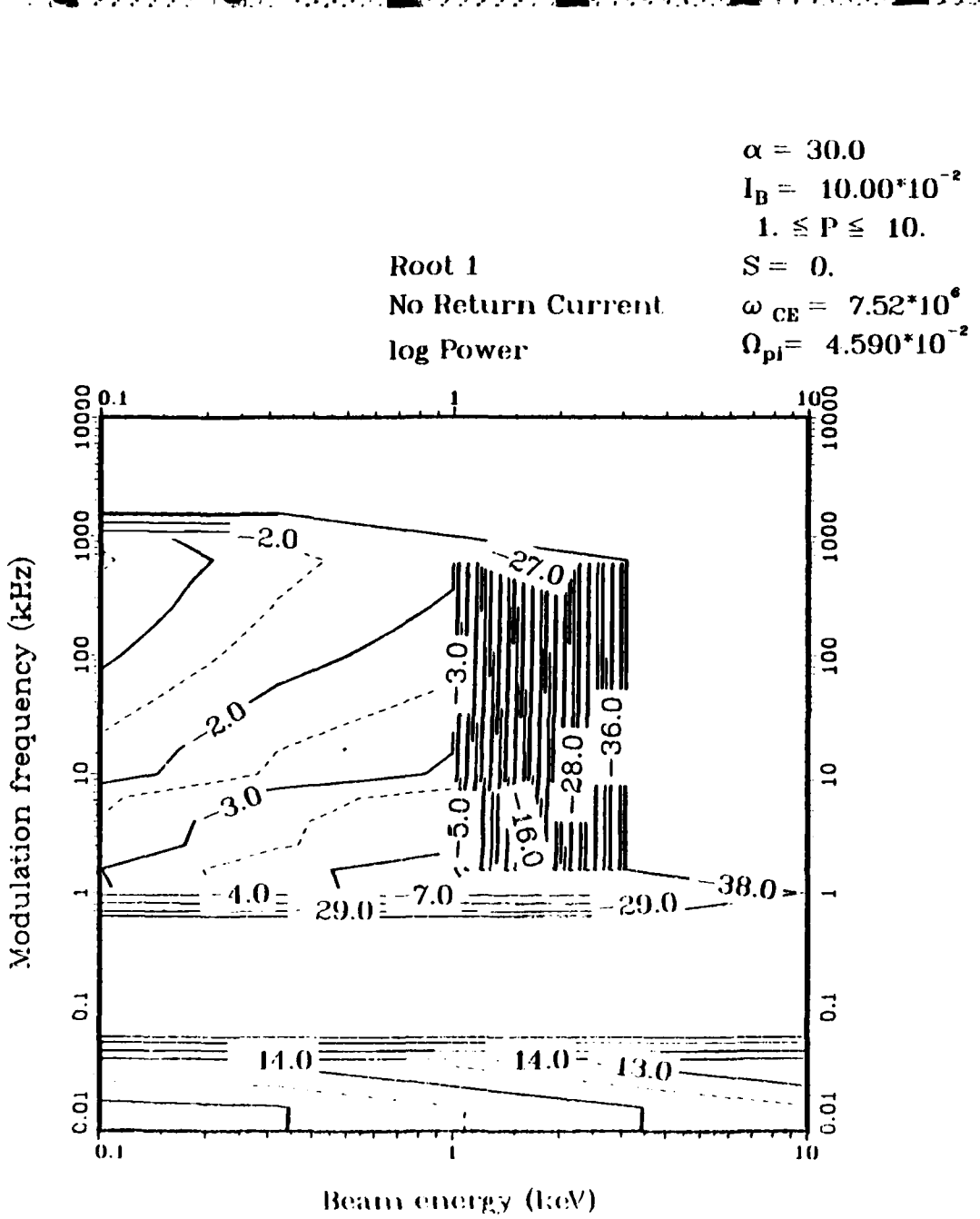

Fig. 72--Daytime radiated power (Cerenkov mode) for VCAP, pitch angle 30 deg (root 1).

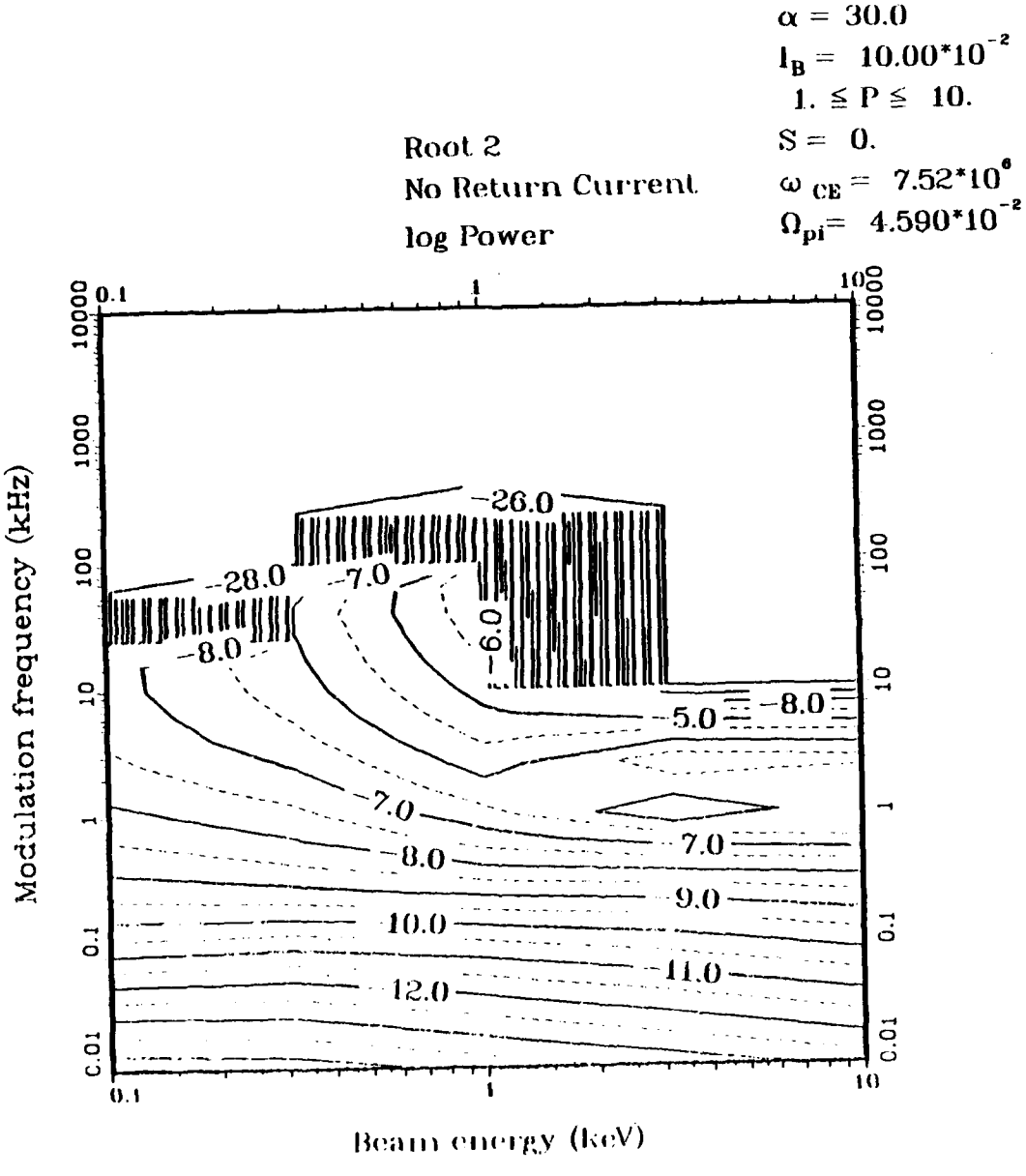

Fig. 73--Daytime radiated power (Cerenkov mode) for VCAP, pitch angle 30 deg (root 2).

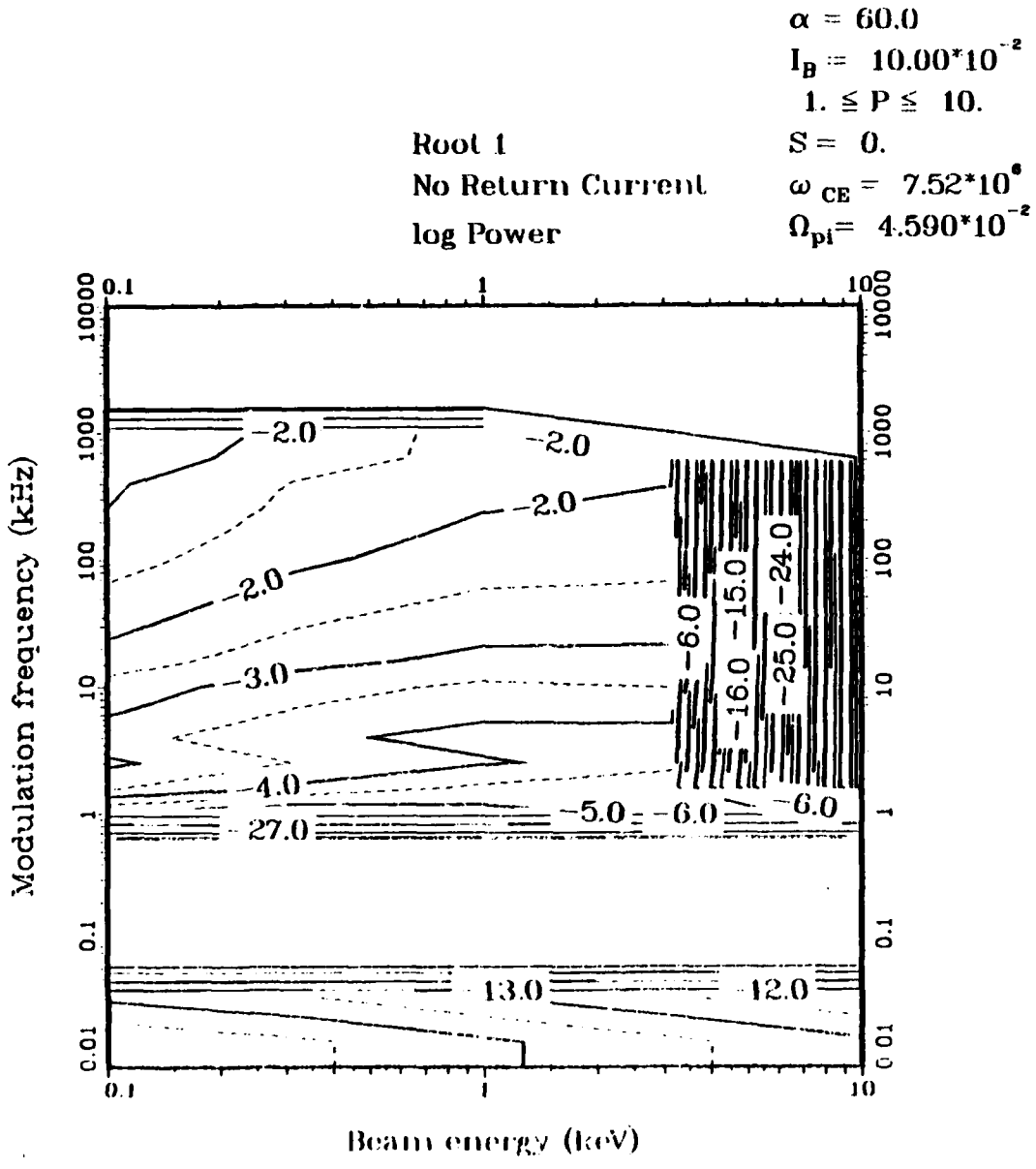

Fig. 74--Daytime radiated power (Cerenkov mode) for VCAP, pitch angle 60 deg (root 1).

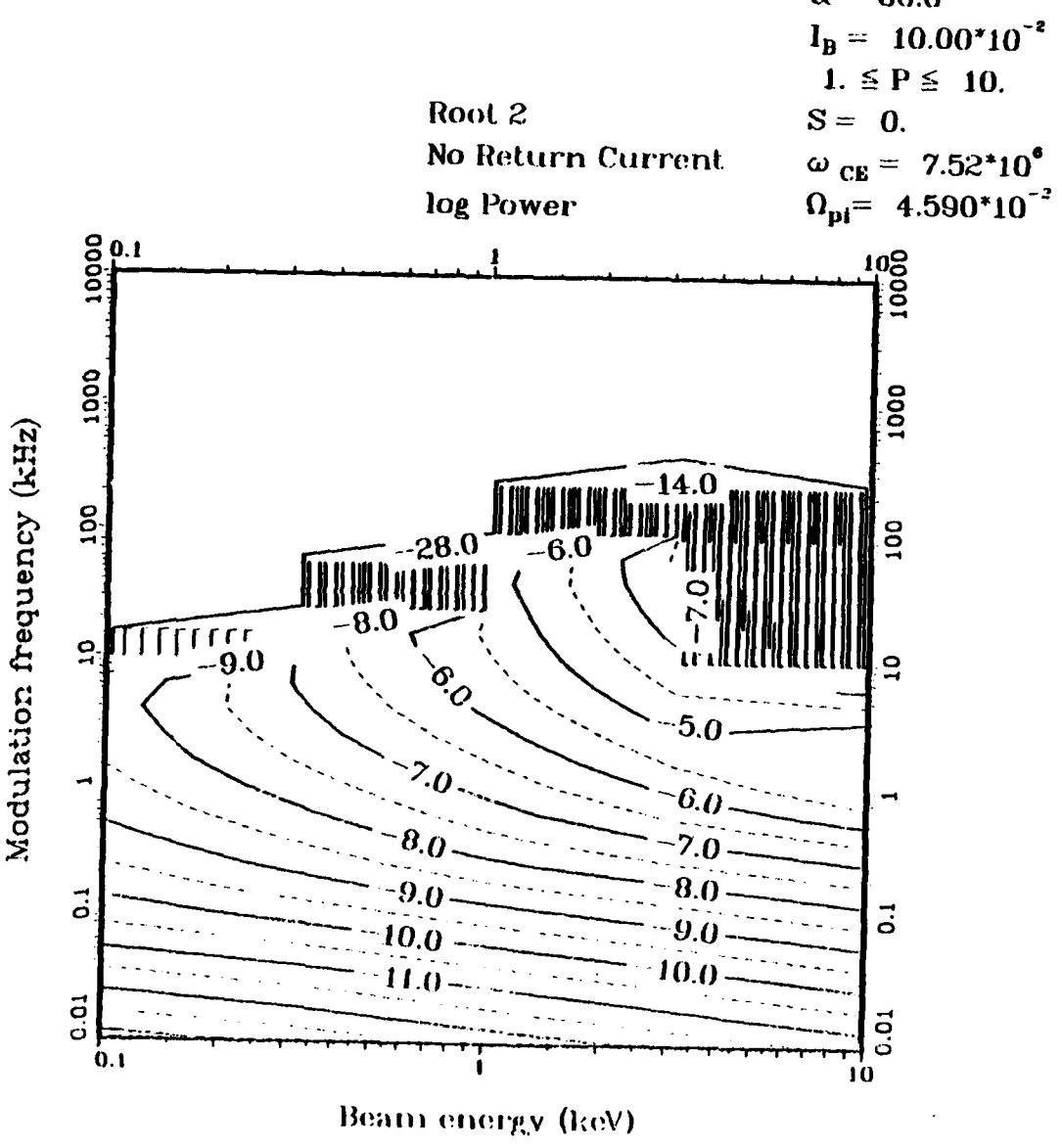

Fig. 75--Daytime radiated power (Cerenkov mode) for VCAP, pitch angle 60 deg (root 2).

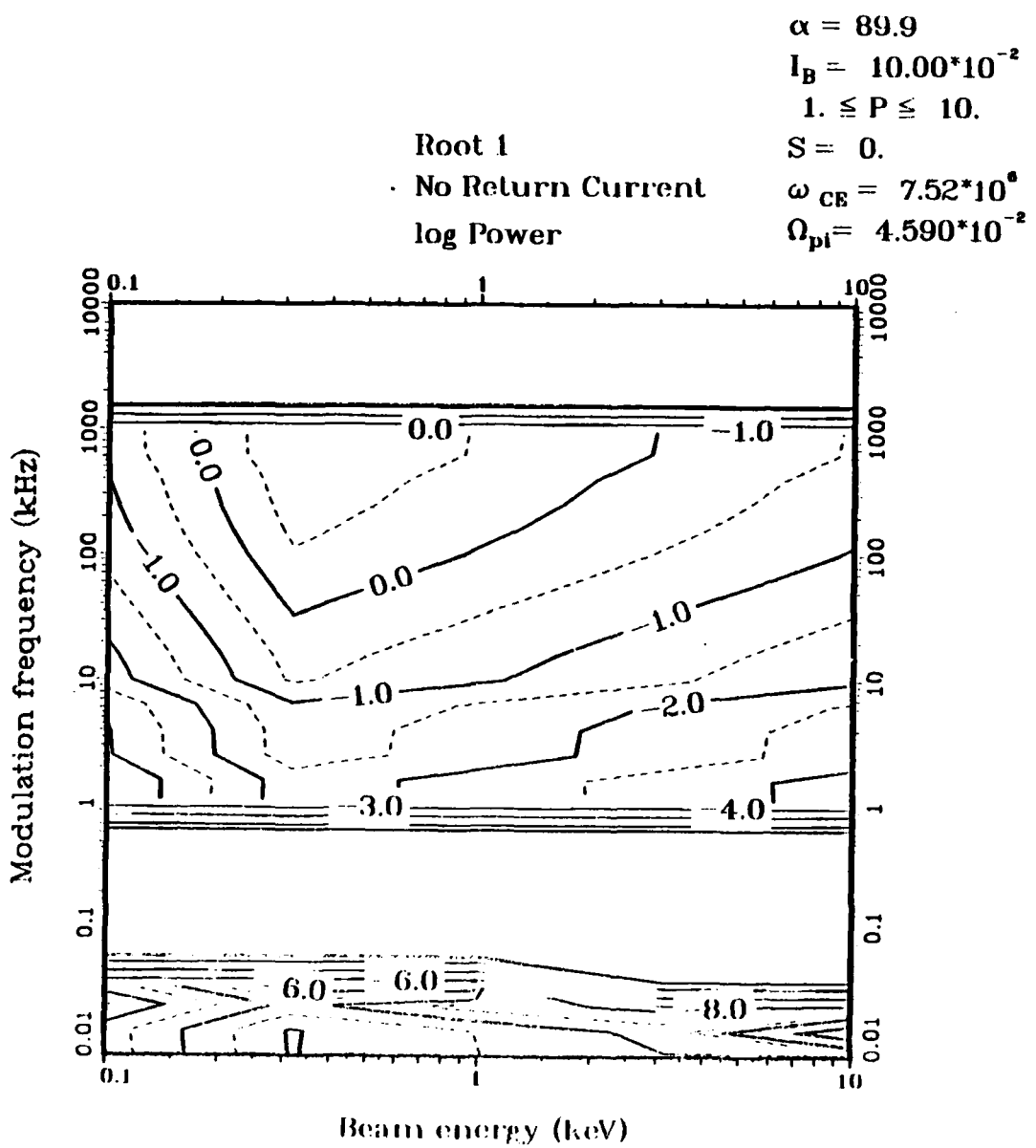

Fig. 76--Daytime radiated power (Cerenkov mode) for VCAP, pitch angle 89.9 deg (root 1).

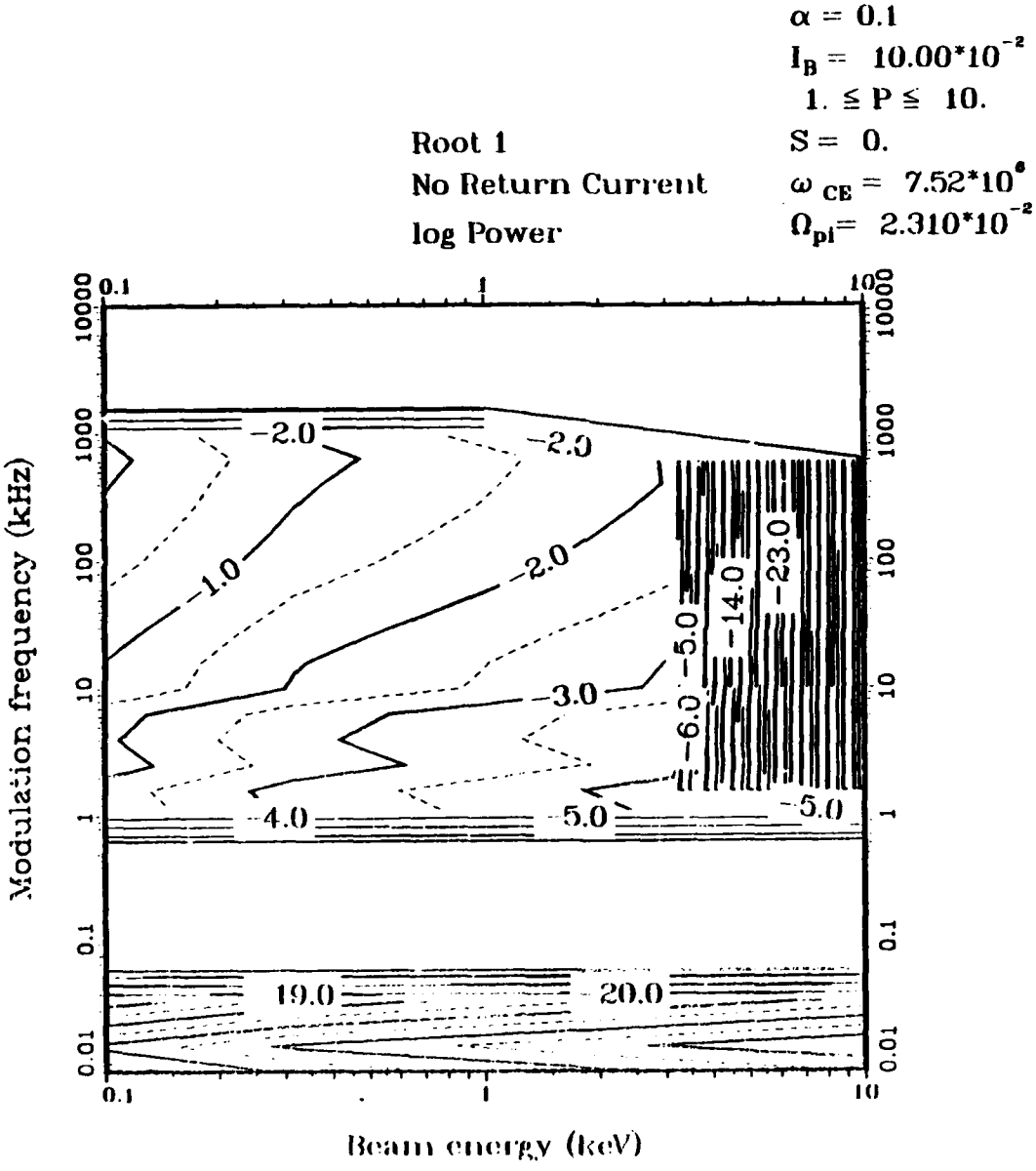

Fig. 77--Nighttime radiated power (Cerenkov mode) for VCAP, pitch angle 0.1 deg (root 1).

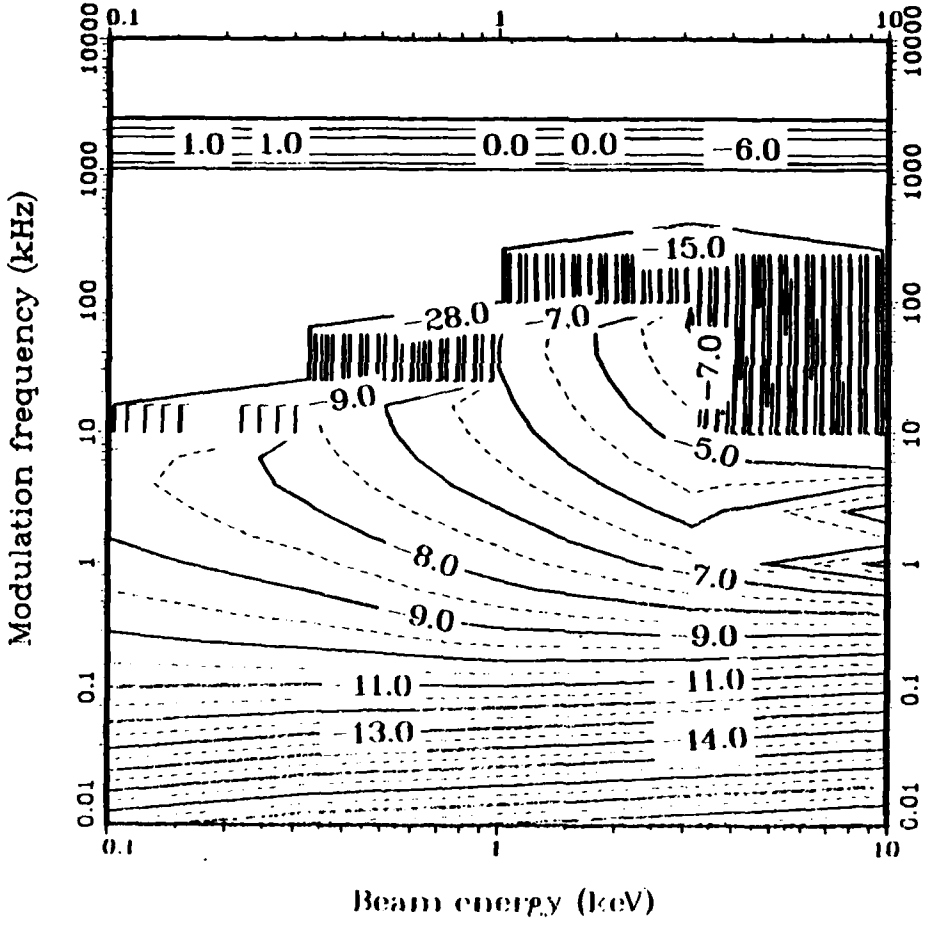

Fig. 78--Nighttime radiated power (Cerenkov mode) for VCAP, pitch angle 0.1 deg (root 2).

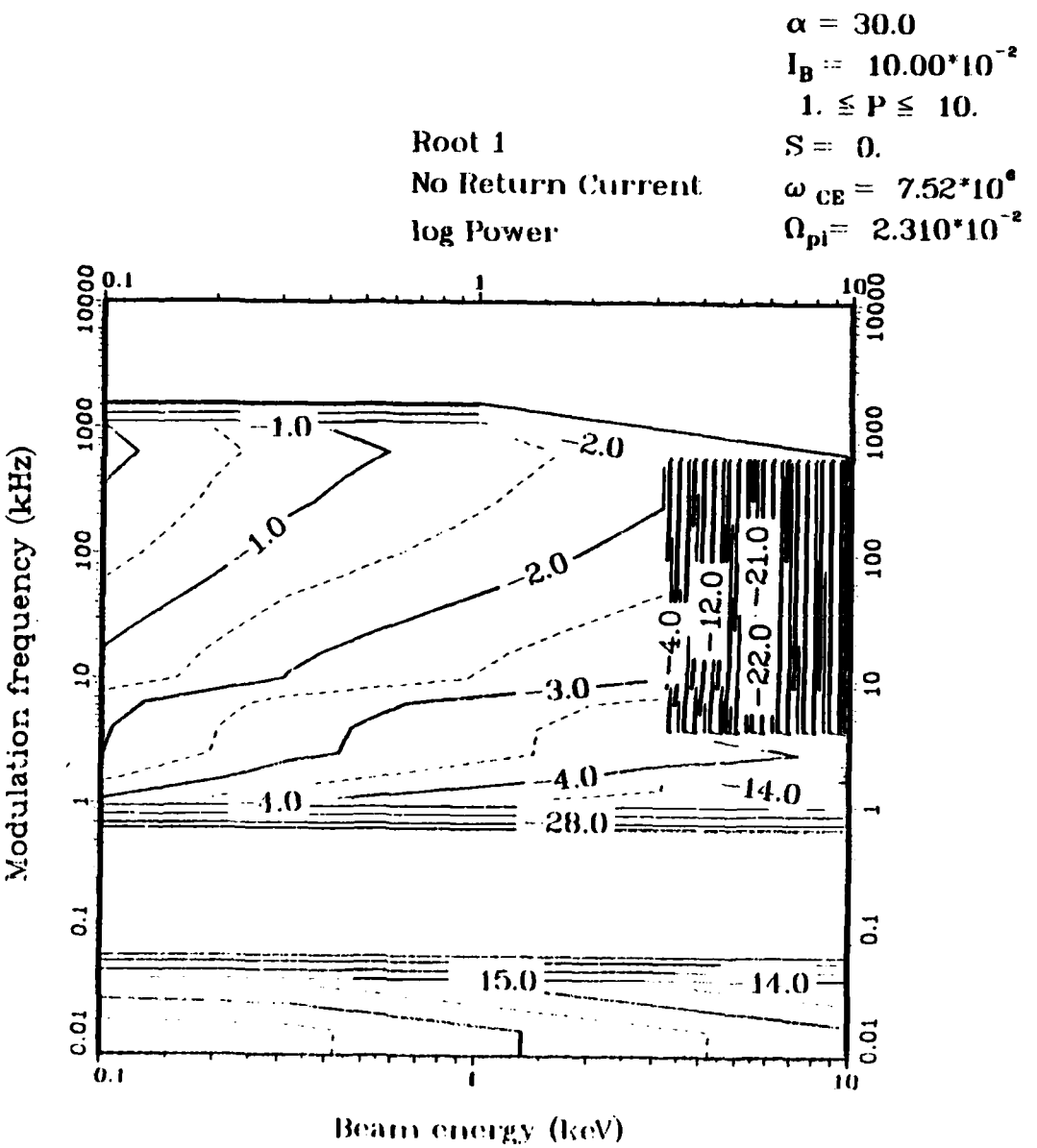

Fig. 79--Nighttime radiated power (Cerenkov mode) for VCAP, pitch angle 30 deg (root 1).

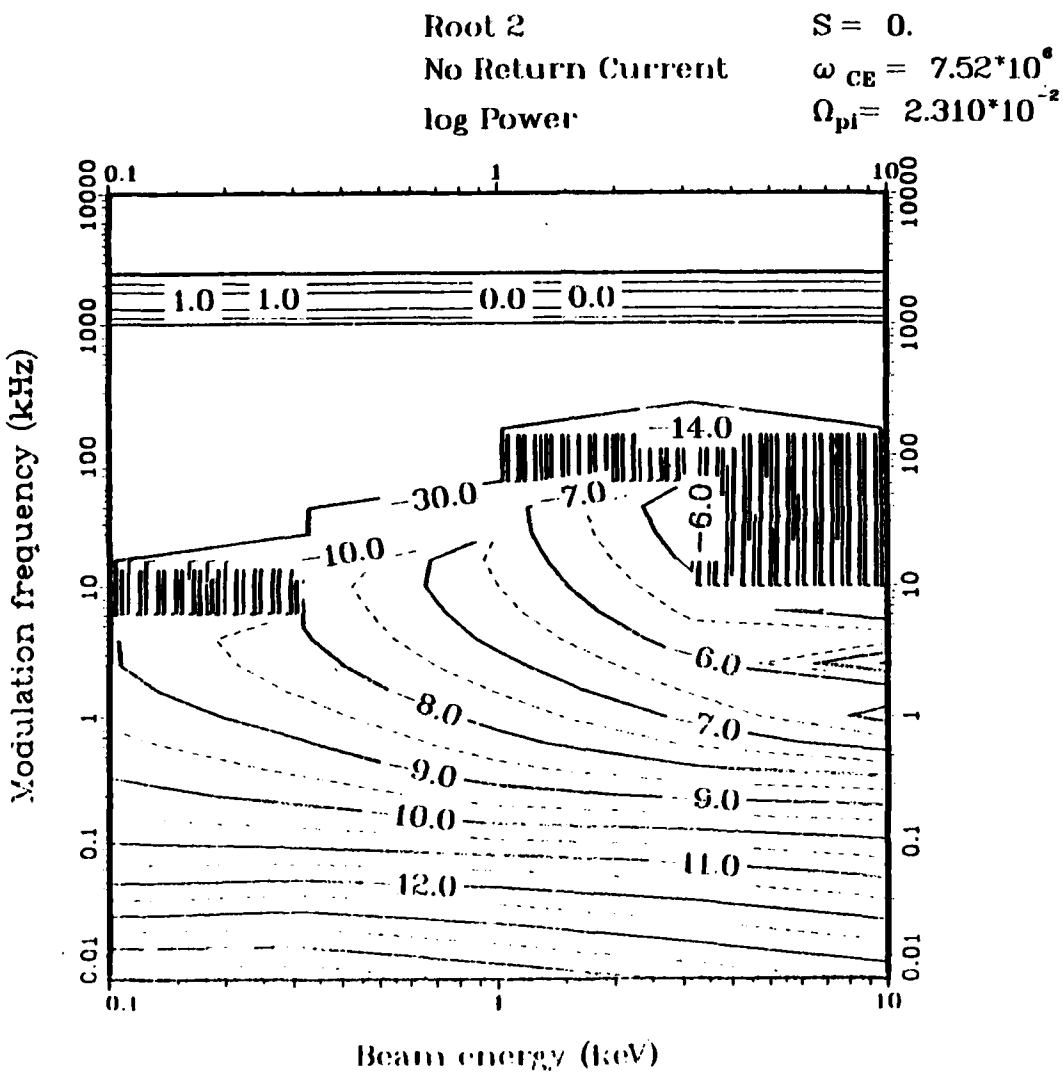

Fig. 80--Nighttime radiated power (Cerenkov mode) for VCAP, pitch angle 30 deg (root 2).

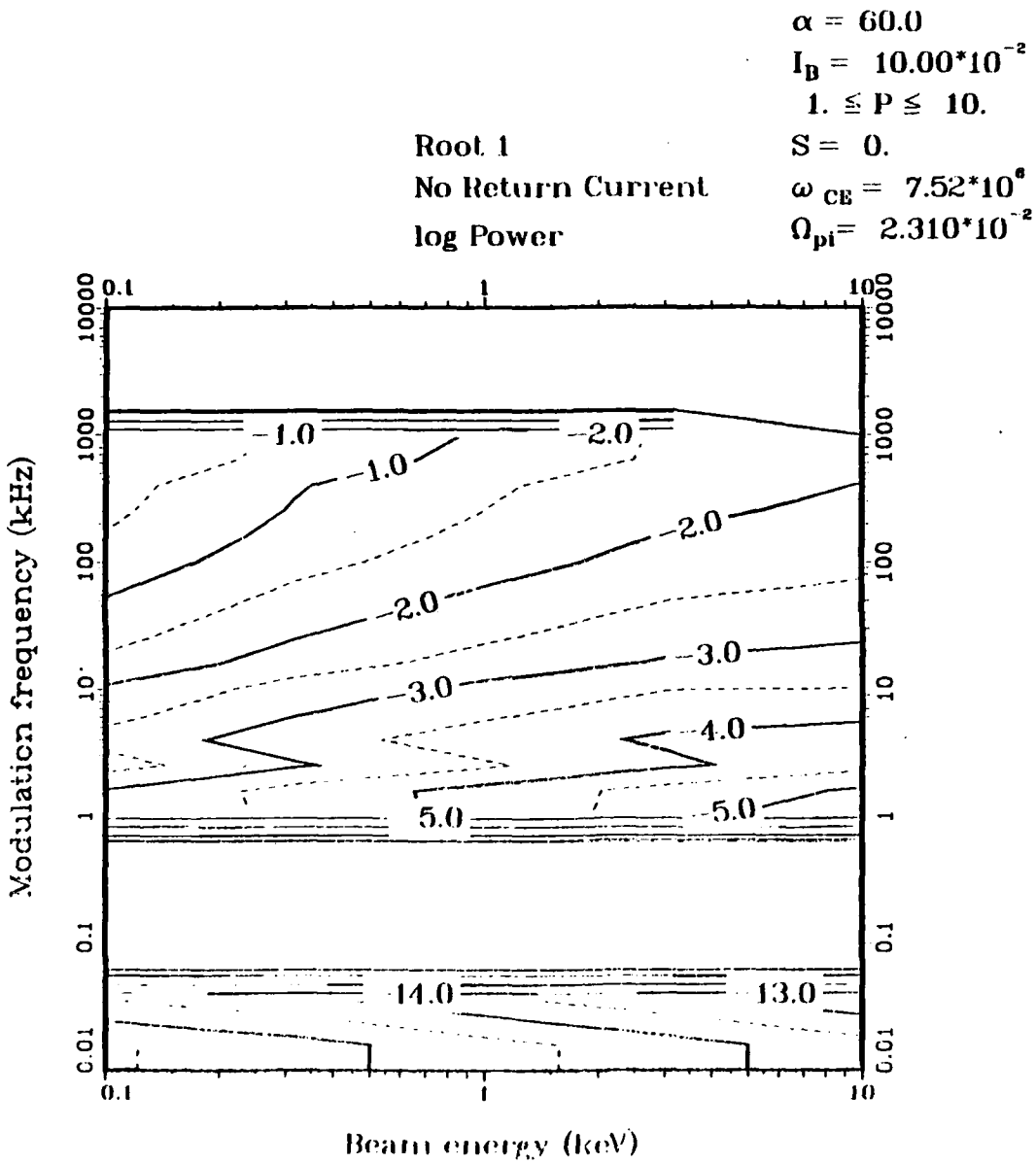

Fig. 81--Nighttime radiated power (Cerenkov mode) for VCAP, pitch angle 60 deg (root 1).

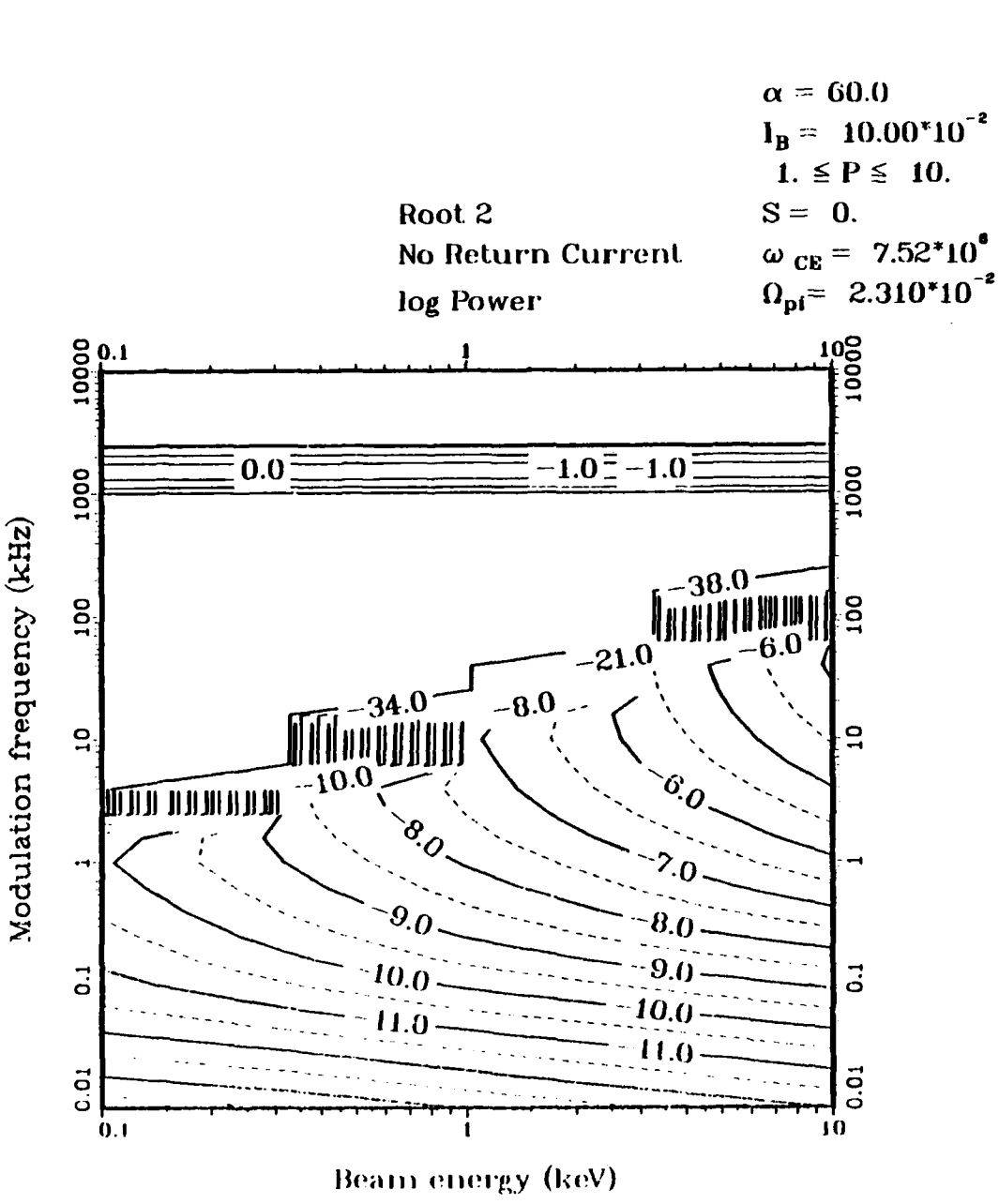

Fig. 82--Nighttime radiated power (Cerenkov mode) for VCAP, pitch angle 60 deg (root 2).

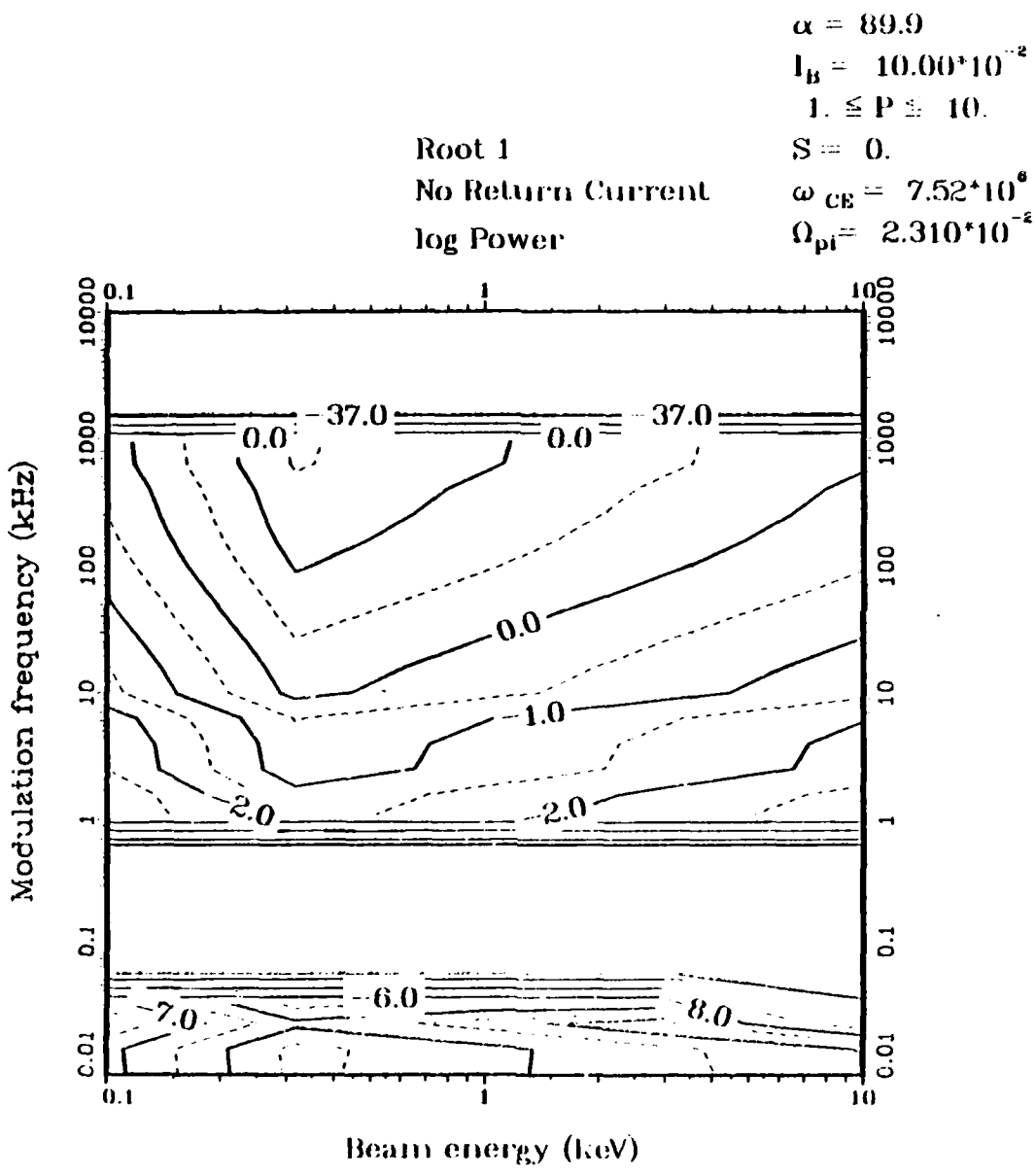

Fig. 83--Nighttime radiated power (Cerenkov mode) for VCAP, pitch angle 89.9 deg (root 1).

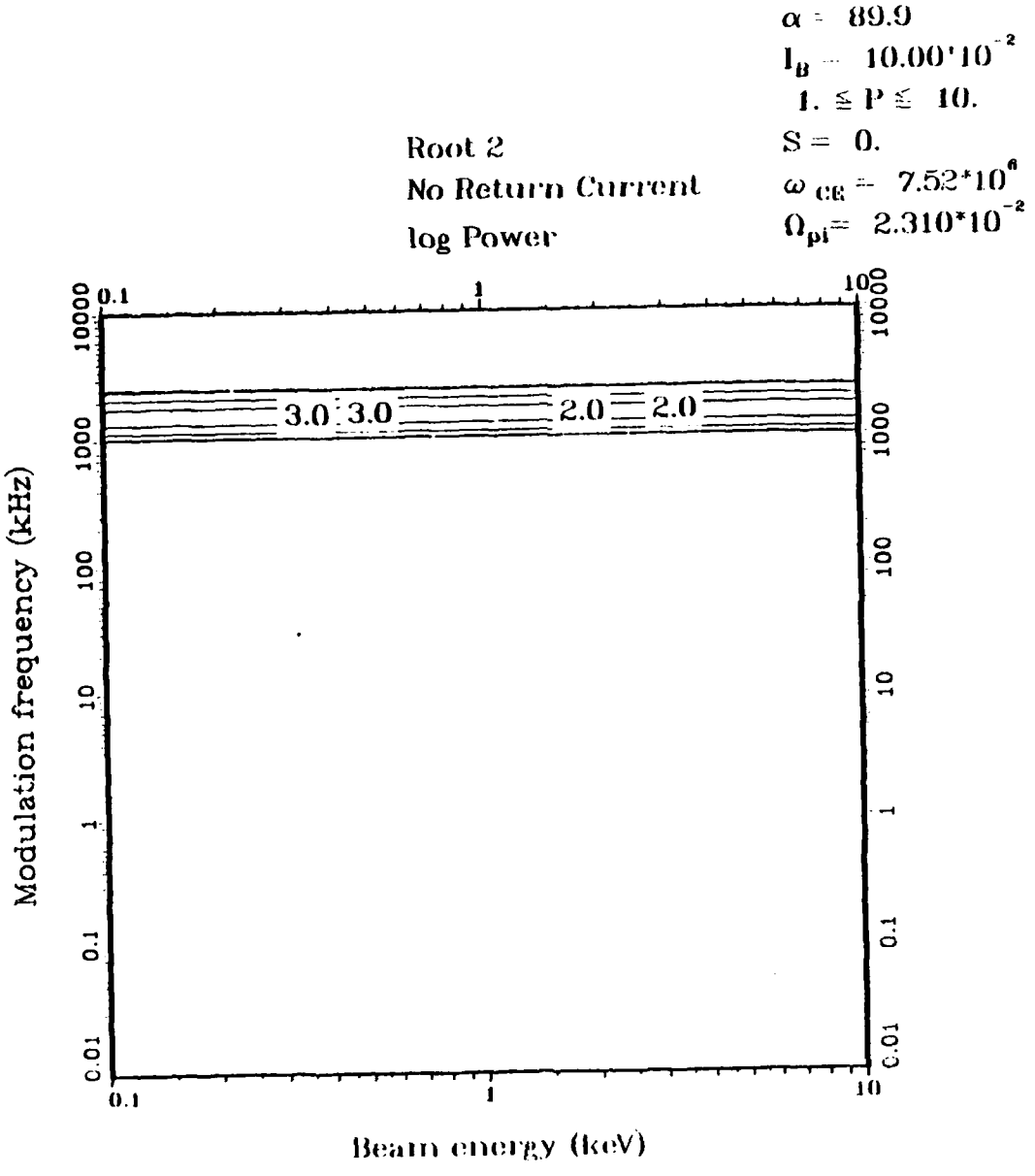

Fig. 84--Nighttime radiated power (Cerenkov mode) for VCAP, pitch angle 89.9 deg (root 2).

VI. SEPAC

The SEPAC experiment is tentatively scheduled to fly on shuttle missions in August 1986, in December 1989, and December 1991. The SEPAC includes an electron gun that presently can be modulated at frequencies from 0.1 to 8.9 kHz. The gun is capable of 12.5 kW emission at highest voltage, which is 7.8 kV. The gun perveance is 2.5×10^{-6} $A/V^{3/2}$, which limits the current possible for a given voltage. An altitude of 275 km and a 57 deg orbit inclination are planned for the August 1986 flight.[10] As in the cases of BERT-I and Spacelab 2, we have assumed ionospheric parameters appropriate to a White Sands overflight.

Table 4 summarizes the calculation parameters. In this set of runs, 20 harmonics were kept, the gun perveance determined the current, and 5 pitch angles were considered. Three pitch angles are presented here: 0.1, 45, and 89.9 deg. Figures 85 through 89 show the power radiated into the Cerenkov mode for daytime emission, and Figs. 90 through 94 show nighttime emission. The perveance reduces beam power and current at low beam energies, therefore, the radiated power decreases as the beam energy decreases. This is opposite to the general tendencies reported for BERT-I and Spacelab 2.

When the beam energy is greater than 1 kV, the power into root 1 is about 0.1 W/m and that into root 2 is about 10^{-3} W/m. For modulation frequencies above 1/2 kHz, much of the power goes into higher harmonics.

TABLE 4.

Ionospheric Parameters for SEPAC Calculation.

Electron Gyrofrequency (Hz)	Ion Gyro-frequency (Hz)	Time	Electron Plasma Frequency (Hz)	Ion Plasma Frequency (Hz)	Lower Hybrid Frequency (Hz)
1.36×10^6	46.1	Day	9.4×10^6	5.49×10^4	7.92×10^3
		Night	3.36×10^6	1.96×10^4	

$\alpha = 0.1$

$\Omega_{pi} = 4.040*10^{-2}$

$1. \leq P \leq 20.$

$S = 0.$

$\omega_{CE} = 8.5450*10^{6}$

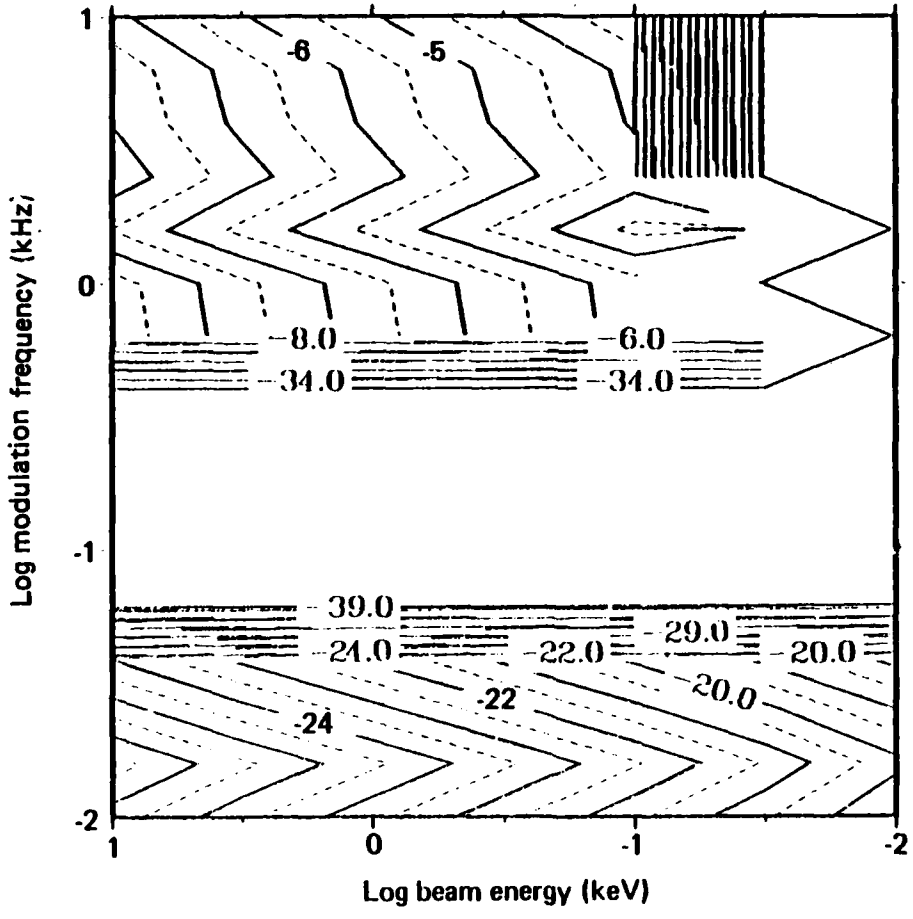

Fig. 85--Daytime radiated power (Cerenkov mode) for SEPAC, pitch angle 0.1 deg (root 1).

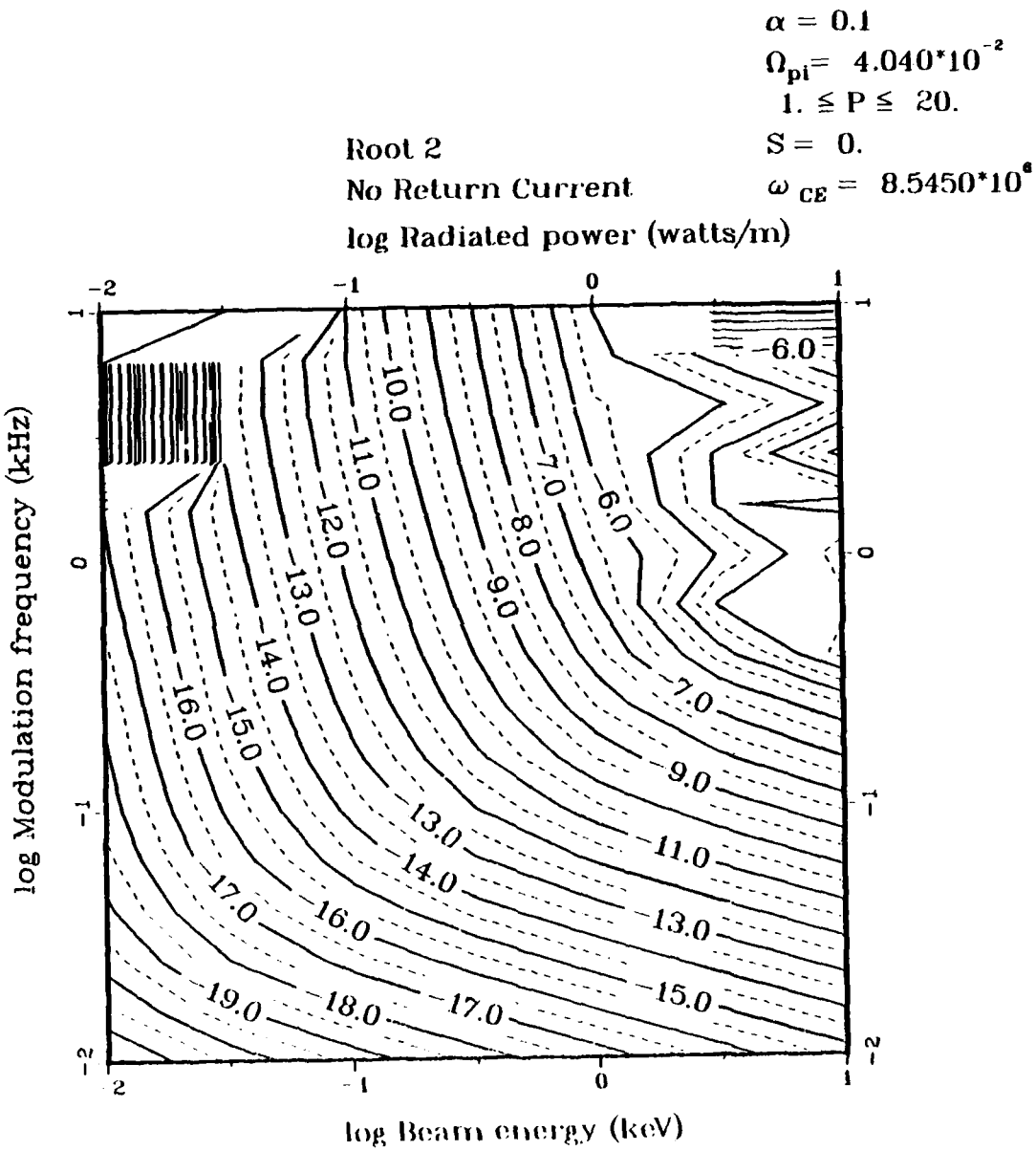

Fig. 86--Daytime radiated power (Cerenkov mode) for SEPAC, pitch angle 0.1 deg (root 2)

$\alpha = 45.0$

$\Omega_{pl} = 4.040*10^{-2}$

$1. \leq P \leq 20.$

$S = 0.$

$\omega_{CE} = 8.5450*10^{6}$

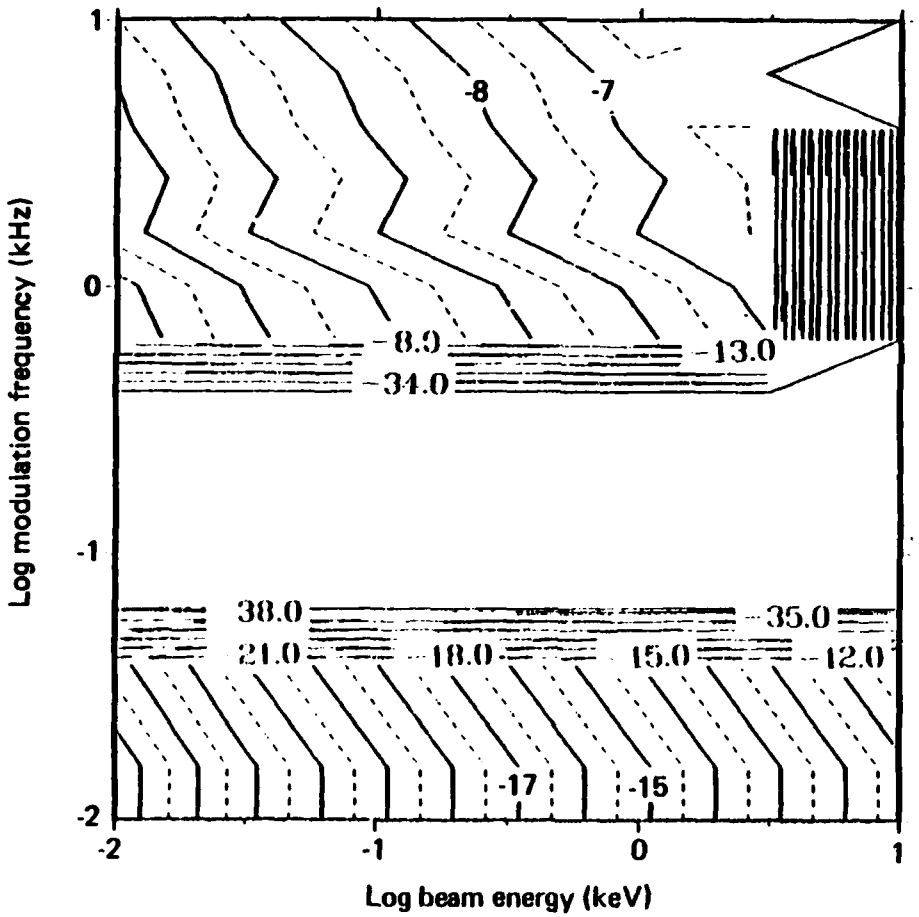

Fig. 87--Daytime radiated power (Cerenkov mode) for SEPAC, pitch angle 45 deg (root 1).

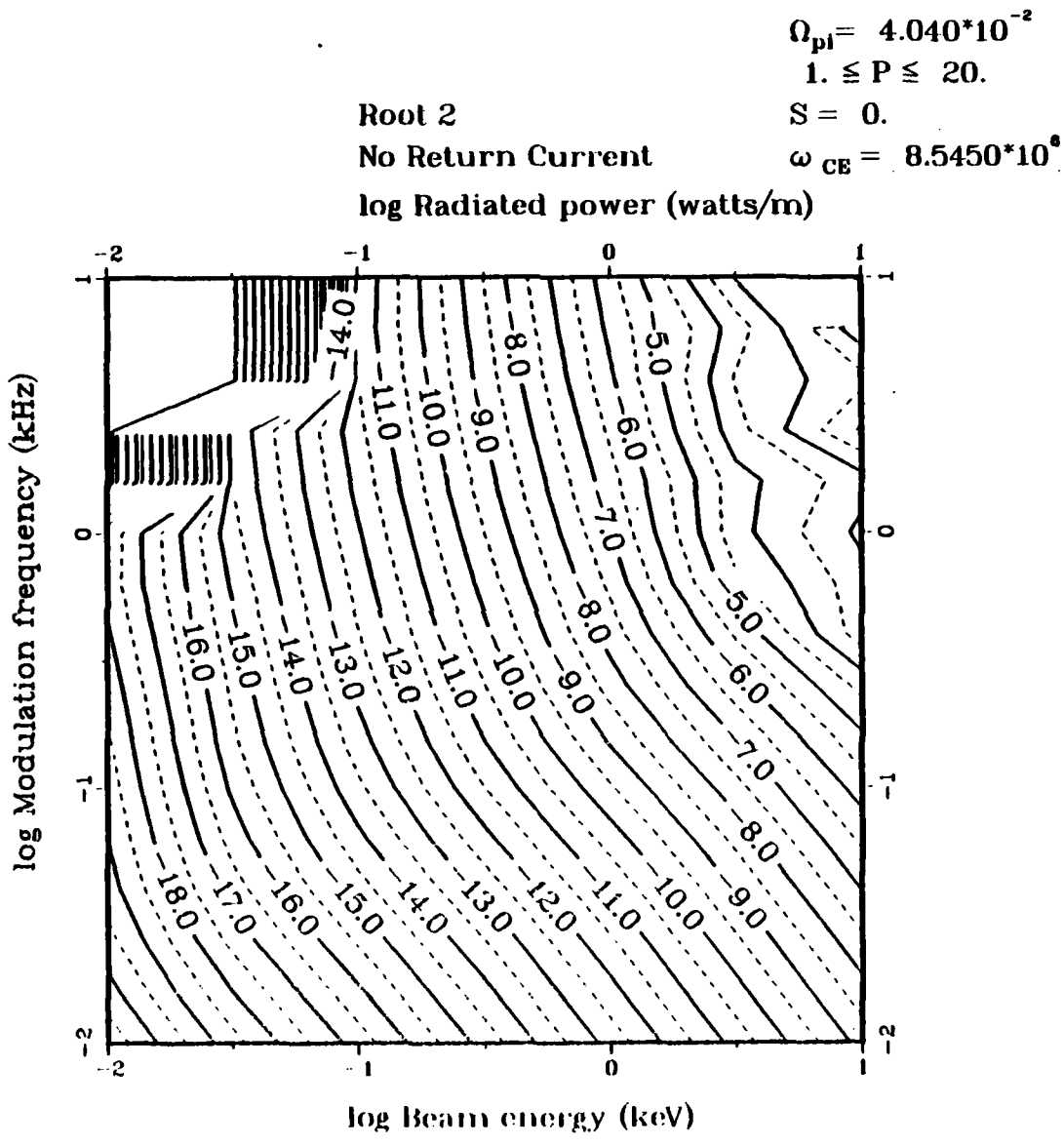

Fig. 88--Daytime radiated power (Cerenkov mode) for SEPAC, pitch angle 45 deg (root 2).

α = 89.9
Ω_{pl}= $4.040*10^{-2}$
1. ≤ P ≤ 20.
S = 0.
ω_{CE} = $8.5450*10^{6}$

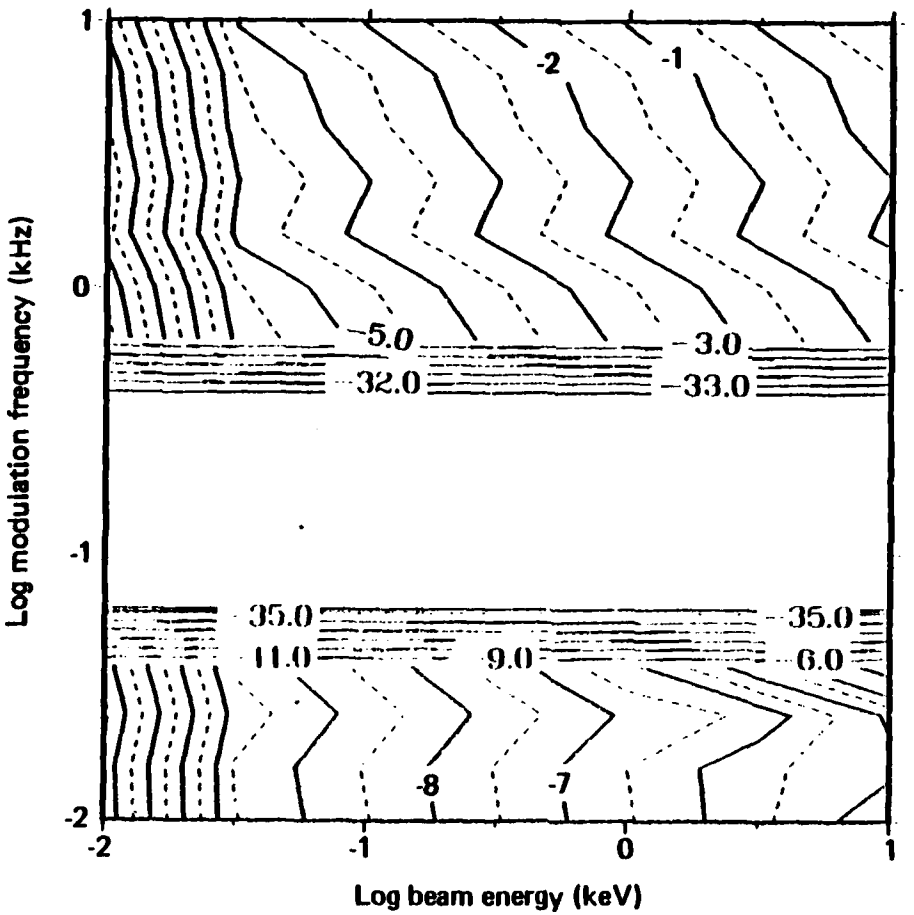

Fig. 89--Daytime radiated power (Cerenkov mode) for SEPAC, pitch angle 89.9 deg (root 1).

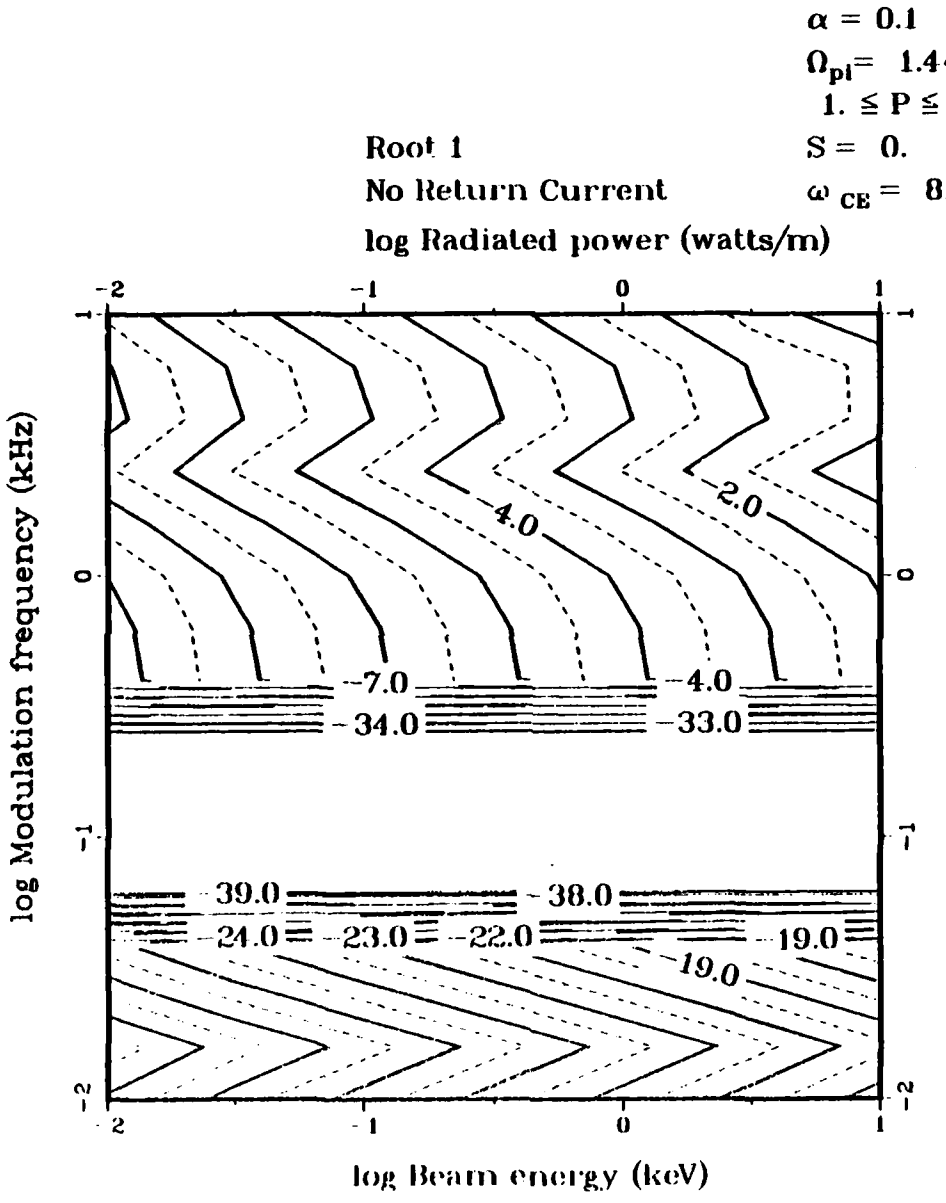

Fig. 90--Nighttime radiated power (Cerenkov mode) for SEPAC, pitch angle 0.1 deg (root 1) .

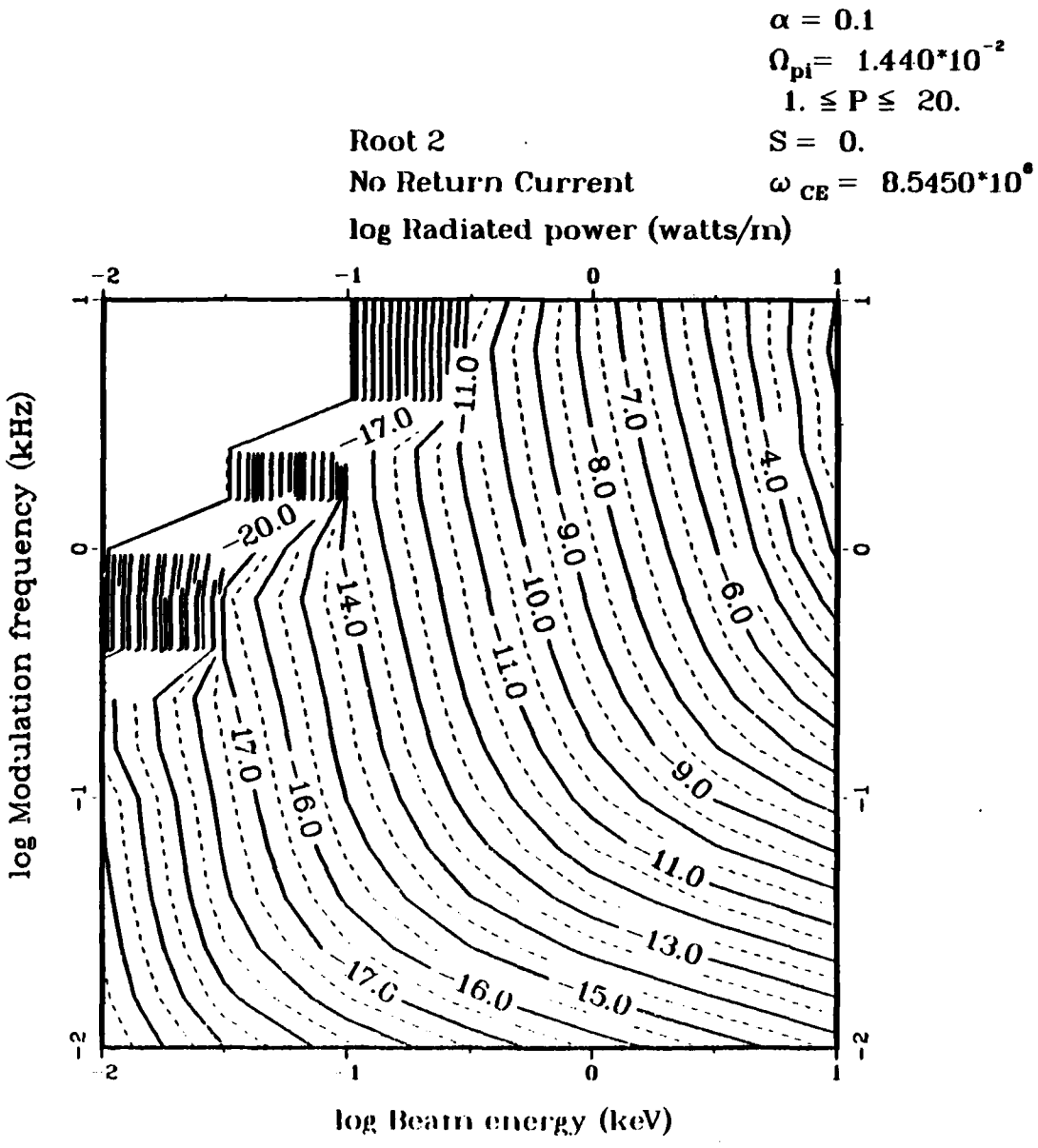

Fig. 91--Nighttime radiated power (Cerenkov mode) for SEPAC, pitch angle 0.1 deg (root 2).

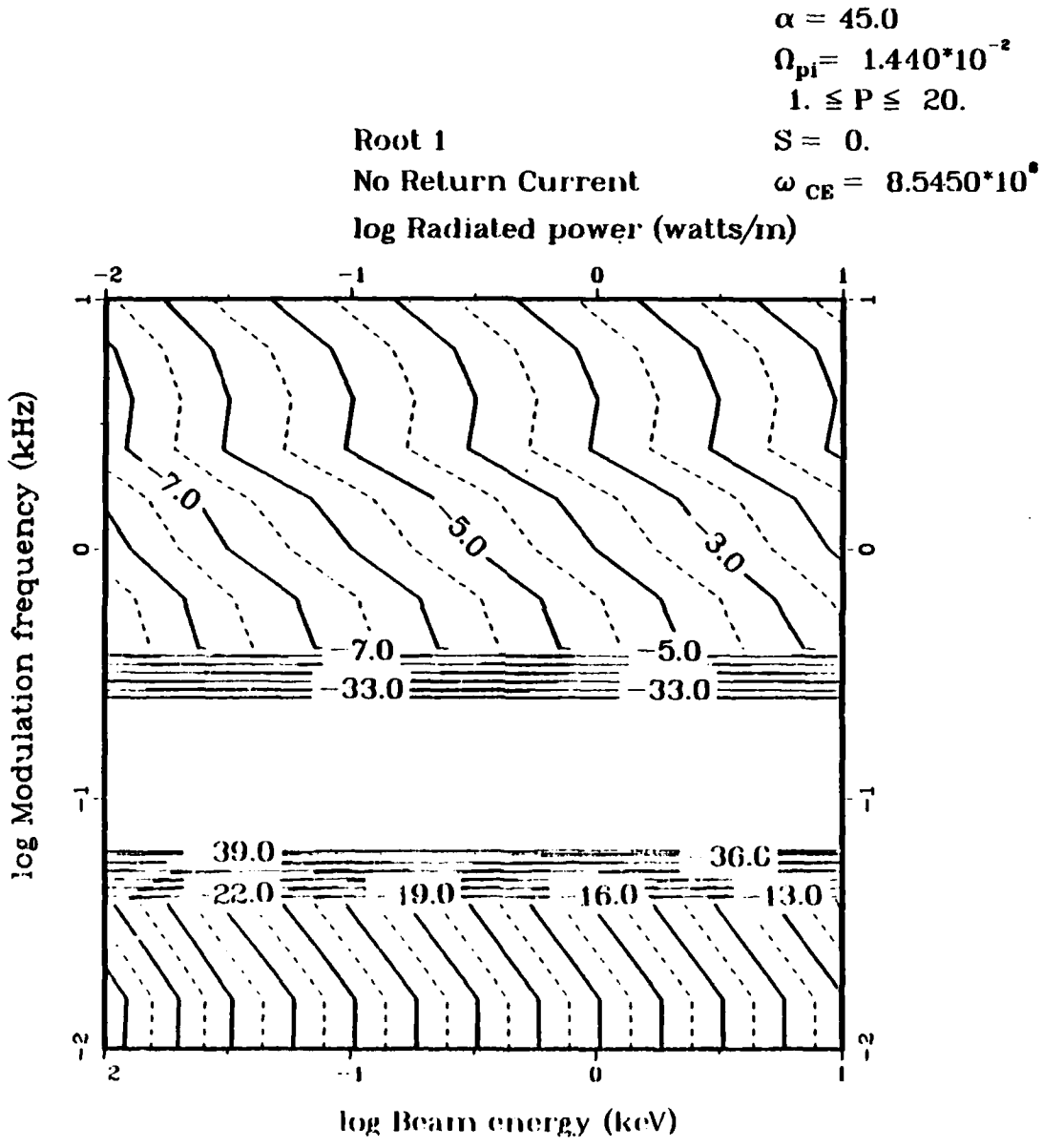

Fig. 92--Nighttime radiated power (Cerenkov mode) for SEPAC, pitch angle 45 deg (root 1).

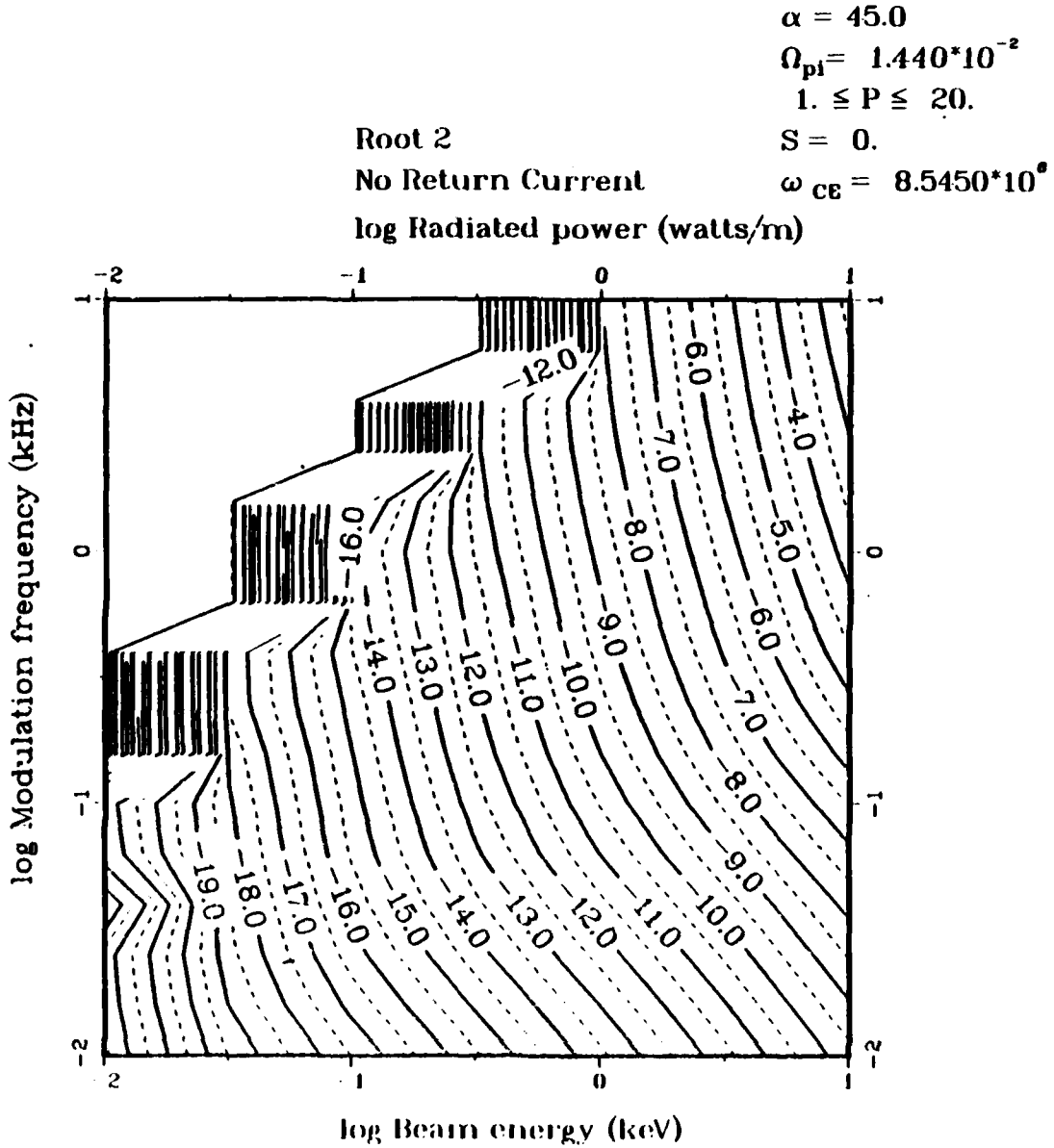

Fig. 93--Nighttime radiated power (Cerenkov mode) for SEPAC, pitch angle 45 deg (root 2) .

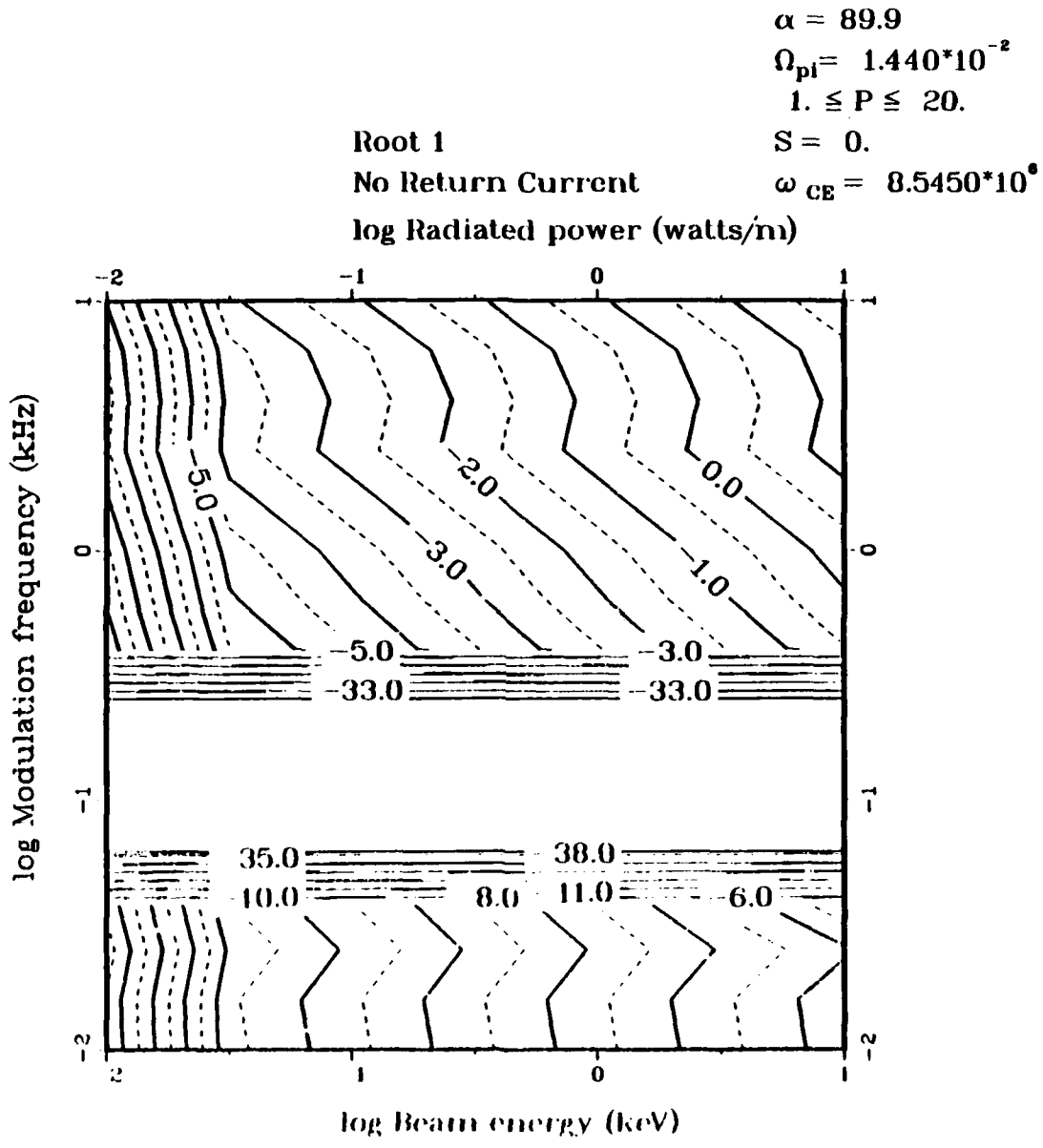

Fig. 94--Nighttime radiated power (Cerenkov mode) for SEPAC, pitch angle 89.9 deg (root 1).

REFERENCES

1. Harker, K. J., and P. M. Banks, *Radiation from Long Pulse Train Electron Beams in Space Plasmas,* STAR Laboratory, Stanford University, California, 1984.

2. Al'pert, Y. L., *The Near-Earth and Interplanetary Plasma,* Vol. 1, Cambridge University Press, New York City, 1983.

3. Booker, H. G., C. M. Crain, and E. C. Field, *Transmission of Electromagnetic Waves through Normal and Disturbed Ionospheres,* The Rand Corporation, R-558-PR, Santa Monica, California, November 1970.

4. Cohen, H., Air Force Geophysical Laboratory, Hanscom Air Force Base, Massachusetts, private communication, December 1984.

5. Tsutsui, M., H. Matsumoto, and I. Kimura, "Laboratory Simulation of Low-Energy Electron Beam Injection by a Japanese Sounding Rocket in Space," *Radio Sci.,* Vol. 19, No. 2, March-April 1984, pp. 503-508.

6. Harker, K. J., *STAR Laboratory,* Stanford University, California, private communication, 1984,

7. Lavergnat, J., and T. Lehner, "Low Frequency Radiation Characteristics of a Modulated Electron Beam Immersed in a Magnetized Plasma," *IEEE Trans. Antennas Propag.,* Vol. AP-32, No. 2, February 1984.

8. Donatelli, D., Air Force Geophysical Laboratory, Hanscom Air Force Base, Massachusetts, private communication, October 1984.

9. Fraser-Smith, A., STAR Laboratory, Stanford University, California, private communication, October 1984.

10. Taylor, W. W. L., TRW, Space and Technology Group, Redondo Beach, California, private communication, October 1984.

MISSION
of
Rome Air Development Center

RADC plans and executes research, development, test and selected acquisition programs in support of Command, Control, Communications and Intelligence (C^3I) activities. Technical and engineering support within areas of competence is provided to ESD Program Offices (POs) and other ESD elements to perform effective acquisition of C^3I systems. The areas of technical competence include communications, command and control, battle management, information processing, surveillance sensors, intelligence data collection and handling, solid state sciences, electromagnetics, and propagation, and electronic, maintainability, and compatibility.

END

FILMED

9-85

DTIC